New Excavations at the Site of Contrebandiers Cave, Morocco

HAROLD L. DIBBLE
Department of Anthropology, 3260 South Street, University of Pennsylvania, Philadelphia, PA 19104, USA; Department of Human Evolution, Max Planck Institute for Evolutionary Anthropology, D-04103, Leipzig, GERMANY; and, Institute of Human Origins, School of Human Evolution and Social Change, Box 874101, Arizona State University, Tempe, AZ 85282, USA; hdibble@sas.upenn.edu

VERA ALDEIAS
Department of Earth and Environmental Sciences, Hayden hall 240, South 33rd Street, University of Pennsylvania, Philadelphia, PA 19104, USA; veraldeias@gmail.com

ESTEBAN ALVAREZ-FERNÁNDEZ
Department of Prehistory, University of Salamanca, C. Cerrada de Serranos S/N, E-37002 Salamanca, SPAIN; estebanalfer@hotmail.com

BONNIE A.B. BLACKWELL
Department of Chemistry, 47 Lab Campus Drive, Williams College, Williamstown, MA 01267, USA; Bonnie.A.B.Blackwell@williams.edu

EMILY HALLETT-DESGUEZ
Institute of Human Origins, School of Human Evolution and Social Change, Box 874101, Arizona State University, Tempe, AZ 85282, USA; hallett.emily@gmail.com

ZENOBIA JACOBS
Centre for Archaeological Science, School of Earth and Environmental Sciences, University of Wollongong, Wollongong, NSW 2522, AUSTRALIA; zenobia@uow.edu.au

PAUL GOLDBERG
Department of Archaeology, 675 Commonwealth Ave., Boston University, Boston, MA 02215, USA; paulberg@bu.edu

SAM C. LIN
Department of Anthropology, 3260 South Street, University of Pennsylvania, Philadelphia, PA 19104, USA; samlin@sas.upenn.edu

ANDRÉ MORALA
Musée National de Préhistoire, Les Eyzies-de-Tayac, FRANCE; andre.morala@culture.gouv.fr

MICHAEL C. MEYER
Centre for Archaeological Science, School of Earth and Environmental Sciences, University of Wollongong, Wollongong, NSW 2522, AUSTRALIA; and, Institute of Geology and Palaeontology, Innrain 52, University of Innsbruck, 6020 Innsbruck, AUSTRIA; michael.meyer@uibk.ac.at

DEBORAH I. OLSZEWSKI
Department of Anthropology, 3260 South Street, University of Pennsylvania, Philadelphia, PA 19104, USA; deboraho@sas.upenn.edu

KAYE REED
Institute of Human Origins, School of Human Evolution and Social Change, Box 874101, Arizona State University, Tempe, AZ 85282, USA; kaye.reed@asu.edu

DENNÉ REED
Department of Anthropology, 1 University Station C3200, University of Texas at Austin, Austin, TX 78712, USA; reedd@mail.utexas.edu

ZELJKO REZEK
Department of Anthropology, 3260 South Street, University of Pennsylvania, Philadelphia, PA 19104, USA; rezek@sas.upenn.edu

DANIEL RICHTER
Department of Human Evolution, Max Planck Institute for Evolutionary Anthropology, D-04103, Leipzig, GERMANY; and, Lehrstuhl Geomorphologie, Universitätsstrasse 30, University of Bayreuth, 95447 Bayreuth, GERMANY; daniel.richter@uni-bayreuth.de

***PaleoAnthropology* 2012: 145–201.** **ISSN 1545-0031**
doi:10.4207/PA.2012.ART74

RICHARD G. ROBERTS
Centre for Archaeological Science, School of Earth and Environmental Sciences, University of Wollongong, Wollongong, NSW 2522, AUSTRALIA; richard_roberts@uow.edu.au

DENNIS SANDGATHE
Department of Archaeology, 8888 University Drive, Simon Fraser University, Burnaby BC V5A-1S6, CANADA; and, University of Pennsylvania Museum of Archaeology and Anthropology, 3260 South Street, University of Pennsylvania, Philadelphia, PA 19104, USA; dms@sfu.ca

UTSAV SCHURMANS
University of Pennsylvania Museum of Archaeology and Anthropology, 3260 South Street, University of Pennsylvania, Philadelphia, PA 19104, USA; schurman@upenn.edu

ANNE R. SKINNER
Department of Chemistry, 47 Lab Campus Drive, Williams College, Williamstown, MA 01267, USA; Anne.R.Skinner@williams.edu

TERESA E. STEELE
Department of Anthropology, One Shields Ave, University of California at Davis, Davis, CA 95616, USA; and, Department of Human Evolution, Max Planck Institute for Evolutionary Anthropology, D-04103, Leipzig, GERMANY; testeele@ucdavis.edu

MOHAMED EL-HAJRAOUI
Institut National des Sciences de l'Archéologie et du Patrimoine, 10001 Rabat, MOROCCO; maelhajraoui@gmail.com

ABSTRACT

New excavations at Contrebandiers Cave, Morocco, began in 2007 and continued through 2010. This site, originally excavated by Roche in the 1950s, contained deposits with Aterian, Iberomaurusian, and Neolithic materials, although the latter were completely removed during Roche's excavations. This report presents an overview of the recent excavations, the stratigraphic sequence of the site, absolute dates based on OSL, TL, and ESR, and detailed data on the lithic (Iberomaurusian, Aterian, and Mousterian) and faunal assemblages, the latter of which includes large mammals, microvertebrates, and marine shells.

INTRODUCTION

Over the past few years, early Late Pleistocene sites across North Africa have received increasing research attention, primarily because of their potential to contribute to the debate on the emergence of anatomically and behaviorally modern *H. sapiens* in Africa. Historically, much of the research on this subject has been centered on East (Horai et al. 1995; McDougall et al. 2005; White et al. 2003) and South African contexts (Klein 2001; Henshilwood et al. 2002; 2009; Marean and Thompson 2003; Marean et al. 2007). However, there are currently a number of active archaeological projects in Morocco, such as at Jebel Irhoud (Smith et al. 2007), Rhafas (Mercier et al. 2007), Ifri n'Ammar (Nami and Moser 2010; Richter et al. 2010), Pigeons Cave at Taforalt (Barton et al. 2005; Belcastro et al. 2010; Bouzouggar et al. 2007), El Mnasra and El Haroura II (Nespoulet et al. 2008; Michel et al. 2010; Stoetzel et al. 2011), and Contrebandiers Cave. The data resulting from these projects are now identifying Morocco as one of the major research areas relating to the modern human origins (Barton et al. 2009; Balter 2011; Bouzouggar et al. 2007; Garcea 2010; Nespoulet et al. 2008; Schwenninger et al. 2010; Van Peer 2001).

For example, there is no doubt that Morocco has produced one of the richest and most complete fossil records of early *H. sapiens* (Hublin 2001). The Jebel Irhoud remains provide some of the oldest evidence (ca. 160 ka) for a *H. sapiens* craniofacial architecture (Hublin 1992; Smith et al. 2007), while a large series of later specimens express some level of continuity with the Irhoud humans. Among these, the Dar-es-Soltane II remains (a cranium of an older man, an infant calvarium, and a mandible of a teenager) are the most complete, while Contrebandiers Cave had previously yielded a mandible, a frontal fragment, and another large cranium fragment (Roche 1976a, 1976b). All of these remains are attributed to fully modern *H. sapiens* (Debénath 1976, 2000; Ferembach 1976, 1985, 1998; Hublin 1993; Ménard 1998; Minugh-Purvis 1993; Roche and Texier 1976; Saban 1998). In addition, there are archaeological industries associated with these hominin fossil remains, traditionally termed Aterian and Mousterian, that express some traits that could be interpreted as reflecting modern behavior (McBrearty and Brooks 2000). Some of these traits include stemmed pieces and bifacial points (which are defining characteristics for the Aterian *sensu stricto*), perforated shell ornaments (Bouzouggar *et al.* 2007; d'Errico *et al.* 2009; Nami and Moser 2010), and the use of ochre and worked bone (El Hajraoui 2004; Nespoulet and El Hajraoui 2004). While the systematics of these industries is in need of updating, there is growing evidence that they date far earlier than was previously thought. For example, Aterian occupa-

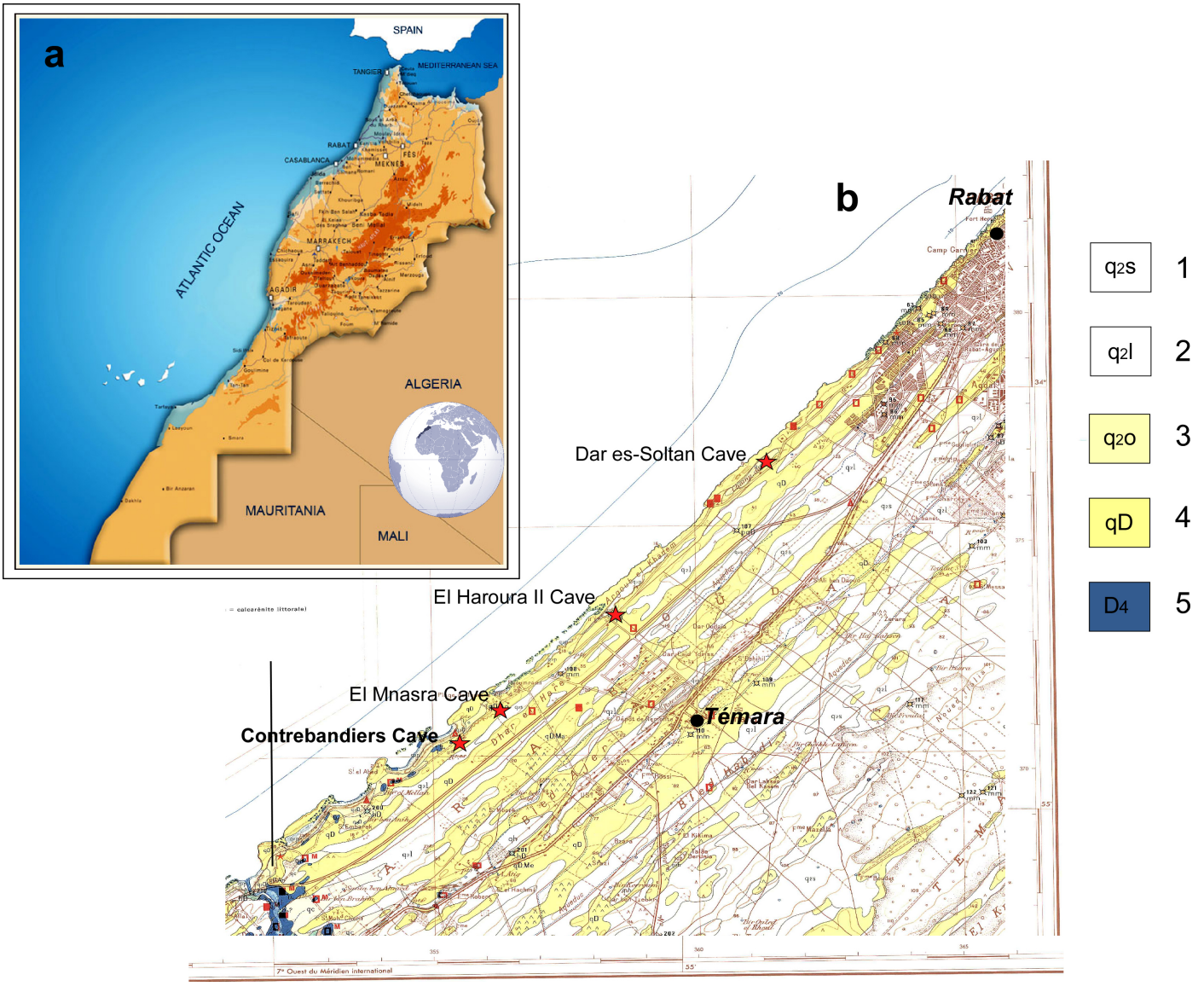

Figure 1. Geographical location of Morocco (a) and geological map of the area of Témara (b) where the red stars show the location of the archaeological sites (adapted from the Carte Geotéchnique de la Région de Rabat, scale 1: 50,000). 1–4 are Quaternary sedimentary deposits. 1: Plateau deposits composed by sandy rubiefied soils, sands of Mamora; 2: Plateau deposits composed by rubified silts attributed to the Soltanian; 3: Marine and litoral deposits, sandy soils of Ouljas (local depressions); 4: Marine and litoral deposits, limestones, and bioclastic limestones; 5: Massive limestones from the Devonian.

tions are dated beyond 80 ka at El Akarit in Tunisia (Reyss et al. 2007), to 60–90 ka in the Libyan Sahara (Cremaschi et al. 1998), and to even earlier dates in Moroccan contexts, such as 110 ka at Dar es-Soltan I (Barton et al. 2009), and 145 ka at Ifri n'Ammar (Richter et al. 2010).

Contrebandiers Cave, also known as Smugglers' Cave (Briggs 1968; Klein and Scott 1986), Témara (Ferembach 1976; Ménard 1998; Vallois and Roche 1958), El Mnasra I (Bouzouggar 1997a) and Grotte d'Oulad Bouchiha/Ouled Bouchikha (Bouzouggar 1997b; Niftah 2003), has a long stratigraphic sequence that contains a succession of lithic assemblages, with good preservation of bone, mollusks, and hominin remains. The site is situated near the town of Témara in the Atlantic coast of Morocco, approximately 16km south from the city of Rabat (33° 55′ 18.23″ N, 6° 57′ 42.41″ W—Figure 1). It was first discovered in 1955 by Roche, who conducted a series of excavations there from 1955 to 1957 (Roche 1969) and then again from 1967 to 1975 (Roche 1976a, b; Roche and Texier 1976). Later, more limited excavations and studies were undertaken by Bouzouggar (Bouzouggar 1997a, b) and Niftah (Niftah 2003; Niftah et al. 2005). The most recent work, a joint Moroccan-American collaboration directed by El-Hajraoui and Dibble (through agreement with the Moroccan Institut National des Sciences de l'Archeologie et du Patrimoine, or INSAP), began in 2007 and has continued through the present. All of the materials recovered from this new excavation are currently stored at INSAP.

There are several goals of the current project—a re-examination of the stratigraphic record, with an emphasis on

establishing the processes that led to the site's formation; the development of a more precise and detailed chronological framework for the site; and, a study of the nature of human occupations at Contrebandiers Cave, with a special focus on the assessment of the differences and/or similarities between the Aterian and Mousterian occupations (see Dibble et al. submitted). In this paper, preliminary results from the recent excavations concerning the stratigraphy, chronology, lithic and faunal assemblages will be presented and discussed.

AN OVERVIEW OF THE SITE, EXCAVATION STRATEGY, AND STRATIGRAPHIC SEQUENCE

Contrebandiers Cave is currently about 250m from the Atlantic Ocean, inland from a beach locally known as Contrebandiers. The cavity is carved into Pleistocene calcarenites and is approximately 30m deep, with an entrance about 28m wide that faces northwest (Figure 2). Roche (1976b) reported that large calcarenite blocks were initially present at the front of the cave overlying the Neolithic layers. Thus, it is probable that a substantial part of the roof collapsed relatively recently, which means that the cave had a significantly different configuration during the Pleistocene and quite possibly even during the Neolithic occupations. At present, there are two visible chimneys, at least one of which directly connects to the plateau area above the site (though it is now partially filled with cement).

When the site was originally discovered, the Paleolithic occupation levels were capped by Neolithic deposits. These Neolithic deposits were almost completely removed during Roche's excavations, and the few remnants consist of organic-rich sediments with ubiquitous shells, locally attached to the cave walls, or pits dug into the underlying sediments. The Iberomaurusian occupations were originally described by Roche to be restricted to an area near the cave's entrance, often in a stratigraphic position described as the infilling of "pits" (Roche 1963; Roche 1976a). The bulk of the roughly 4m-thick deposits contains Aterian and Mousterian assemblages. Archaeological excavations have exposed the cave's floor only in the central area of the site where its topography is overall inclined towards the mouth of the cave (Figure 3).

At the start of our work, a standard 1-m grid system was established as close as possible to the grid used in preceding excavations (see Figure 2). The excavation grid was tied to the Moroccan geodesic system, with the zero point at Contrebandiers (located in the back wall in the interior of the cave) positioned at 11.333m above sea level (a.s.l.). The excavation methodology employed at the site is based on methods described elsewhere (Dibble et al 1995, 2007; McPherron and Dibble 2002). This excavation strategy involves point-proveniencing all objects larger than 25mm with a Total Station, using software developed by McPherron and Dibble (2002; see also http://www.oldstoneage.com/software/default.shtml). Certain objects smaller then 25mm were also point-provenienced, including all teeth, *Nassarius* sp. shells, and human remains; geological, dating, and other samples were provenienced in the same manner. During excavation, all of the sediments were collected in 7-liter buckets, and an individual Unit-ID number was attributed to each bucket, while the three-dimensional location of each bucket was recorded at the center of the area from where the sediments were excavated (typically an area covering about 0.25m^2). These sediments were then wet screened on the site using 1cm (coarse) and 2mm (fine) mesh. In addition, although a sample of buckets were also screened with 1mm mesh in order to test for bias in the recovery of microvertebrate remains. Complete and fragmentary shell (both terrestrial and marine), microvertebrates, and small pieces of lithics and bone recovered from the screens were not assigned individual numbers, but were instead treated as aggregated data. The data recorded in the field were ultimately transferred into our own GIS program, which provides a means of integrating other data derived from the analysis of the excavated objects.

Previous archaeological trenches nearly cut the site into three separate areas. The biggest trench, roughly paralleling the mouth of the cave just at the current dripline, can be seen in Figure 4a and 4b. This trench was excavated to bedrock and reached all the way to the cave wall on the west. Another trench, smaller and more irregular (perhaps due to post-excavation erosion), extended back into the cave at roughly right angles to the first. The area of this second trench (Figure 4c) is referred to here as the Central Excavation Area (CEA).

The first priority for the new excavations was to establish a site-wide stratigraphy by creating a clean and continuous section around the periphery of the earlier trenches. To accomplish this as quickly as possible, various excavation areas, or sectors, were defined along the periphery on the old trenches (Sector I, Sector II, Sector III and Sector IV; see Figure 2). In addition, a 2-m square test pit was opened at the back of the cave in order to assess the stratigraphic sequence and archaeological potential in this area of the site; it is designated as Sector V. As work progressed, the stratigraphy was defined for each sector independent of the others; individual stratigraphic units were then designated as a combination of the sector number along with the stratigraphic layer (e.g., I-2, II-1, IV-2, etc.). Thus, Layer IV-2 (i.e., Layer 2 from Sector IV) is not necessarily equivalent to Layer V-2 (i.e., Layer 2 in Sector V). By 2010, the excavation in Sectors I, II, and III (the CEA) progressed to a point that allowed direct stratigraphic correlation among these sectors, and a stratigraphic succession was implemented for the CEA deposits, designating the units in a numeric sequence (from top to bottom). The stratigraphic sequence for sectors IV and V remains separate and independent, since there are no direct physical links between these excavation areas and the CEA.

THE STRATIGRAPHIC SEQUENCE

The general stratigraphic correlations of the exposed profiles of Contrebandiers are shown in Figure 5. The correspondence between our lithostratigraphic nomenclature and previous published stratigraphic descriptions by Roche

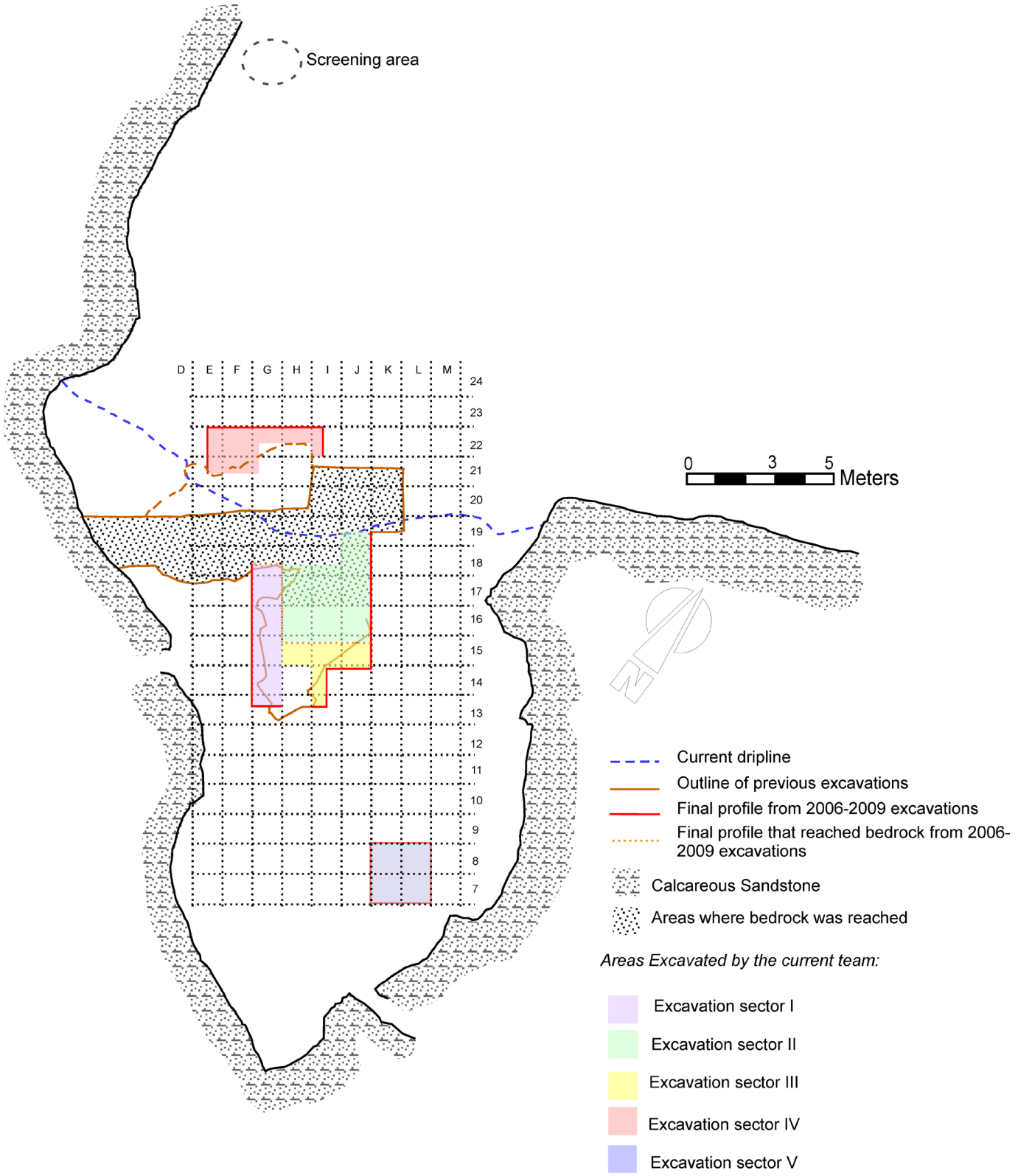

Figure 2. Map of Contrebandiers cave showing excavation grid and the main sectors of current excavations at the site.

(1976b) and Roche and Texier (1976) is presented in Table 1, along with traditionally-defined industrial affiliations.

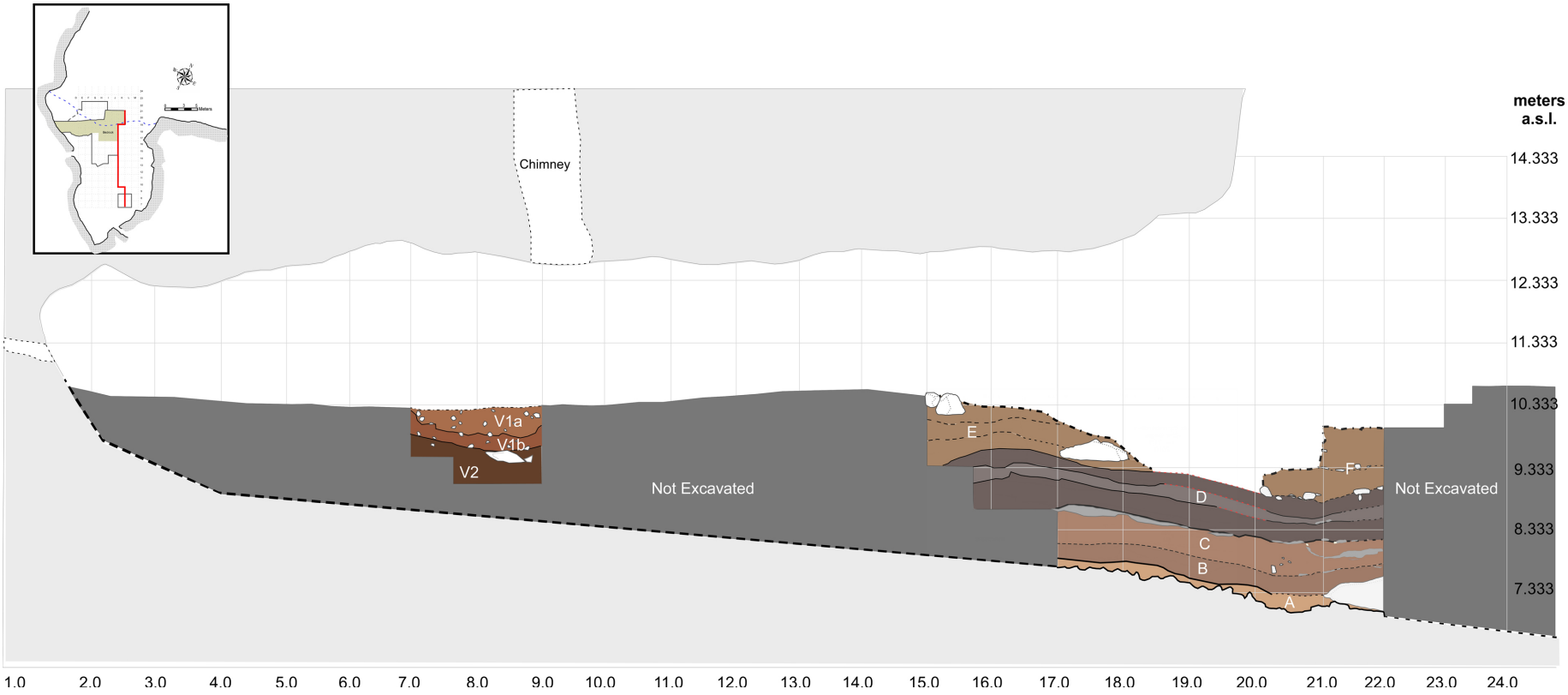

Figure 3. Schematic view of the stratigraphic deposits and their absolute altimetry. See grid map in the figure for location of the drawn profile.

Figure 4. Photographs of Contrebandiers Cave in 2006, before excavation began at the site. Note the existing trenches excavated during previous work at the site in the Central Excavation Area (CEA). a-b) Photographs of the main trench roughly parallel to the cave mouth; c) view of the smaller trench that extended towards the back of the cave.

Central Excavation Area (Figures 6 and Figure 7)

Six major lithostratigraphic units are distinguished in the CEA. These units are, with minor exceptions, comparable to the archaeological layers, which are referred to here as Layers. The color designations for each unit are based on the Munsell soil color chart, taken in shade, on dry sediments. From bottom to top, the units are as follows:

Unit A (Archaeological Layer 7)**:** 12 to 26cm thick. This is a tabular lithostratigraphic unit characterized by reddish brown (5YR 5/4) shell-rich sands with brownish yellow mottles (10YR 6/6) that vary from loose to strongly cemented towards the base. This cementation of Unit A makes its distinction from the cave's floor difficult to establish in certain areas. Overall, the deposits are massive or with discrete horizontal internal bedding, moderately sorted, with rare well-rounded cm-size calcarenite clasts (<7cm); interstitial red clays and foraminifera were also observed. A large (>1m) calcarenite block is visible in the profile of squares K 21/22. These deposits constitute the basal sediments in the cave and have an apparent dip towards the entrance of the cave, following the natural inclination of the bedrock. Localized bioturbation is visible (typically with diameter of roughly 1.5cm, some likely due to wasp activity), which may be responsible for the gradual contact with the overlying deposits, and common incorporation of the coarse grains in the above strata. No archaeological material was observed within this unit in the field, although mm-size bones and coprolites were identified in thin section.

Unit B (Archaeological Layer 6c)**:** ~30cm thick. This unit is composed of moderately loose sandy clay, mostly yellowish red (5YR 4/6) though with reddish brown areas (5YR 3/4), and with occasional concreted areas and domains where weakly developed bedding is apparent. Occasional calcarenite clasts (~ 7 to 15cm) are present, along with mm-size charcoal fragments. Lenticular indurated Fe/Mn-rich crusts, roughly 1cm thick, were identified (specifically in Squares J/I 18–16), as well as local phosphatization of the sediments. Anthropogenic inputs are present as discrete combustion areas, identified by ash and carbonaceous

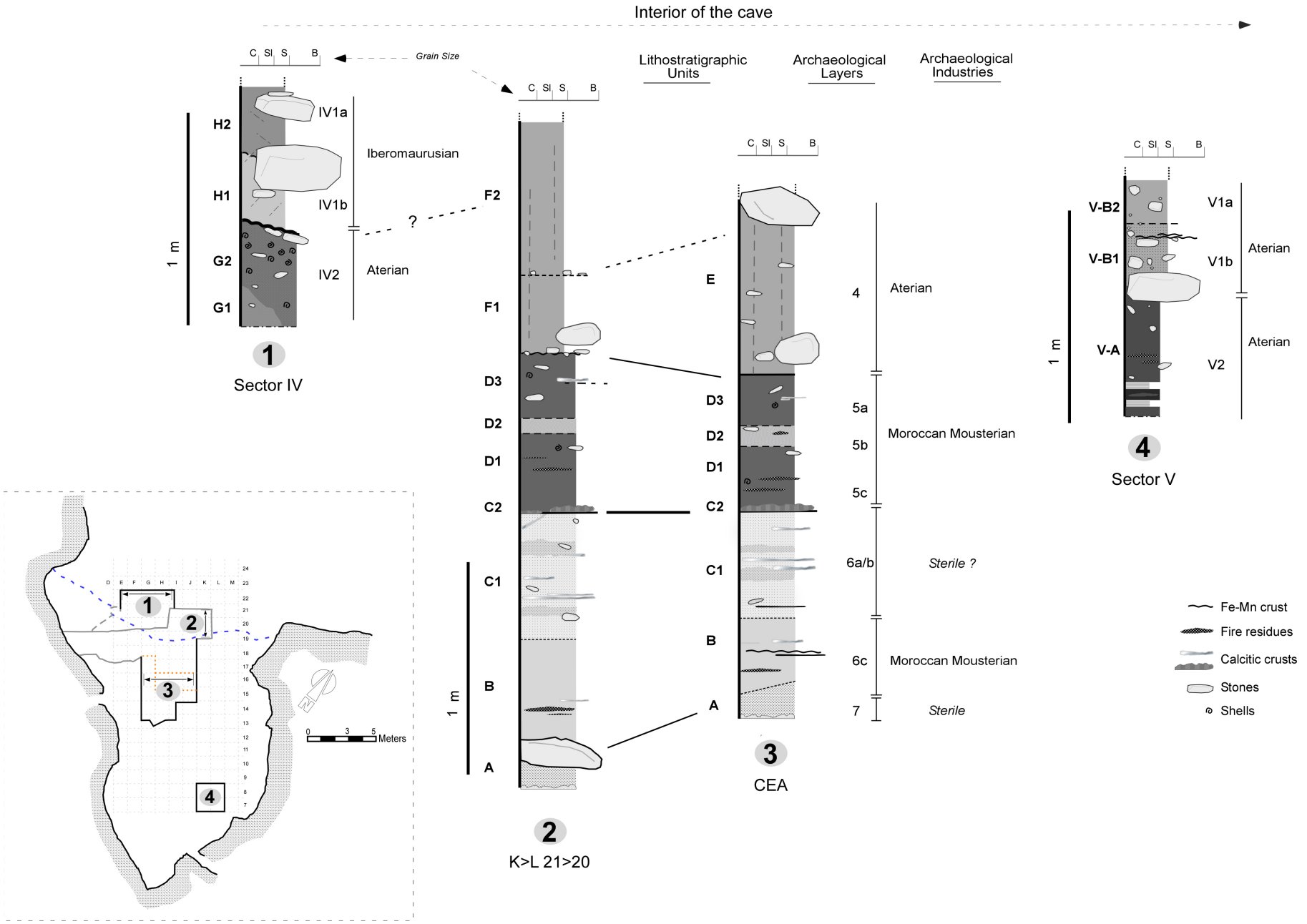

Figure 5. Schematic stratigraphic columns of the deposits exposed at Contrebandiers cave, showing the correspondence between the lithostratigraphic units and the archaeological layers. The numbered circles below each column denote the excavation sectors where the description were made—see also cave map at bottom left corner of the figure for location within the site's grid system. The width of the columns represents grain size (C clay, SL silt, S sand, and B Boulders).

TABLE 1. SYNTHESIS OF THE MAIN STRATIGRAPHIC SEQUENCE IN THE CENTRAL EXCAVATION AREA (CEA) OF CONTREBANDIERS CAVE (with correlation with published stratigraphy from Roche [1976b]).

Archaeological Layers	Lithostratigraphic Unit	Roche (1976b) Stratigraphy	Archaeological Industries
4a	F2	8?	Aterian
4b			
4c			
4d	F1	9/10	
4e			
5a	D3	11a	Mousterian
5b	D2	11b	
5c	D1	11c	
5d			
6a/b	C2 (crust)	12	
	C1	13a/13b/13c	
6c	B	13d/14/15?	
7	A	16	Sterile

Figure 6. View of the Central Excavation Area (CEA) at the end of the 2010 season.

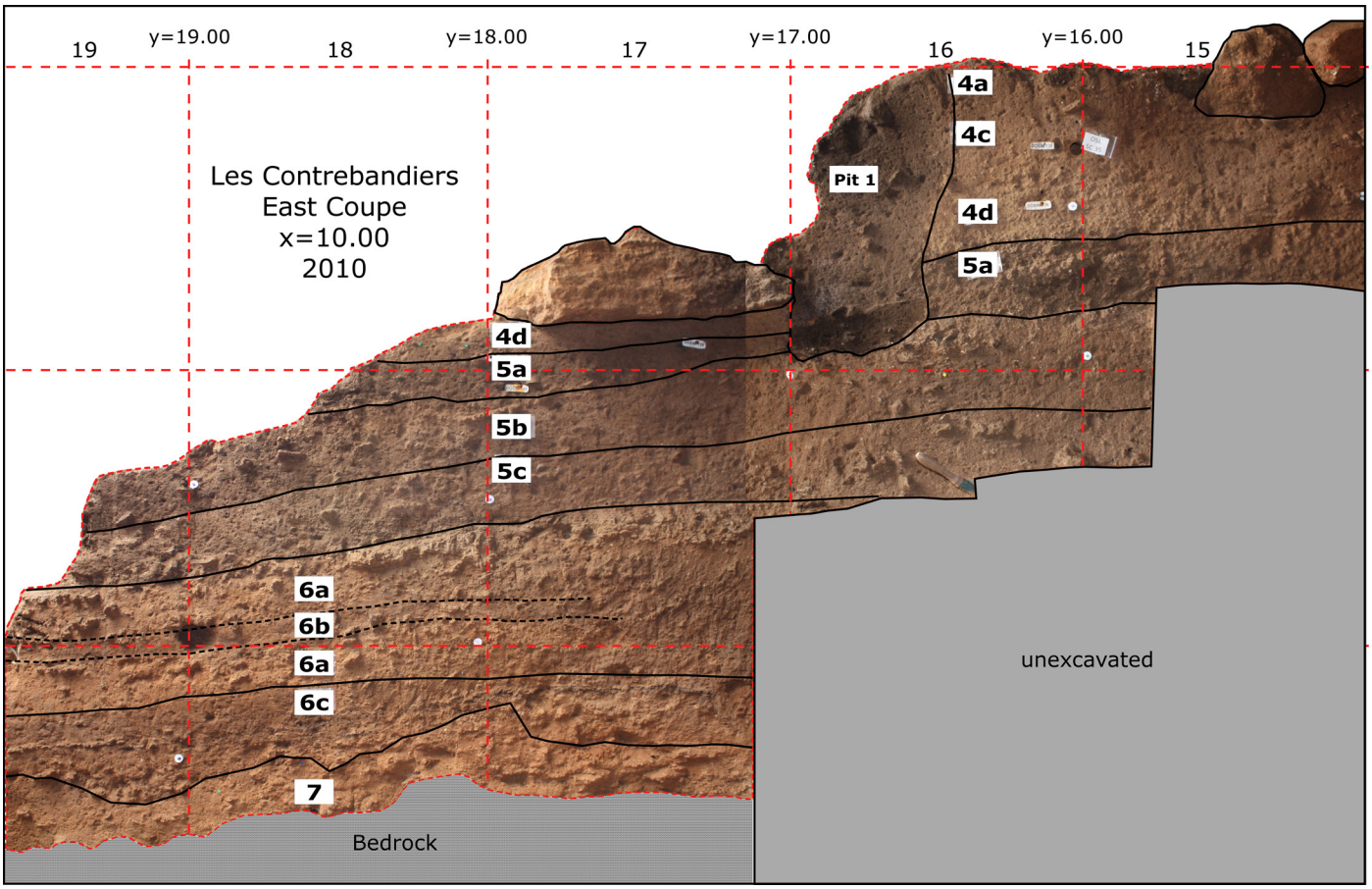

Figure 7. Photograph and drawing of the deposits in the grid East profile (squares J>K 19–15) of the Central Excavation Area (CEA), showing the archaeological layers .

accumulations in association with artifacts (Mousterian), though these inputs are less frequent than in the above Unit D. Biological activity is represented by mm-size plant roots and wasp burrows. The lower contact is somewhat gradual with unit A.

The next unit, *Unit C* (Archaeological Layers 6a/b), is subdivided into two subunits. *Subunit C1* is 45 to 60cm thick, light brown (7.5YR 5.5/4) silty sands interfingered with darker yellowish brown (10YR 4/4) sediments that are laterally and vertically discontinuous. Lenticular carbonate-cemented crusts (typically 3 to 5cm thick) are common throughout the unit, as are areas that are more phosphatic in nature. As in Unit B, lenticular indurated Fe/Mn-rich crusts are present, for example in Squares H17–18. Overall, this unit has extremely rare anthropogenic inputs in the excavated areas. *Subunit C2* is comprised of a heavily cemented and somewhat continuous indurated calcareous crust of variable thickness (typically 5 to 10cm) that caps Unit C. Above Unit C, the deposits dip more markedly in different directions.

Unit D (Archaeological Layers 5a, 5b, 5c, and 5d) is, on average, 80cm thick. Its lower boundary with Unit C is sharply inclined, and Unit D seems to truncate Unit C in some areas. Unit D is generally composed of silty sands, and it is subdivided into three main facies based on composition and color. Throughout this unit the archaeological materials continue as representative of what has been traditionally called Mousterian.

Subunit D1 (~45cm thick) is dark brown (10YR 4/3), more organic deposit with abundant human inputs, namely charcoal specks, ash, stone tools, shells, and bones. Human fossil remains were identified in this unit during the 2009 field season. The deposits are locally cemented, and cm to dm-size bioturbation is common, reflecting a clear increase in earthworm and wasp activity. The irregular nature of several of the cemented lenses shows that bioturbation occurred prior to the cementation of the deposits by calcium carbonate. Rock fragments >10cm are rare, and when present, are mainly calcarenite.

The above *Subunit D2* (~15cm thick) is brown/dark brown (7.5YR 4/4), though lighter than subunit D1, and with relatively fewer ash accumulations and the charcoal specks are smaller and scattered. These deposits are locally cemented by calcium carbonate.

Subunit D3 (~20cm thick) is composed of dark brownish (7.5YR 3/2) deposits similar both in color and composition to those in Subunit D1, although with rarer ashy deposits, at least in the excavated areas; artifacts and faunal remains continue to be frequent. Several dip directions can be recorded in Unit D—a general inclination towards the cave's entrance in Squares J/K 19–16, and flattening in the area of K/L 20–22. In Squares H18–15 and G18–16, Unit D seems to

Figure 8. View of Sector IV, looking north.

be dipping in the opposite direction, roughly towards the interior of the cave. The dips appear to be controlled by the presence of a swallow hole that was active in the area of squares G-H 15/13.

Unit E (Archaeological Layer 4): (thickness unknown because sediments were removed by previous excavations—the more extensively preserved deposits are 110cm thick, e.g., in Squares J14-I14). The description of this unit throughout the site is hampered by the widespread excavations in the past, in addition to the presence of Neolithic pits that disrupt the deposits. The associated archaeological lithic industry is attributable to the Aterian due to the presence of tanged pieces. Unit E is composed of reddish yellow (7.5YR 6/6) silty sands, which are overall extremely bioturbated. Mottled pockets consisting of slightly darker brown clayey silts are attributed to burrows. Decimeter-size roof spall occurs in several profiles throughout the site at the base of this unit, and towards its upper boundary in Squares J-I 13–15. Besides these roof fall accumulations, clasts of about ~5cm in diameter occur locally in the unit. Common human inputs (bones, shells, lithics) are present, as well as cm-size grass roots and localized calcite-cemented areas. The lower boundary with Unit D is sharp, and Unit E seems to truncate the underlying deposits, at least in Squares H-J/15–16.

Unit F (no archaeological equivalent)**:** ~120cm thick in Squares K/L21 and K/L22. This unit consists of well-sorted reddish yellow (7.5YR 6/6) fine silt with reddish domains, and exhibiting a stone line with clasts from 5 to 10cm in diameter.

Excavation Sector IV (Figures 8 and 9)

Excavation in this sector, which is located on the northern side of Roche's main trench and thus independent from the other excavation areas, descended only slightly more than a meter below the present surface. Only two main stratigraphic units have been identified so far. From bottom to top, the units are as follows:

Unit G (Archaeological Layer IV-2)**.** The unit has a wavy, somewhat concave geometry, with a sharp, truncated upper limit. Although the excavated area is limited, in this area the upper limit is inclined toward the interior of the cave in Squares E/F 22–21. Due to its geometry, Unit G varies in thickness from ~20 to ~80cm, although its lower boundary was not reached during excavations. Overall, the deposits of *Subunit G2* are crumbly pebbly silty sands characterized by a lateral variability in color - from light yellowish brown (10YR 6/4) to pale brown (10YR 6/3) and an abundance of stones. The unit gradually varies from almost clast-supported (with stones typically in the 3 to 15cm range) and ubiquitous shells in its concave area, to extensively cemented matrix-supported deposits towards the north. Anthropogenic inputs are common, characterized by an Aterian lithic assemblage, with abundant complete shells that occur locally with darker brown sediments within its concavity. Finally, slightly darker, well-indurated brown sediments, with rare ~5cm stones occur towards the base of this unit in Squares H21/20. These deposits are designated as *Subunit G1* and have been only partially excavated; the contact and differentiation with G2 is not clear at present.

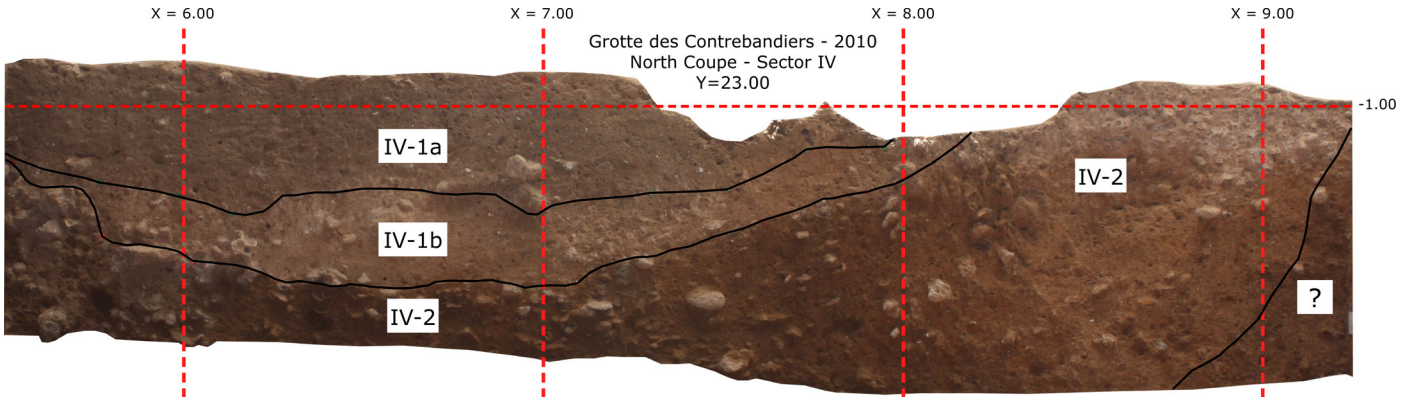

Figure 9. Photograph and drawing of the deposits in Sector IV (looking north), showing the archaeological layers.

Unit H (Archaeological Layers IV-1a and IV-1b), which is ~ 60cm thick, unconformably overlies the sediments of Unit G in a cut/fill type of structure. The deposits are loose and moderately sorted; based on color and composition; they can be subdivided into two subunits. The color varies from yellowish brown (10YR 5/6 in Subunit H2, archaeological Layer IV-1a) to light brown silty sands (7.5YR 6/4 in Subunit H1, archaeological Layer IV-1b). Extensive dm-size roof spall is present in both subunits, and there is an increase of stones (usually smaller than 20cm) in *Subunit H1*. The distinction between Subunits H1 and H2 is gradual and hampered by bioturbation, principally wasp cocoons. The origin of the 'pockets' that characterize *Subunit H2*, and the overall erosional contact with unit G are still unclear at present. These are the only layers that contained Iberomaurusian, along with numerous bone fragments, and marine shells. The top of this unit was truncated by previous excavations.

Excavation Sector V (Figure 10)

Sector V is a 2-m square test pit near the back of the cave (see Figure 2). Although only ~130cm was excavated here, two main lithostratigraphic units were defined. Combined with somewhat distinct lithological characteristics, the roughly 5m that separates this excavation sector from the central area of the cave precludes for the moment any attempt at direct correlation between the deposits. Consequently, the lithostratigraphic nomenclature for this sector remains independent. Both units contain archaeological industries with tanged pieces (Aterian).

Unit V-A (Archaeological Layer V-2): the lower limit of this unit was not reached during excavation. Currently, the unit is ~70cm thick in the deepest areas. The deposits are loose dark reddish brown (2.5YR 3/4) to dusky red (10R 3/3) silty sands with common charcoal specks; large dm-size roof spall blocks characterize the top of the unit. Anthropogenic sediments are expressed by the presence of features rich in charcoal and ash. Bioturbation is visible, including wasp cocoons and rodent burrows. This unit is also distinguished by irregular yellow (2.5Y 7/6) clayey lenses that are discontinuous throughout the deposits, and there is a clear decrease in stones throughout in comparison with unit V-B.

Unit V-B (Archaeological Layers V-1a and V-1b) varies in thickness from ~30 to 60cm and overall dips towards the west. Based on color and composition differences, this unit was subdivided into two subunits, from bottom to top. *Subunit V-B1* (Archaeological Layer V-1b) is reddish brown (2.5YR 4/4) silty sand with abundant ~15cm darker brown mottles regularly distributed throughout the deposits. These darker mottles can largely be attributed to animal burrows, namely wasps and rodent burrowing, some of which are clearly recent. In addition, modern cm-size roots were observed, providing further evidence of bioturbation in this area of the cave. This subunit is characterized by frequent stone lines (the stones vary from 5 to 15cm in diameter), and by larger dm-sized blocks of roof spall that mark its lower boundary. The sediments are clearly phosphatic, often resulting in the decalcification of the calcarenite stones, although mm-size size shell fragments (probably from both marine mollusks and terrestrial snails) are still observed. Anthropogenic inputs include stone tools and bone fragments. *Subunit V-B2* (Archaeological Layer V-1a) is a dark reddish brown (2.5YR 3/4), moderately sorted, fine silty sand, fairly loose and with occasional stones (5 to 10cm in diameter) and mottles of darker coloration. These darker mottles are mainly due to reworking of the sediments by bioturbation, although some can also be attributed to phosphatization and local disaggregation of the roof spall. This subunit is better expressed in the grid south areas of squares K-L 7. The presence of irregular, roughly 1cm thick, phosphatic and Fe-Mn indurated crusts is observed. These crusts pinch out towards north.

ABSOLUTE DATING OF THE DEPOSITS AT CONTREBANDIERS CAVE

A principal goal for the new excavations at Contrebandiers Cave is to determine or constrain the ages for the various artifact assemblages, which requires an accurate and precise chronology for the sedimentary and archaeological sequences. To achieve this objective, a multi-method dating approach involving electron spin resonance (ESR), thermoluminescence (TL), and optically stimulated luminescence (OSL) techniques was adopted to provide complementary

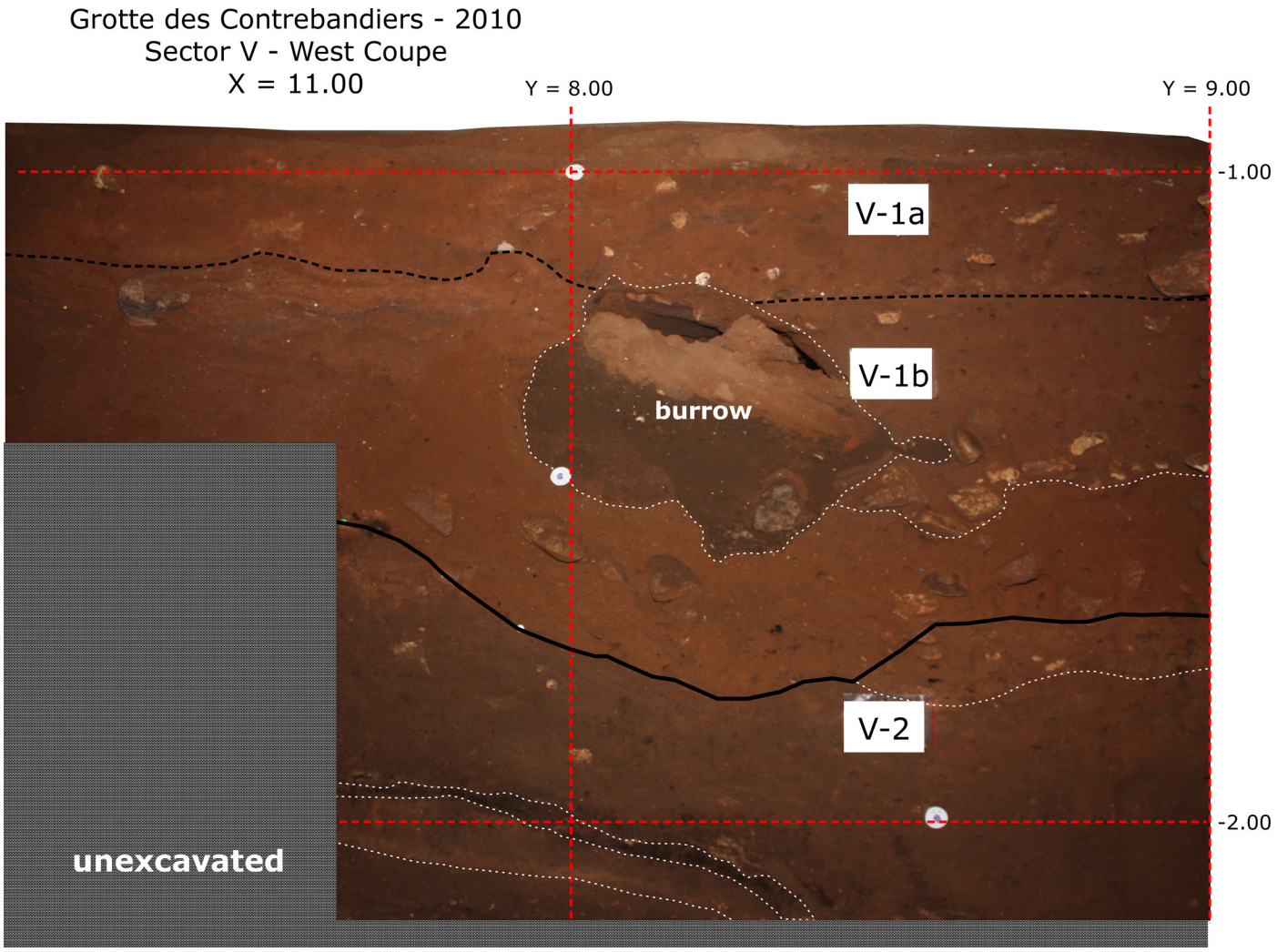

Figure 10. Photograph and drawing of the deposits in Sector V grid West profile, showing the archaeological layers.

data sets and avoid shortcomings in any single technique or sample type. All three techniques rely on the same physical principles—ages are calculated by measuring the total accumulated ionizing radiation stored in the crystal structure within the mineral compared to the total radiation dose rate arising from within and without the sample (Aitken 1985).

However, each method focuses on different materials. ESR was used to date hydroxyapatite in tooth enamel, TL to date burnt flint, and OSL to date quartz grains from sediments—and these different materials reflect different events in terms of their deposition. So, for example, TL dating of a burned lithic artifact reflects the time when it came into contact with fire, but not the manufacture of the artifact itself. On the other hand, ESR dating assumes that humans were the agents for the use and disposal of the animal, and thus directly dates that activity. However, an advantage of OSL is that it can date ubiquitous quartz grains with either geological or archaeological associations. In this case, the date reflects the last time the grains were zeroed by sunlight before burial and thus provides a date for the sedimentary context of the artifacts. As such, the three techniques can be considered semi-independent methods. Age agreement between these three chronometric methods indicates that the events are quasi-synchronous, and that the dates have a strong probability of being accurate.

OSL DATING OF QUARTZ SEDIMENTS

Again, ages obtained by OSL dating provide estimates of the time elapsed since the dated mineral grains were last exposed to sunlight. By measuring grains individually, those with aberrant OSL properties can be identified and discarded from the data set, and grains with bright signals, which are in agreement with the underlying physical and mathematical models, can be selected for determination of the equivalent dose (D_e), which is divided by the environmental dose rate to calculate the OSL age (Jacobs and Roberts 2007). With single-grain analysis, it is also possible to directly check the stratigraphic integrity of archaeological deposits for possible effects of post-depositional disturbance (e.g., mixing by anthropogenic or other processes) and to assess the adequacy of pre-depositional light exposure (David et al. 2007; Jacobs 2010; Jacobs and Roberts 2007; Jacobs et al. 2006, 2008; Lombard et al. 2010; Roberts

TABLE 2. OSL SAMPLES COLLECTED DURING THE 2007 AND 2008 ARCHAEOLOGICAL EXCAVATIONS PRESENTED IN STRATIGRAPHIC ORDER.*

Sample name	Year collected	Square	Archaeological Layer
CENTRAL EXCAVATION AREA			
SC21	2008	I14	4c
SC35	2010	J15	4c
SC20	2008	I14	4d
SC8	2007	I15	4d
SC7	2007	I15	4d
SC16	2008	K19	5a
SC15	2008	K19	5b
SC19	2008	J16	5c (top)
SC14	2008	K19	5c
SC6	2007	J19	5c
SC13	2008	K19	5c
SC28	2010	I16	5c
SC2	2007	J19	5c
SC1	2007	J19	5c (base)
SC18	2008	J16	6a
SC29	2010	I16	6a
SC12	2008	K19	6b
SC3	2007	J19	6b
SC11	2008	K19	6c
SC17	2008	J18	6c
SC4	2007	J19	6c
SC10	2008	K19	6c
*SC40	2010		6c
*SC41	2011	G14	Pit feature
*SC42	2011	G14	Pit feature
SC5	2007	J19	7
SC9	2008	K19	7

et al. 1998). By contrast, the determination of D_e values and OSL ages from multi-grain aliquots, as used by Barton et al. (2009) and Schwenninger et al. (2010) to date archaeological sediments from Contrebandiers Cave and other nearby sites, can conceal the pre- and post-depositional history of a sample, by averaging out the effects of mixing processes or insufficient light exposure (Arnold and Roberts, 2009; Duller 2008). This can give rise to inaccurate D_e estimates (and, hence, OSL ages), which may be further compromised if the multi-grain aliquots contain grains with aberrant OSL behaviors. Owing to the inherent benefits of single-grain analysis, therefore, we used this approach as our tool of choice to construct an OSL-based chronology of improved accuracy and precision for the complex archaeological sequences at Contrebandiers Cave.

A total of 46 sediment samples was collected for OSL dating from Contrebandiers Cave during the 2007 (n=8), 2008 (n=18), 2010 (n=14) and 2011 (n=6) excavation seasons. Samples were collected from the CEA, Roche's trench, and Sectors IV and V (see Figure 2) and, together, span the entire archaeological sequence revealed thus far at Contrebandiers Cave. Ten of the samples were collected from non-archaeological layers, such as the beach sands at the base of the sedimentary sequence (Layer 7), the bedrock floor and wall of the cave, and the breccia cemented to the wall. Final OSL ages have been obtained for 31 of the 46 samples collected, all from the pre-Iberomaurusian layers and the beach sands at the base of the excavation; dating of the remaining 15 samples (mostly associated with the Iberomaurusian, the breccia cemented to the walls, the bedrock, and

TABLE 2. (continued)

Sample name	Year collected	Square	Archaeological Layer
SECTOR IV AND ROCHE'S TRENCH			
*SC27	2010	F22	1b
*SC25	2008	F22	1b
*SC24	2008	F22	1b
SC30	2010	F22	IV-2
SC39	2010	I22	IV-2
SC37	2010	L21	IV-2b
*SC46	2011	K21	RT-4
	2010	I21	RT-4
SC32	2010	J21	RT-4
SECTOR V			
SC23	2008	L7	1b
SC34	2010	L7	2
BRECCIATED SEDIMENTS ON WALLS			
*SC43	2011	L21	East wall
	2011	Beyond grid	South wall
*SC45	2011	Beyond grid	South wall
*SC36	2010	A19	West wall
*SC33	2010	Outside limits of main excavation	
CAVE ROCK			
*SC22	2008	Outside cave	Calcareous sandstone
*SC38	2010	Outside cave	
*SC26	2008	J21	

*The Sector and archaeological layer from which each sample was collected is shown alongside its archaeological association.

the Neolithic) is in progress. Table 2 lists the samples collected, their stratigraphic positions, and their archaeological associations. At each sampling location, sediment for OSL dating was collected either in opaque plastic tubes in the daytime or in black plastic bags beneath a black tarp, using only a red-filtered flashlight for illumination. Cemented samples were struck off the wall with a hammer as a block and the outer light-exposed surfaces were removed in red light in the laboratory. Additional sediments for environmental radioactivity and moisture content determinations were collected in clear, zip-lock plastic bags.

To determine the D_e for individual grains, we applied the single-aliquot regenerative-dose (SAR) procedure, which contains a number of internal checks of sample suitability and validation tests of experimental conditions (e.g., Galbraith et al. 1999; Jacobs et al., 2006; Murray and Wintle 2000). We used the same instrumentation and methods of data collection and analysis as those employed to date archaeological sediments from a range of Middle Stone Age sites in southern Africa (Jacobs et al. 2008) and elsewhere in Morocco (Jacobs et al. 2012); experimental details specific to the samples from Contrebandiers Cave are provided in Jacobs et al. (2011). To determine the environmental dose rate for each of the samples, the beta dose rate was measured directly using a low-level beta counter and, for the majority of samples, the gamma-ray dose rate was obtained from *in situ* gamma-ray spectrometry. These methods give the combined beta and gamma dose rates associated with the radioactive decay of naturally occurring ^{238}U, ^{235}U, ^{232}Th (and their decay products), and ^{40}K in the materials surrounding the dated grains. When *in situ* gamma spectrometry was not possible, the gamma-ray dose rate was ob-

tained from a combination of thick-source alpha counting and beta counting. Corrections to the beta and gamma dose rates for grain size and moisture content followed standard procedures (see Jacobs et al. 2008). Account also was taken of the cosmic-ray dose rate (Prescott and Hutton 1994), including adjustments for the latitude, longitude and altitude of the site, and the depth and density of sediment and rock overburden at each sample location as well as for the internal alpha dose rate to the quartz grains. The D_e values, environmental dose rate data, and OSL ages are summarized, in stratigraphic order, in Table 3; this list includes the 31 samples collected from Layers 4–6, IV-2, V-1, V-2, and the beach sand samples (Layer 7) for which final ages are also presented in Jacobs et al. (2011). A chi-squared test of age homogeneity (based on Galbraith [2003]) indicates that the individual ages within each of the archaeological layers (e.g., Layer 4) are statistically consistent and can, therefore, be combined; see Jacobs et al. (2011) for detail. The weighted mean OSL ages are also listed in Table 3.

Three major events emerge from the OSL chronology. First, the deposition of the basal beach sands (Layer 7) dates to 126±9 ka, or during the Last Interglacial (MIS 5e). Second, this was followed by the deposition of two layers containing so-called Mousterian (i.e., without tanged pieces) with weighted mean dates between 122±4–5 (Layer 6c) and 115±3 ka (Layer 5a-c), and then the base and top of Layer 4, which contains an Aterian assemblage, dated to 107±4 and 96±4 ka, respectively. Third, the grand weighted mean ages for the Mousterian (116±3 ka) and the Aterian (103±3 ka) suggest an occupation hiatus between them (see Jacobs et al., 2011for detailed explanation). As will be discussed below, however, the inclusion of results from the other dating techniques does not support a significant interval between them. Nonetheless, and in spite of the methodological concerns mentioned above, this OSL chronology overall is in line with age estimates obtained previously for Mousterian assemblages at Contrebandiers Cave and other sites in the vicinity (Barton et al. 2009; Jacobs et al. 2012; Schwenninger et al. 2010).

PRELIMINARY TL AGES ON BURNED ARTIFACTS

TL dating determines the last time a mineral, including lithic artifacts, was heated to a high temperature (>300°C). While the dates reflect a phenomenon that took place after an artifact was made or used, the temporal association between artifact deposition and the time it was burned is usually good. Natural fires rarely occur in caves (see discussion in Alperson-Afil et al. 2007), and the heat from natural fire penetrates little into underlying sediment (Bellomo 1993) and is inadequate to heat shallowly buried lithics to the extent necessary for TL dating (Richter 2007). Because only a small fraction of the lithic material from Contrebandiers Cave shows traces of heating, the unlikely occurrence of natural fires in a cave can be excluded, and the heating, therefore, attributed to human activities. Thus, the association between the sample and the event dated is established and related to the anthropogenic combustion features recovered.

Fifty-four artifacts from Contrebandiers Cave that showed macroscopic traces of heating, such as potlid fractures, crazing, and reddening (Richter 2007), were submitted for TL analysis. Among these, 42 comprised suitable material and were large enough for TL analysis. Small pieces from the edges of these lithics, and subsequently from the sample's interior, were tested for their suitability (Table 4) and of these, 14 samples passed the test for having been completely zeroed in antiquity (Richter 2007). Preliminary results are reported here for nine of those samples that were collected from Layers IV-2, 5a, 5b, and 5c.

Multiple-aliquot additive regeneration (MAAR) protocols (Aitken 1985) were used to measure the paleodose by linear regression analysis, in conjunction with an additive approach to determine the α sensitivity for each individual sample. The ionizing radiation rates were determined by neutron activation analysis (NAA) to measure the internal dose rate and by insertion of γ-Al_2O_3:C dosimeters in the site to determine the external (γ and cosmic) dose rate contribution. The preliminary cosmic-ray dose rates were taken as measured by the dosimeters. The external dose rates for layers for which ages are reported here were based on between 2 and 8 dosimeters (see Table 4), with more dosimetry pending further analysis. So far, the external dose rates do not exhibit unusually large variation between layers or excavation areas, nor within layers. This is similar to what was observed for the *in situ* γ spectrometry measurements associated with the OSL ages.

The resulting preliminary TL ages (Table 5) show two apparent age clusters around 90 ka and 115 ka and an obvious outlier at 180 ka. The clusters, however, have no stratigraphic significance. Therefore, a simple average of the data from Layer IV-2 can provide a first preliminary age estimate of ~91 ka (MIS 5c) for the last heating for these samples. Similar preliminary results were obtained for Layers 5a and 5b, but more samples are needed to investigate any age relationships.

ESR DATING OF TOOTH ENAMEL

In tooth enamel, ESR dating determines the time at which the hydroxyapatite in tooth enamel began to accumulate dose from ionizing radiation. To calculate the accumulated dose, the ESR peak height was measured using the additive dose method. The internal dose rate was calculated from the concentrations of radioactive elements, principally U and its daughters in the sample itself, while the external dose rate was determined from the radioactive elements in the sediment by NAA. Since fossil teeth absorb U after deposition, the U uptake history must either be calculated through coupled ESR-^{230}Th/^{234}U dating (e.g., Falgueres et al. 2007) or modelled. The early uptake (EU) model, which assumes that the measured U accumulated soon after the tooth's deposition, provides a minimum age, unless U loss occurred recently. The linear uptake (LU) model, which assumes that the U accumulated at a constant rate throughout the tooth depositional history, gives a median age. The recent uptake (RU) model, which assumes that the U accu-

TABLE 3. OSL AGES FOR SEDIMENT SAMPLES FROM CONTREBANDIERS CAVE.

Sample code	Dose rates (Gy/ka)				D_e	Age[b,c]
	Beta	Gamma	Cosmic	Total[a]	(Gy)	(ka)
Aterian (Layer 4 in the CEA, Layers IV-2, V-1b, and V-2)						
SC30	0.56±0.03	0.34±0.03	0.13±0.01	1.06±0.07	—	Indeterminate
SC39	0.40±0.03	0.34±0.03	0.14±0.01	0.92±0.06	88.3±3.3	96±8
SC37	0.57±0.04	0.40±0.03	0.14±0.01	1.13±0.07	114.8±6.9	101±9
SC31	0.62±0.04	0.47±0.03	0.11±0.01	1.23±0.07	113.2±4.8	92±6
SC32	0.64±0.04	0.47±0.04	0.13±0.01	1.27±0.08	123.2±5.1	97±7
				Weighted mean		**96±4**
SC21	0.57±0.03	0.34±0.01	0.09±0.01	1.04±0.05	106.7±3.1	103±6
SC35	0.62±0.04	0.44±0.03	0.09±0.01	1.18±0.07	124.1±7.3	105±9
SC20	0.75±0.04	0.38±0.01	0.09±0.01	1.26±0.06	130.4±4.9	104±7
SC8	0.47±0.03	0.35±0.01	0.09±0.01	0.94±0.05	101.7±5.4	108±9
SC7	0.59±0.03	0.39±0.01	0.10±0.01	1.11±0.06	130.0±5.9	117±9
SC23	0.77±0.03	0.29±0.01	0.09±0.01	1.18±0.05	133.0±5.2	113±7
SC34	0.79±0.05	0.34±0.01	0.09±0.01	1.25±0.07	133.4±7.2	107±9
				Weighted mean		**107±4**
Mousterian (Layers 5a–c)						
SC16	0.52±0.03	0.29±0.01	0.11±0.01	0.95±0.04	112.6±5.9	118±9
SC15	0.53±0.03	0.30±0.01	0.11±0.01	0.97±0.05	112.6±5.0	116±8
SC19	0.40±0.02	0.25±0.01	0.09±0.01	0.78±0.04	97.4±4.5	124±9
SC14	0.43±0.02	0.31±0.01	0.11±0.01	0.88±0.04	99.6±2.9	113±7
SC6	0.55±0.04	0.36±0.01	0.10±0.01	1.04±0.06	118.5±3.9	114±8
SC13	0.52±0.03	0.33±0.01	0.10±0.01	0.99±0.05	110.4±3.4	112±7
SC1	0.48±0.03	0.34±0.01	0.10±0.01	0.95±0.06	108.6±3.5	115±8
SC28	0.57±0.04	0.45±0.01	0.09±0.01	1.14±0.06	130.5±5.6	115±8
SC2	0.66±0.04	0.45±0.02	0.10±0.01	1.24±0.07	1.40.8±6.3	114±8
				Weighted mean		**115±3**
Essentially archaeologically sterile (Layers 6a-b)						
SC18	0.61±0.04	0.38±0.01	0.09±0.01	1.11±0.06	126.4±3.9	114±6
SC29	0.70±0.04	0.39±0.02	0.09±0.01	1.21±0.07	131.9±4.6	109±7
SC12	0.59±0.03	0.35±0.01	0.10±0.01	1.08±0.05	127.8±5.8	119±8
SC3	0.62±0.04	0.43±0.02	0.10±0.01	1.19±0.07	126.6±6.1	107±8
				Weighted mean		**112±4**
Mousterian (Layer 6c)						
SC11	0.59±0.03	0.33±0.01	0.10±0.01	1.05±0.05	127.7±6.3	122±9
SC17	0.52±0.03	0.34±0.01	0.08±0.01	0.98±0.05	116.3±3.0	119±7
SC4	0.50±0.03	0.36±0.01	0.10±0.01	0.99±0.06	118.5±3.4	120±8
SC10	0.51±0.03	0.30±0.01	0.09±0.01	0.94±0.05	121.9±5.0	130±9
				Weighted mean		**122±5**
Beach sands (Layer 7 in Sector II)						
SC5	0.28±0.02	0.20±0.01	0.09±0.01	0.61±0.03	75.1±5.7	123±11
SC9	0.27±0.02	0.20±0.01	0.09±0.01	0.59±0.03	78.1±7.7	132±15
				Weighted mean		**126±9**

[a]Includes assumed internal alpha dose rate of 0.03±0.01 Gy/ka.

[b]Total uncertainty includes a systematic component of ±2.5% associated with laboratory beta-source calibration.

[c]Total uncertainty (expressed at 1σ) represents the quadratic sum of all random and systematic uncertainties.

TABLE 4. TESTS FOR TL DATING SUITABILITY.

Layer	Total	Too small	Tested samples	Not sufficiently heated	Passed 1st heating test	Sufficiently heated	Associated dosimeters
IV-1a	2	1	1	1		0	
IV-1b	1		1	1		0	2
IV-2	10	3	7		2	5	7
V-1b			0			0	3
V-2	3	1	2			2	5
4c			0			0	1
4d	11	1	10	5	4	1	7
5a	18	5	13	5	4	4	9
5b	3		3	1	1	1	2
5c	5	1	4	2	1	1	10
6a	1		1	1		0	
6c			0			0	4
CB2			0			0	2
CB3			0			0	2
CB4			0			0	2
for OSL			0			0	4
Total	**54**	**11**	**42**	**16**	**12**	**14**	**60**

mulated very late in its burial history, provides the maximum possible age (Ikeya 1982; Grün 2006; Grün et al. 1988; Blackwell et al. 1992). Isochron analyses can identify when multiple U uptake events or U loss has occurred (Blackwell et al. 2001, 2002; Blackwell 2006; Rink 1997). Significant U leaching from teeth rarely occurs in teeth younger than 200 ka, and is usually associated with diagenetic mineralization (Blackwell et al. 2000, 2002), something that did not occur in the teeth from Contrebandiers Cave. Isochron analyses have not been completed for the teeth reported here.

TABLE 5. PRELIMINARY TL DATING RESULTS.

Sample code	Archaeological Layer	Age (ka)
CONT-33	IV-2	87±11
CONT-34	IV-2	87±10
CONT-36	IV-2	115±11
CONT-37	IV-2	80±11
CONT-39	IV-2	85±11
CONT-53	IV-2	179±14
CONT-5	5a	89±16
CONT-28	5a	92±14
CONT-52	5b	89±14
CONT-50	5c	116±13

Since γ radiation penetrates ~30cm through most sediment and rock, β , ~3mm, and α, ~20μm, the sedimentary dose rates can vary over short distances in sites with thin or inhomogeneous layers (Brennan et al. 1997), such as at Contrebandiers Cave. Therefore, sedimentary dose rates are calculated by volumetrically averaging the dose rates from each layer and sedimentary component. Throughout the tooth's burial history, the sedimentary dose rate may not remain constant due either to changes in sedimentary water or radioactive element concentrations or varying cosmic dose rates due to changing burial depth.

At Contrebandiers Cave, 35 subsamples from nine teeth collected from Layers 5a and 5b in the CEA, and Layers IV-1b and V-1a (sectors IV and V, respectively—Table 6) were prepared using standard ESR dating protocols (Blackwell 1989). The enamel aliquots were irradiated using ^{60}Co γ radiation with doses ranging from 0 to 2560Gy at ~62–156mGy/s, and annealed at 90°C for 3 days to remove any short-lived interference signals (Skinner et al. 2000). Spectra for the aliquots were collected using a JEOL RE1X ESR spectrometer at 9.45GHz at 2.0mW, under 100kHz field

TABLE 6. ESR DATING SAMPLES FROM CONTREBANDIERS CAVE.

ESR Sample #	Excavation ID	Archaeological Layer	Grid Coordinates X (m)	Y (m)	Z (m)	Species	Tooth
PT47A	E22-237	IV-1b	5.934	22.237	1.469	*Bos primigenius*	deciduous premolar
PT47B	E22-237	IV-1b	5.934	22.237	1.469	*Bos primigenius*	deciduous premolar
PT46	E21-28	IV-1b	5.669	21.736	1.478	*Alcelaphus buselapus*	molar
AT1	L7-29	V-1a	12.636	7.951	1.197	Hippotragini	left deciduous molar 1/2
PT45	L8-103	V-1a	12.427	8.151	1.333	bovid/cervid	deciduous molar
FT95	L8-120	V-1a	12.544	8.689	1.362	*Equus*	upper molar
FT94	K8-87	V-1a	11.418	8.544	1.413	*Equus*	upper deciduous
FT93	G18-94	5a	7.931	18.544	1.836	*Equus*	upper molar
PT44	I15-334	5a	9.919	15.274	1.876	*Bos primigenius*	2nd molar
FT83	J18-65	5a	10.47	18.065	2.104	cervid/bovid	cheek - premolar?
FT84	J17-428	5b	10.789	17.791	2.22	cervid/bovid	cheek - premolar?

modulation 0.5mT. The spectra were scanned, centered at 360mT with an 8 min sweep time, with the receiver gain selected to maximize the signal intensity relative to the noise. To calculate the sedimentary dose rates, 26 samples of sedimentary components were analyzed for U, Th, and K using NAA. The accumulated doses and their uncertainties (Table 7) were calculated by plotting the peak heights against added dose, assuming an exponential growth curve. The ages, dose rates, and their uncertainties were calculated using Rosy (v. 1.4.2), which corrects for β and γ dose rate attenuation by water, enamel and dentine density and thicknesses, and tissue composition (Brennan et al. 1997). To measure the modern sedimentary water concentration, three representative sediment samples were dried and weighed. Although the modern water content averaged 10 wt%, 15±5% was assumed here since past climates have been wetter and sea levels have been higher in the past which would raise the time-averaged water concentration somewhat. Changing the water concentration by 5% only changes the ages by approximately 2–3%.

In all the enamel, the U concentrations measured <1ppm, while in the dentine, U concentrations ranged from ~1.7 to ~ 15.7ppm. Teeth from Sectors IV and V had lower dentinal U concentrations, averaging ~ 2–4ppm. In Layer 5 in the CEA, however, PT44 and FT84 had dentinal U concentrations >10ppm, while FT83 and FT93 had near 7ppm. All come from the deepest samples analyzed. Moreover, the U concentrations increase with depth. This may indicate a significant change in U uptake. In teeth exposed to seawater during burial, U concentrations tend to be higher (Blackwell et al. 2002). Therefore, these high U concentrations might indicate that these teeth have been exposed to saline groundwater, and in this case, because the teeth would absorb U at a different rate, the RU model might be a better uptake model for calculating the ages for those teeth. On the other hand, there is no geological evidence of a saline environment. Because the LU model gives median ages, and LU ages are usually more reliable for teeth in 50–500 ka range (see references in Blackwell 2006), the LU ages will be assumed to more accurately reflect the tooth's age, except for the four where a recent uptake model with U uptake rate parameter, p>2, more likely has occurred. Nonetheless, for all teeth except FT83 and FT84, the model ages do not differ significantly at the 95% confidence limit.

The sedimentary dose rates (see Table 7), which were determined with different methods, vary from as low as 200 to 750μGy/a for γ and β. To test the effects of changing $D_{ext}(t)$ on all the model ages for the teeth from Contrebandiers Cave, the ages for a typical subsample, FT95en4, were recalculated by varying the external dose rate from 0.0 to 2.0mGy/a, while all other variables were held constant (Figure 11). To calculate the age for FT95en4, the external dose rate was assumed to be 372±25μGy/a. At the 95% confidence limit (i.e., 2 σ errors), the LU ages for FT95en4 did not differ significantly from that reported in Table 7, until the external dose rate fell below 325μGy/a or exceeded 550μGy/a. Hence, minor inaccuracies or uncertainties in the external dose rates used here should not significantly affect the age accuracy, unless more than 75% *éboulis* filled the 30cm sphere around a tooth. Moreover, this means that minor differences in the cosmic dose rates selected for calculating the ages have a minor effect.

For Layer IV-1b, the average ESR ages are 53±5 ka for the LU model, but could be as old as ~65 ka when assuming RU (Table 8). For Layer V-1a, the teeth averaged 91±5 ka (LU), but could be as old as ~111 ka with the RU model. These data suggest that a significant hiatus in deposition occurred between the deposition of much of the cave and

TABLE 7. SEDIMENTARY DOSE RATES.

Sample		Context			Concentrations			External Dose Rates[1]	
Sample ID	N Samples	Archaeological Layer	Square	Depth (m)	[U] (ppm)	[Th] (ppm)	[K] (wt%)	From β Sources[2] (mGy/y)	From γ Sources[3] (mGy/y)
2008SMG8	1 (bulk sediment)	IV-1b	E22	1.469	1.1±0.02	2.32 ± 0.16	0.34 ± 0.01	0.098±0.011	0.274±0.019
2008SMG6	1 (bulk sediment)	IV-1b	E21	1.478	1.36±0.02	2.67±0.18	0.42±0.01	0.12±0.012	0.329±0.023
Layer V-1a	8	V-1a	L7-K8	1.197	1.59±0.2	3.74±0.28	0.48±0.17	0.164±0.036	0.41±0.049
2007.37a	1 (attached sediment)	4	J15	1.155	1.57±0.02	3.04±0.2	0.39±0.01	0.132±0.013	0.359±0.025
Layer 5a	6	5a	G18-J18	1.836	2.98±1.76	2.44±1.24	0.29±0.13	0.169±0.068	0.447±0.18
Layer 5a[4]	5	5a	G18-J18	1.836	2.28±0.48	2.85±0.78	0.3±0.15	0.15±0.035	0.4±0.07
2007.35a	1 (bulk sediment)	5b	J18	2.245	1.25±0.02	2.24±0.16	0.33±0.01	0.107±0.011	0.288±0.02
Layer 5c	4	5c	H18-J17	2.181	1.81±0.37	2.33±0.3	0.32±0.05	0.124±0.02	0.286±0.038
2008SMG27	1 (éboulis)		L8		1.28±0.02	0.67±0.07	0.01±0.01	0.069±0.006	0.175±0.013
2008SMG28	1 (éboulis)		L/K		1.07±0.02	See note 5	0.12±0.01	0.004±0.002	0.009±0.003
2008SMG24	1 (cemented sediment)	5b			1.42±0.02	2.09±0.15	0.32±0.01	0.109±0.013	0.29±0.02
2008SMG25	1 (bone)	5b			7.25±0.02	See note 5	0.32±0.01	0.306±0.061	0.753±0.05
Detection limits[6]					~ 0.01–0.02	~ 0.2–0.4	~ 0.001–0.002		

[1]Analyzed by NAA, and calculated with sedimentary water concentration, W_{sed}= 15.±5.wt%

[2]Calculated with the dentine thickness for the closest tooth enamel water concentration, W_{en}=2.±2.wt%
enamel density, ρ_{en}=2.95±0.02g/cm^3
sedimentary density, ρ_{sed}=2.66±0.02g/cm^3

[3]Calculated using cosmic dose rate, $D_{cos}(t)$=0.000±0.000mGy/y

[4]Means without FT93sed, which may have contained dentine flaked from the tooth.

[5]Value below detection limit: assumed to be 0.0±0.0 for calculations.

[6]Typical NAA detection limits depend on the sample mass and mineralogy.

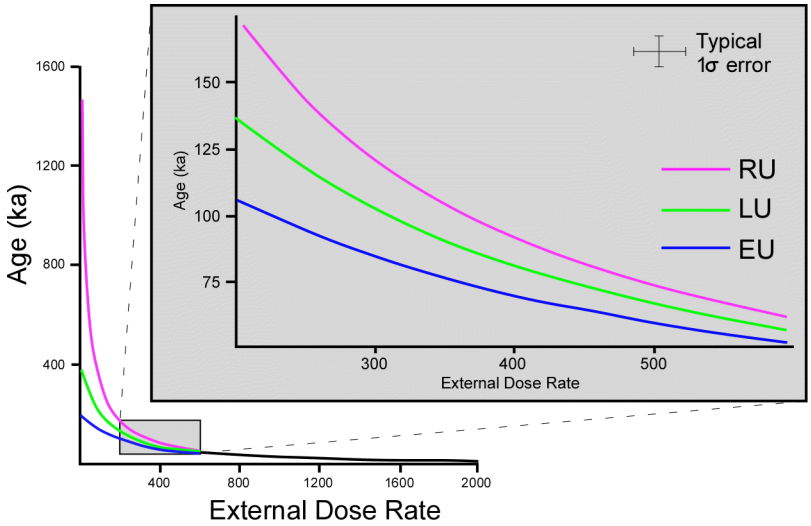

Figure 11. ESR ages vs. external dose rates, Dext(t), for FT95en4. Initially, Dext(t) equaled 372 ±25 μGy/y. The ages decreased as Dext(t) increased, as do the differences between the model ages. At the 95% confidence limit (2σ errors), significant differences in the calculated LU age occurred, if $D_{ext}(t)$ either fell below 325 μGy/y or exceeded 550 μGy/y. For the EU age, significant changes occurred when $D_{ext}(t)$ fell below 300 μGy/y or surpassed 480 μGy/y. For the RU age, significant changes only occurred when $D_{ext}(t)$ dropped below 330 μGy/y or exceeded 425 μGy/y.

Layer IV-1b. As noted above, an erosional unconformity occurs beneath Layer IV-1b. For Layer 5, the teeth average 94±8 ka assuming recent uptake (RU), with individual ages ranging from ~90 to 118 ka.

Although several more teeth need to be dated from each layer to ensure that reworking has not occurred, and more layers remain to be dated, these first ESR ages from Contrebandiers Cave indicate that the cave was inhabited during MIS 5 and early MIS 3.

TABLE 8. MEAN ESR AGES.

Tooth	N Samples	Archaeological Layer	U Concentrations Enamel	U Concentrations Dentine	Accumulated Dose (Gy)	ESR Ages[1] EU ka ±1σ	ESR Ages[1] LU ka ±1σ	ESR Ages[1] RU ka ±1σ
PT47A	2	IV-1b	0.39±0.02	3.98±0.42	18.28±1.62	40.6±4.7	54.1±7.2	64.9±9.4
PT47B	2	IV-1b	0.51±0.22	1.72±1.03	18.33±0.94	38.1±2.6	48.2±3.4	59.7±4.6
PT46	2	IV-1b	0.26±0.02	3.82±0.75	21.36±0.89	44.3±2.8	56.3±3.9	70.6±5.3
Weighted mean		**IV-1b**				**41.3±4.8**	**52.5±5.4**	**65.2±6.3**
AT1	2	V-1a	0.07±0.07	3.82±0.46	47.27±1.26	80±4.2	109.2±6.6	132.2±9.1
PT45	1	V-1a	0.1±0.02	3.44±0.38	57.99±1.35	82.8±7.2	105.3±11	120.9±14.4
FT94	6	V-1a	0.18±0.06	4.35±0.28	41.75±0.49	67.9±1.6	86.3±2.1	107.8±3.1
FT95	4	V-1a	0.06±0.04	3.33±0.2	41.76±0.49	80.1±2.4	93.9±3	107.7±3.9
Weighted mean		**V-1a**				**73.8±7.3**	**91.4±7.7**	**110.5±8.3**
FT93	4	5a	0.3±0.07	6.74±1.2	53.58±1.77	61±4.8	83.6±7.9	117.4±17.9
FT83	1	5a	0.27±0.02	7.13±0.31	46.7±2.25	64.5±7.7	88.7±6.2	123.2±9.7
PT44	11	5a	0.69±0.18	13.75±2.24	42.87±0.31	43.7±0.7	65.3±1.1	89.7±1.9
FT84	1	5b	0.26±0.02	15.7±0.65	51.03±1.05	47.1±2.3	70.4±3.5	114.8±7.4
Weighted mean		**5a/b**				**45±5.7**	**67.4±6**	**94.4±7.8**

[1]Abbreviations: EU=assuming early U uptake, p=-1.
LU=assuming linear (continuous) U uptake, p=0.
RU=assuming recent U uptake, p=2.

Calculated using α efficiency factor, k_α=0.15±0.02
initial U activity ratio, $(^{234}U/^{238}U)_0$=1.20±0.20
tooth density, ρ_{mol}=2.96±0.02g/cm^3
radon loss from the shells, Rn_{mol}=0.±0.vol%
sediment density, ρ_{sed}=2.66±0.02g/cm^3
cosmic dose rate, $D_{cos}(t)$=0.0±0.0μGy/a
sedimentary water concentration, W_{sed}= 15.0±5.00wt%

SUMMARY OF THE ABSOLUTE CHRONOLOGY

For true confidence in a site's dating, at least two independent methods should be used in order to avoid systematic errors that could skew the results for any one method. Here, we summarize the results from the three methods used at Contrebandiers Cave. While minor differences among the ages from the different methods may arise from minor variability in the sedimentary mineralogy across the layers and from layer to layer, the agreement here is striking. For each layer, the ages from the three methods agree well within statistical uncertainties (2σ uncertainty=95% confidence interval).

In Sector IV, there is an erosional unconformity that, in places dips at almost 35° and separates Layers IV-1b (Iberomaurusian) and IV-2 (Aterian). Thus far, only ESR ages were used to date Layer IV-1b, though the TL and OSL ages for Layer IV-2 agree well and are stratigraphically consistent with the ESR dates for Layer IV-1b. Therefore, these dates suggest that samples from Layer IV-2 were deposited during MIS 5c, while those from Layer IV-1b were deposited during early MIS 3, after an erosional event that may have truncated Layer IV-2 deposits. Additional dates from this layer, and from other Iberomaurusian assemblages, will be needed to confirm these ages.

For Layers 4–7 within the CEA, the weighted means of all three methods yield consistent results, and the ESR and TL ages overlap with the OSL ages within the 1σ uncertainties (Figure 12). These ages indicate that Layers 4 through 7 were all deposited during early to mid MIS 5—Layers 7 and 6c probably formed during MIS 5e, Layer 5 within MIS 5c and 5d, and Layer 4 probably during MIS 5c. However, if one considers the ages with their associated uncertainties, then Layer 4, with tanged pieces, cannot be statistically distinguished from the lower layers without such pieces by the combined current age estimates provided by the three methods. When the ages of all of the assemblages containing tanged pieces (IV-2, 4, V-1, and V-2) are compared with those that do not (Layers 5–6), the overlap is quite clear. As summarized in Dibble et al. (submitted), even when examined from a regional perspective, a chronological distinction between these two industrial variants is not apparent.

THE LITHIC INDUSTRIES FROM CONTREBANDIERS CAVE

THE ATERIAN AND MOUSTERIAN LITHIC ASSEMBLAGES

The 2007–2010 excavations recovered over 2,700 lithic objects from the Aterian and Mousterian layers (Table 9, Figures 13–25). Although Roche considered all of the pre-Iberomaurusian deposits to be Aterian, the absence of tanged pieces in Roche's collections in the lower layers had already led some researchers to question the attribution of these layers as Aterian (Bouzouggar 1997a). In his overview of the lithic material from one of the lower layers (his Layer VII, which corresponds to our Layer 5), Bouzouggar (1997b) mentioned a very low percentage of Aterian elements, but without elaborating on those elements (but see Bouzouggar 1997b: 204: Fig. 137). His conclusion was that due to the non-diagnostic lithic typology it was difficult to ascertain the cultural attribution of this layer (Bouzouggar 1997b: 198). Unquestionable attribution of all of the pre-Iberomaurusian contexts in the cave to the Aterian is not supported by our own work either, in that tanged pieces are found in Layers 4a–4e, IV-2, and V-1a, V-1b, and V-2, and there is an absence of them in Layers 5a–5d and 6a–6c. It should be noted here that the three stemmed pieces from V-2 occurred near the top of that layer, and therefore there is some possibility that they may be intrusive. But given that the presence or absence of tanged pieces is the criterion for attributing assemblages to either the Aterian or Mousterian, respectively, it is now more likely that Contrebandiers Cave includes examples of both assemblage groups. As discussed in detail by Dibble et al. (submitted), the distinction between these two assemblage groups is based entirely on the presence or absence of stemmed or bifacial pieces, but in virtually every other respect, including chronology, they are indistinguishable. While that study concludes that they are the same industry, and part of the pan-African Middle Stone Age (rather than as part of the Eurasian Middle Paleolithic), in this paper we will continue to refer to them by their traditional labels in order to provide continuity with the bulk of the published studies on these Maghrebian industries.

Throughout the Aterian and Mousterian assemblages, tool production is relatively low. Among the scrapers (Table 10), simple single scrapers tend to dominate; the more reduced types are represented by a few double and convergent forms, while transverse scrapers are absent. Notches and denticulates represent the bulk of the other retouched types. Stemmed pieces, both "points" and other stemmed types, are rare, though present, in most of the assemblages except for the lower layers (5–6) of the CEA. So-called "Upper Paleolithic" types and truncated-faceted pieces are also present, but relatively rare.

In terms of technology, the percent of Levallois technique varies from zero to a high of 12.5% in Layer 4B, but the overall average is quite low at 3.3% (Table 11). Among the cores (Table 12) there is a very low representation of Levallois, though some of the single-surface and the one Mousterian disc from Layer 5B may have yielded some Levallois flakes during their reduction. These core types are all fairly small, with an average length of just 4.29cm. There are some Kombewa flakes and cores, which together with the truncated-faceted pieces and small cores suggests some production of small flakes (Dibble and McPherron 2006). Morphological blades (whose lengths are greater than twice their widths) are present, though there are no blade cores and extremely rare crested blades. There are also a few *éclats débordants.* The most prevalent recognized form is naturally-backed pieces, however. Plain platforms are the most common throughout the assemblages, followed by cortical platforms; dihedral and faceted platforms are much more rare (Figure 26).

The dimensions of various lithic classes are remarkably

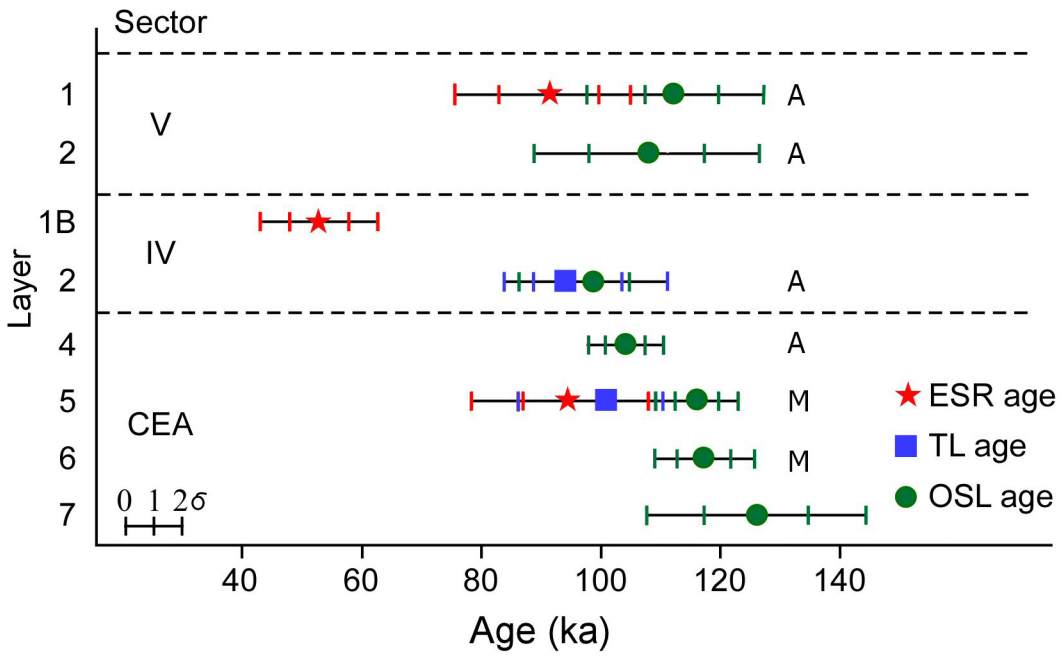

Figure 12. Summary of Weighted Mean Ages. As the different sectors have not been correlated stratigraphically, the ages are shown for each sector individually. However, the lithics associated with each layer are indicated: A—Aterian; M—Mousterian. Within the Central Excavation Area (CEA), the ages derived from all methods agree well within their uncertainties at the 1σ level. For Layer 4 in the CEA, Layer V-1 in Sector 5, and Layer IV-2 in Sector 4, all their ages agree within their associated 2σ uncertainties, suggesting that they are contemporaneous and correlate with MIS 5d-5b. Considering the associated uncertainties, the ages for the layers containing Aterian vs. Mousterian assemblages cannot be distinguished. Ages for Layers IV-1b and IV-2 are stratigraphically consistent, but a protracted erosional hiatus occurred between them.

TABLE 9. BREAKDOWN OF LITHICS BY MAJOR ARTIFACT CLASS AND LAYER.

Level	Flakes	Tools	Flake Fragments	Tool Fragments	Cores	Core Fragments	Shatter	Manuports & Hammerstones	Artifacts per m3
4A	30	2	10	4	5	1	13	0	232.1
4B	29	6	4	1	3	1	9	1	482.1
4C	55	9	14	3	6	1	12	1	236.5
4D	111	27	25	2	3	7	48	4	157.4
4E	1	1	0	1	0	0	2	0	238.1
5A	136	8	43	6	5	5	126	2	492.6
5B	133	7	45	5	9	4	65	2	203.0
5C	278	8	84	8	10	6	88	1	170.8
5D	6	0	0	0	2	0	1	0	91.8
6A	9	1	0	0	2	1	1	0	9.3
6B	6	1	2	0	1	1	2	1	16.4
6C	34	6	6	1	2	0	6	0	33.0
IV-2	366	42	107	21	20	10	121	2	582.4
V-1A	31	9	10	3	14	6	8	20	86.4
V-1B	41	5	4	0	14	9	7	20	108.2
V-2	118	15	34	3	19	11	48	5	133.4

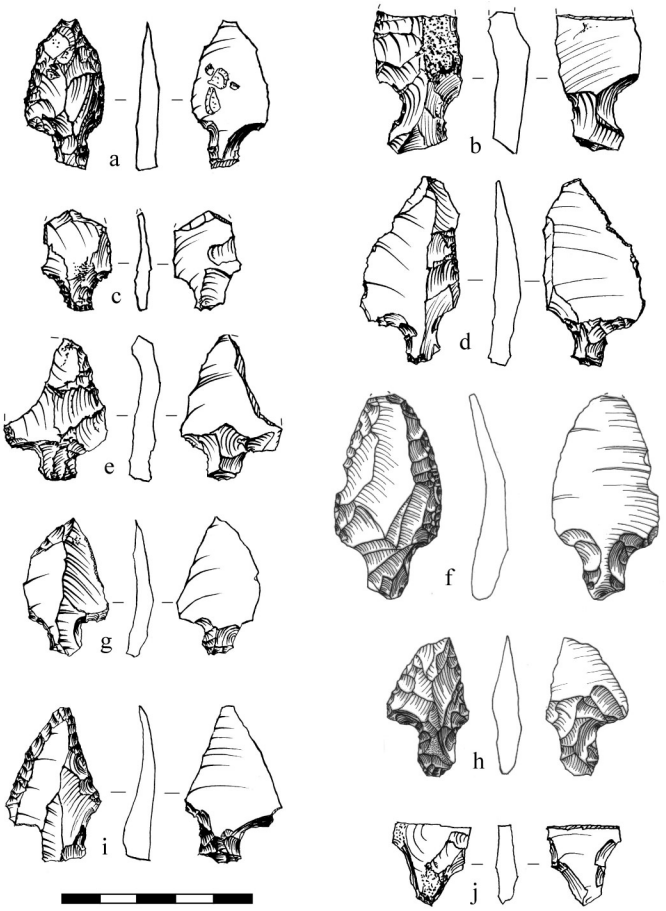

Figure 13. Tanged pieces from the Aterian assemblages.

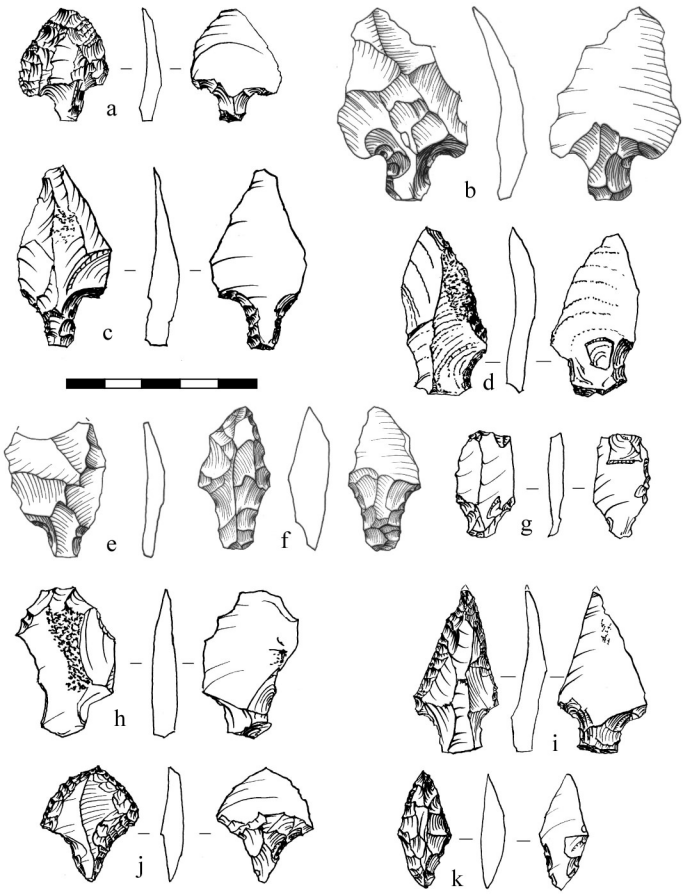

Figure 14. Tanged pieces from the Aterian assemblages.

uniform across the major stratigraphic units (Figure 27), with only unretouched flakes being statistically different among the various assemblages (F=9.99, df=3, p=0.000002).

Although detailed studies of the raw materials represented among these assemblages has not been completed, it is already clear that a large variety of minerals (quartz) and rocks were used, including sedimentary (limestone, calcarenite, sandstone, flint, and chalcedony), metamorphic (quartzite), and igneous (lava, basalt, and diorite) types (Figure 28). There is also a great deal of variability in cortex, indicating that some materials were collected from primary deposits and others from either alluvial or coastal deposits. Flint and chalcedony, in particular, exhibit a great deal of variability in terms of color and texture, suggesting multiple origins for these rocks.

The predominant raw materials of retouched lithics are chalcedony, flint, and quartzite, although they are used differently. First, while most of the unretouched flakes, cores, and notched tools are more or less equally found on the finer grained materials (flint and chalcedony), as well as the coarser ones (quartzite), in all of the layers the ratio of retouched to unretouched objects is higher with chalcedony and flint than it is with quartzite (Table 13), indicating either the preference for chalcedony and fine-grained flint as opposed to quartzite, or/and somewhat constrained supply of the former raw materials over the later. In addition, the fact that scrapers and stemmed pieces are predominantly associated with the fine grained materials suggests a preference for these raw materials on these kinds of tools (Figure 29). Levallois technology follows this pattern to a degree, though it is less pronounced. It is also clear that objects made on the finer grained materials tend to be smaller than those made on quartzite (Figure 30). Whether the difference in lithic artifacts size made on different raw material reflects distinct sizes and shapes of the original nodules or greater reduction of fine grained materials as opposed to coarser ones is unknown at this time.

In addition, the number of objects made on different raw materials is not the same throughout all the layers in the cave (see Table 13). Material from Layers 5 and V-1 has a lower representation of chalcedony and flint as compared to other layers, while Layers 5 and V-2 have a higher representation of the locally available quartz and limestone.

Overall, the density of lithic artifacts is extremely low throughout all of the excavated layers (see Table 9). The number of blanks (complete or proximal flakes, retouched or not) per 7-liter bucket of excavated sediment rarely exceeds 2, and in most layers is less than 1 (Figure 31). Likewise, the number of complete or proximal flakes recovered in the coarse screen fraction (1cm) and smaller than the 2.5cm cutoff is low. This raises the possibility that smaller lithic objects were removed from the site through natural processes, and there are pronounced inclinations of the objects, both from Sector IV (oriented toward the back of

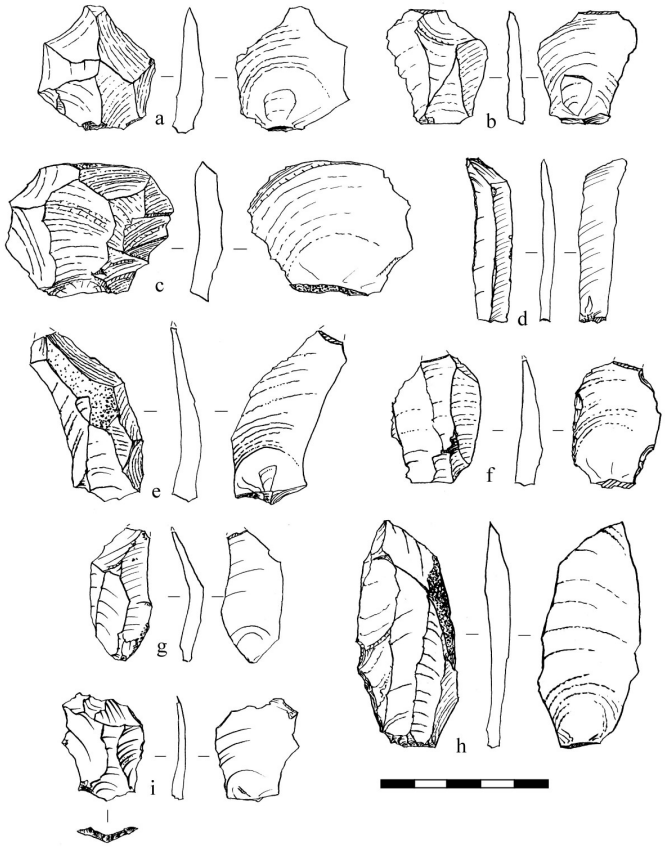

Figure 15. Levallois flakes from the Aterian assemblages.

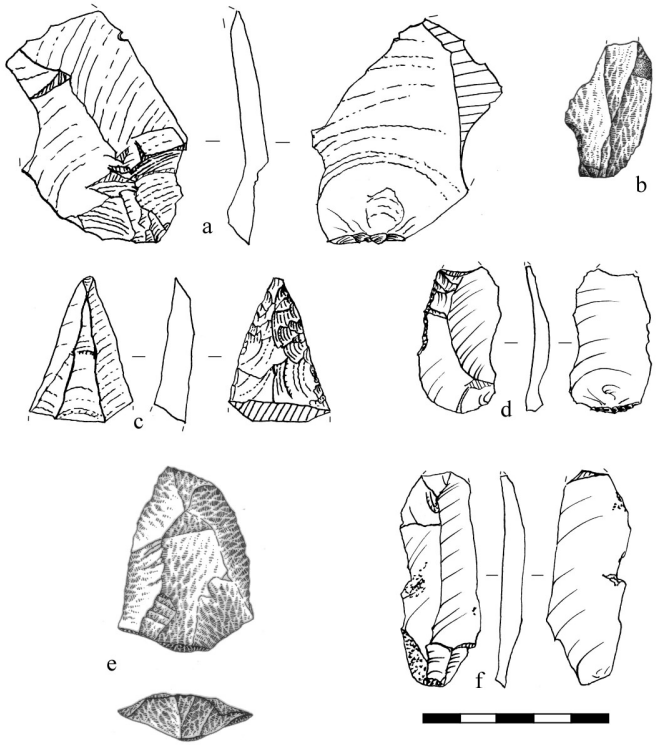

Figure 16. Levallois flakes from the Aterian assemblages.

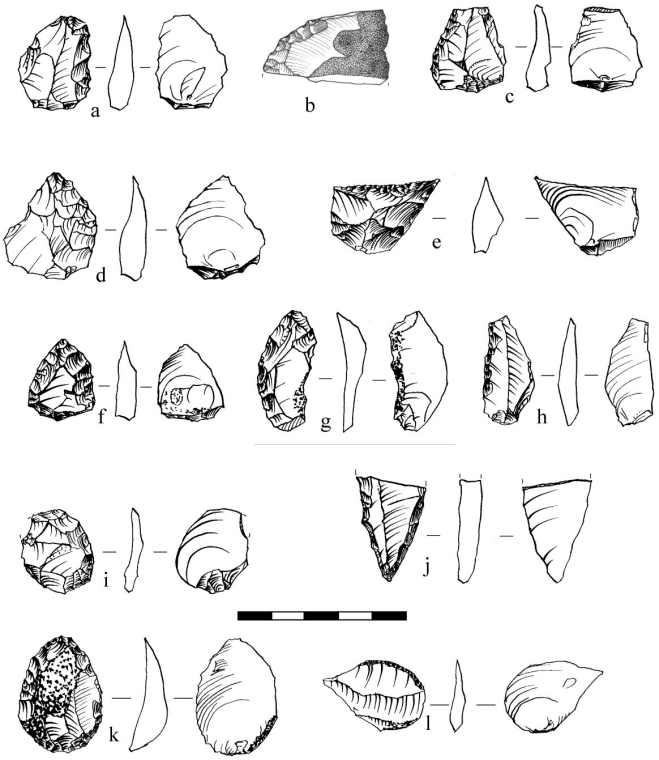

Figure 17. Scrapers from the Aterian assemblages.

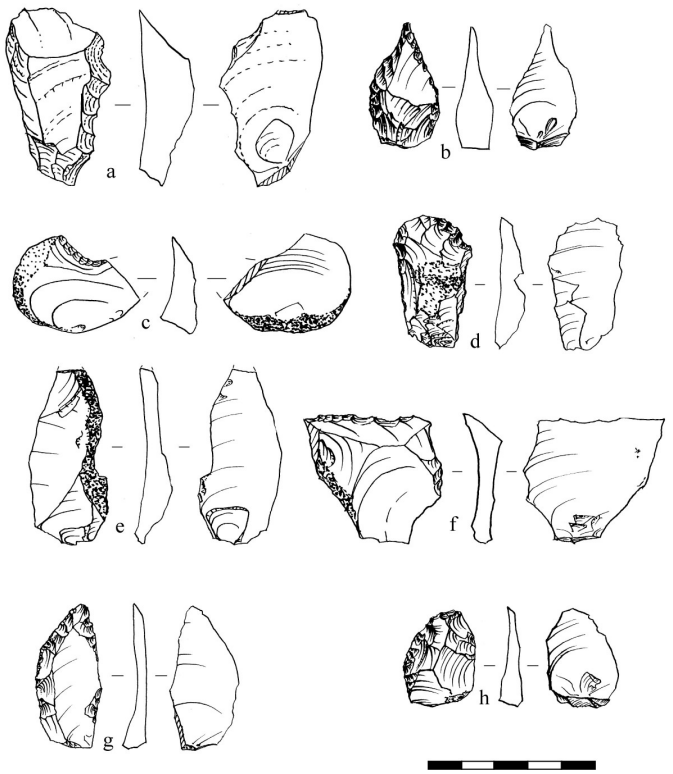

Figure 18. Retouched tools from the Aterian assemblages. a: denticulate; b: borer; c: notch; d: endscraper; e, f: naturally-backed knives; g: convergent scraper; h: double scraper.

TABLE 10. RAW COUNTS OF BORDIAN TYPES BY LAYER.*

TYPE	IV-2	4A	4B	4C	4D	4E	5A	5B	5C	5D	6A	6B	6C	V-1A	V-1B	V-2
Typical Levallois flake	13	-	2	1	1	-	-	-	-	-	1	-	-	2	-	1
Atypical Levallois flake	5	1	1	2	1	-	1	-	5	-	-	-	4	-	-	-
Pseudo-Levallois point	3	-	-	-	-	-	-	-	1	-	-	-	1	-	-	1
Mousterian point	1	-	-	1	-	-	-	-	-	-	-	-	-	-	-	-
Straight single scraper	6	-	2	3	-	-	-	2	1	-	-	-	-	2	-	1
Convex single scraper	11	2	-	-	1	-	1	2	-	-	-	-	1	-	-	1
Concave single scraper	2	-	-	-	1	-	-	-	1	-	-	-	-	-	-	-
Double straight-convex scraper	2	-	-	1	-	-	-	-	-	-	-	-	-	-	-	-
Double Convex scraper	2	-	-	-	1	-	-	-	-	-	-	-	-	-	-	-
Double Concave-convex scraper	1	-	-	-	-	-	-	-	-	-	-	-	-	-	-	-
Straight convergent scraper	1	-	-	-	-	-	-	-	-	-	-	-	-	-	-	-
Convex convergent scraper	3	1	-	-	1	-	-	-	-	-	-	-	-	-	-	-
Dejete scraper	1	-	-	1	-	-	-	-	-	-	-	-	-	-	-	-
Scraper on interior	-	-	-	-	-	1	-	-	-	-	-	-	-	1	-	-
Typical endscraper	2	-	-	1	1	-	-	-	-	-	-	-	1	-	-	-
Atypical endscraper	-	-	-	-	-	-	-	-	1	-	-	-	-	-	-	-
Typical burin	-	-	-	1	-	-	-	-	-	-	-	-	-	-	-	-
Typical percoir	-	-	-	-	1	-	1	-	-	-	-	-	-	-	-	-
Typical backed knife	-	-	-	-	-	-	-	-	-	-	-	-	1	-	-	-
Naturally-backed knife	7	-	-	2	3	-	1	2	3	-	1	-	1	1	3	2
Raclette	-	-	-	-	-	-	-	-	-	-	-	1	-	-	-	-
Truncation	-	-	-	-	2	-	-	-	-	-	-	-	-	-	-	-
Notch	4	1	-	-	3	-	7	7	8	-	-	-	1	1	1	6
Denticulate	7	1	-	1	7	-	5	1	7	1	1	-	3	4	2	4
Bec burinante alterne	-	-	-	-	-	-	-	-	-	-	-	-	-	-	-	1
Retouch on interior	-	-	-	-	2	-	1	-	-	-	-	-	1	-	-	-
Abrupt/alternating retouch	10	1	1	-	1	-	3	1	3	-	-	-	1	2	2	2
Bifacial retouch	1	-	-	-	-	-	-	-	-	-	-	-	-	-	-	-
End-notched flake	3	-	1	-	-	-	-	-	-	-	-	-	-	1	-	-
Tanged point	4	-	1	2	1	-	-	-	-	-	-	-	-	-	1	2
Tanged tool	6	-	2	1	2	-	-	-	-	-	-	-	-	2	-	1
Chopper	-	1	-	1	-	-	-	-	1	-	-	-	-	3	1	2
Chopping-tool	-	-	-	-	-	-	-	-	-	-	-	-	-	4	5	1
Divers	4	1	1	-	-	-	-	-	-	-	-	-	-	-	-	1
Bifacial foliates	1	-	-	-	-	-	-	-	-	-	-	-	-	-	-	-
Truncated-Faceted piece	4	-	-	-	1	-	-	1	1	-	-	-	-	1	1	1

*(Bordes 1961; Debénath and Dibble 1994).

the cave) and in the CEA (oriented somewhat toward the mouth of the cave). However, and contrary to this interpretation, there is little indication of edge damage (Figure 32), which would be expected if the objects had moved significantly. Thus, it is more likely that the low artifact densities are reflecting more ephemeral occupations than significant post-depositional/erosional constrains.

Studies of cortex can yield some information concerning how materials were both imported in, and exported from, the site. Overall, for the five layers studied so far

TABLE 11. SUMMARY OF LITHIC MATERIALS AND VARIOUS TYPOLOGICAL AND TECHNOLOGICAL INDICES.*

	IV-2	4A	4B	4C	4D	4E	5A	5B	5C	5D	6A	6B	6C	V-1A	V-1B	V-2
Real Count:	100	9	11	18	29	1	20	15	31	1	3	1	15	23	15	26
Essential Count	61	7	7	13	21	1	14	12	19	1	1	1	7	18	10	20
Comp + Prox Flakes	366	30	29	55	111	1	136	133	278	6	9	6	34	31	41	118
Frags + Shatter	228	23	13	26	73	2	169	110	172	1	1	4	12	18	11	82
Cores + Core frags	30	6	4	7	10	-	10	13	16	2	3	2	2	20	23	30
Manuports + Hammerstones	2	-	1	1	4	-	2	2	1	-	-	1	-	20	20	5
TYPOLOGICAL INDICES																
Real Count																
ILty	18.0	11.1	27.3	16.7	6.9	0	5.0	0	16.1	0	33.3	0	26.7	8.7	0	3.8
IR	29.0	33.3	18.2	27.8	13.8	100	5.0	26.7	6.5	0	0	0	6.7	13.0	0	7.7
IAU	0	0	0	0	0	0	0	0	0	0	0	0	0.1	0	0	0
I	18.0	11.1	27.3	16.7	6.9	0	5.0	0	16.1	0	33.3	0	26.7	8.7	0	3.8
II	33.0	33.3	18.2	33.3	13.8	100	5.0	26.7	9.7	0	0	0	13.3	13.0	0	11.5
III	2.0	0	0	11.1	13.8	0	5.0	0	3.2	0	0	0	13.3	0	0	0
IV	7.0	11.1	0	5.6	24.1	0	25.0	6.7	22.6	100	33.3	0	20.0	17.4	13.3	15.4
Essential Count																
IR	47.5	42.9	28.6	38.5	19.0	100	7.1	33.3	10.5	0	0	0	14.3	16.7	0	10.0
IAU	0	0	0	0	0	0	0	0	0	0	0	0	0.1	0.0	0	0
II	54.1	42.9	28.6	46.2	19.0	100	7.1	33.3	15.8	0	0	0	28.6	16.7	0	15.0
III	3.3	0	0	15.4	19.0	0	7.1	0	5.3	0	0	0	28.6	0	0	0
IV	11.5	14.3	0	7.7	33.3	0	35.7	8.3	36.8	100	100	0	42.9	22.2	20.0	20.0
TECHNOLOGICAL INDICES																
IL	5.2	4.3	12.5	7.4	3.0	0	0.6	0.5	1.4	0	8.3	9.1	10.9	2.7	0	3.3
IF	16.9	22.2	25.0	15.2	9.1	0	8.0	7.5	7.9	0	20.0	16.7	15.8	31.3	21.6	4.8
IFS	8.2	14.8	20.8	8.7	5.5	0	5.3	5.0	3.5	0	10.0	16.7	10.5	15.6	16.2	1.6
Ilam	3.4	11.1	12.9	15.9	3.0	0	2.1	2.4	1.9	0	0	0	0	7.0	4.4	4.8
Débordant	4.1	0	6.5	4.8	4.5	0	3.6	2.4	1.9	0	0	0	8.3	0	8.9	3.2
Natural Back	6.0	8.3	3.2	4.8	3.8	0	7.1	9.4	5.3	0	12.5	0	8.3	7.0	6.7	6.5

*For definitions of the indices, see Debénath and Dibble (1994).

TABLE 12. BASIC CORE TYPES BY LAYER.

Archaeological Layer	Single Surface	Levallois	Mousterian Disc	Pyramidal	Prismatic	Kombewa	Chopper / Chopping Tool	Globular	Inform	"Tested"
IV-2	8	-	-	-	1	1	1	-	12	3
4A	1	-	-	-	-	-	1	-	-	1
4B	1	-	-	-	-	-	-	-	2	-
4C	4	1	-	-	-	-	-	-	-	2
4D	1	-	-	-	-	-	-	-	3	1
5A	2	-	-	-	-	1	-	-	3	-
5B	2	-	-	-	-	1	-	-	7	2
5C	2	-	-	1	-	1	-	-	6	3
5D	-	-	-	-	-	1	-	-	1	-
6A	2	-	-	-	-	-	-	-	-	-
6B	-	-	1	-	-	-	-	-	1	-
6C	-	-	-	-	-	1	-	-	1	-
V-1A	1	-	-	-	-	-	-	3	10	3
V-1B	2	1	-	-	-	-	2	1	14	1
V-2	7	1	-	-	-	-	-	2	11	6

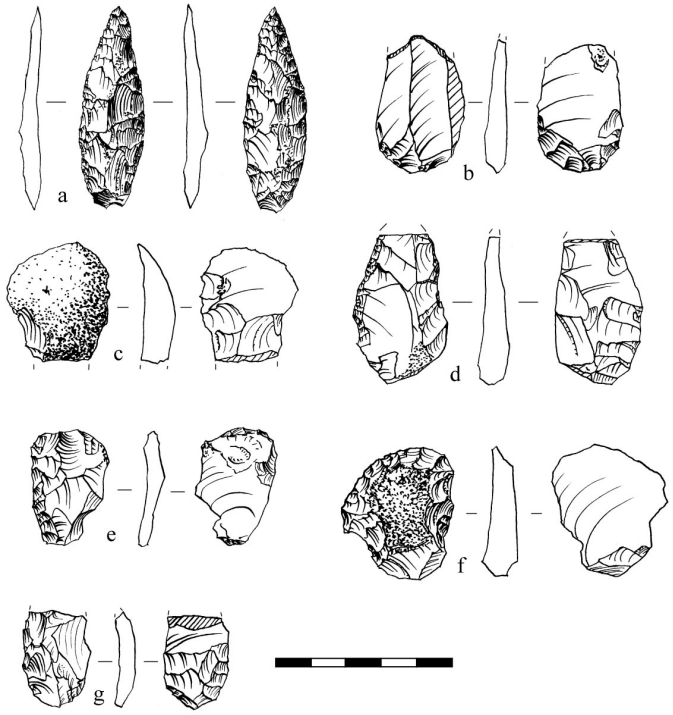

Figure 19. Retouched tools from the Aterian assemblages. a: bi-facial foliate; b, c: truncated-faceted pieces; d: truncated-faceted piece on a scraper; e, f: scrapers with tang(?); g: flake with bifacial retouch.

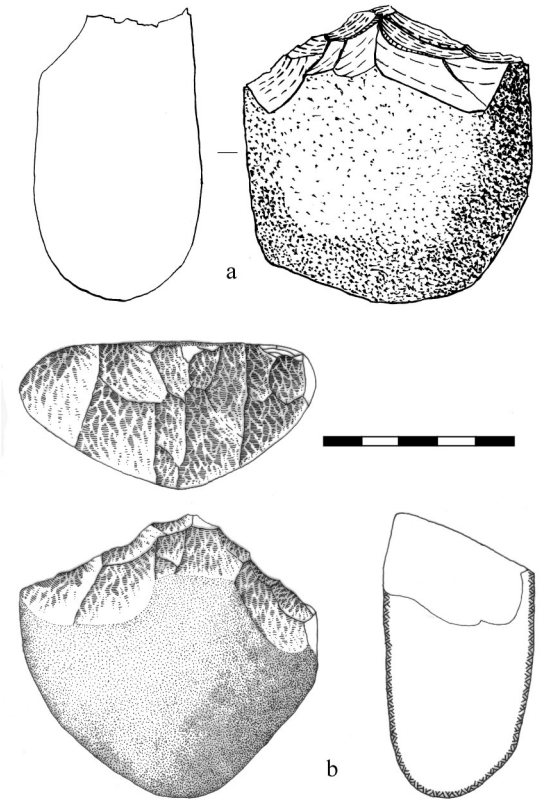

Figure 20. Core tools from the Aterian assemblages.

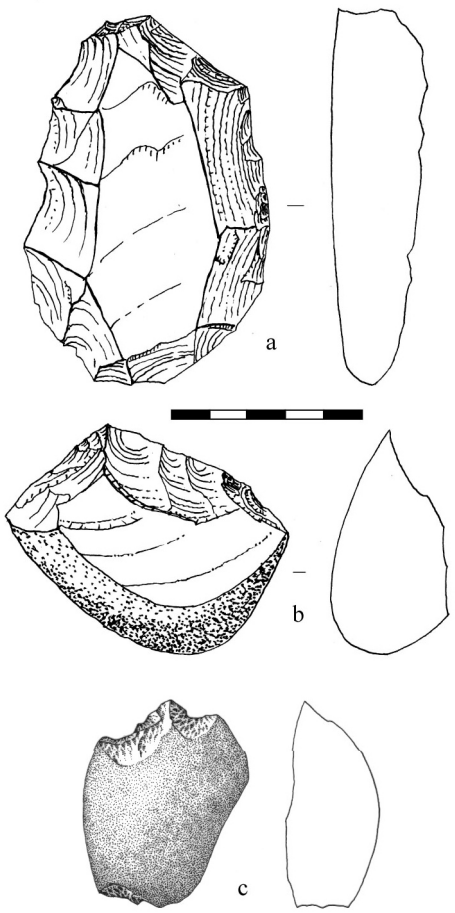

Figure 21. Core tools from the Aterian assemblages.

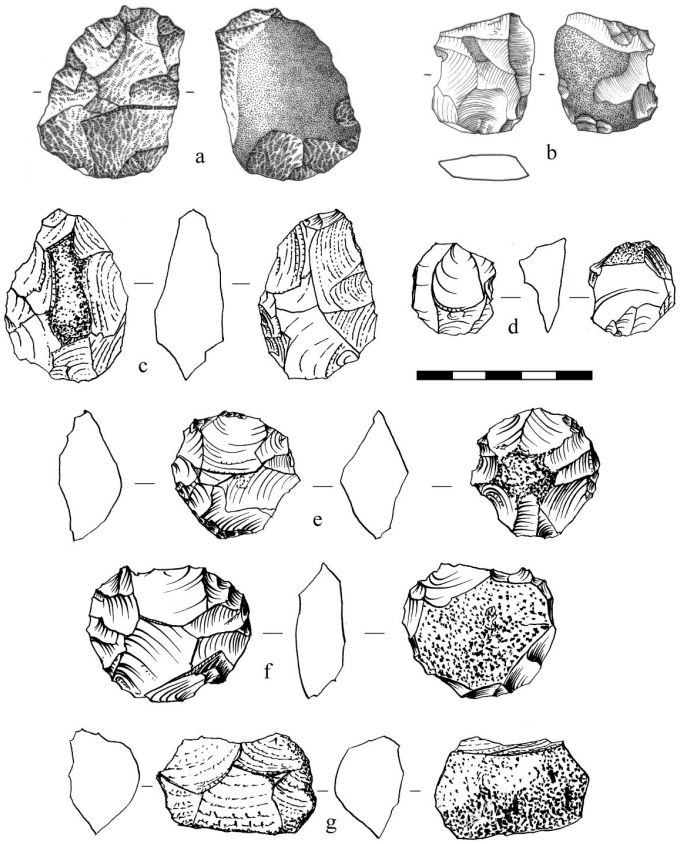

Figure 22. Cores from the Aterian assemblages.

TABLE 13. BREAKDOWN OF RAW MATERIAL INPUT (counts in percentages) AND RETOUCHED LITHICS PER BLANKS RATIO BY LAYERS.

Raw material makeup (%)					
Layer	**Chalcedony and Flint**	**Quartzite**	**Quartz**	**Limestone**	**Other**
IV-2	36	48	5	4	7
4 (all)	38	45	7	1	9
5 (all)	21	38	13	10	18
6 (all)	39	48	3	3	7
V-1 (all)	20	63	6	1	10
V-2	32	35	12	1	20
Retouched artifacts / Blanks					
Layer	**Chalcedony and Flint**	**Quartzite**	**Quartz**	**Limestone**	**Other**
IV-2	0.36	0.01	N/A	N/A	N/A
4 (all)	0.42	0.07	N/A	N/A	0.05*
5 (all)	0.16	0.02	0.02	0.01*	0.01*
6 (all)	0.21	0.13	N/A	N/A	0.5*
V-1 (all)	0.42	0.12	0.25*	N/A	0.5*
V-2	0.19	0.1	0.06*	N/A	0.11

*=one retouched artifact.

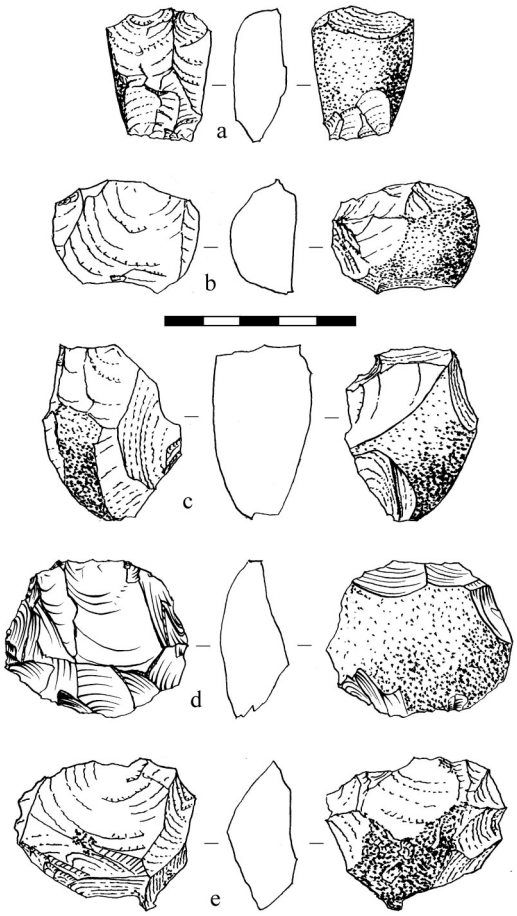

Figure 23. Cores from the Aterian assemblages.

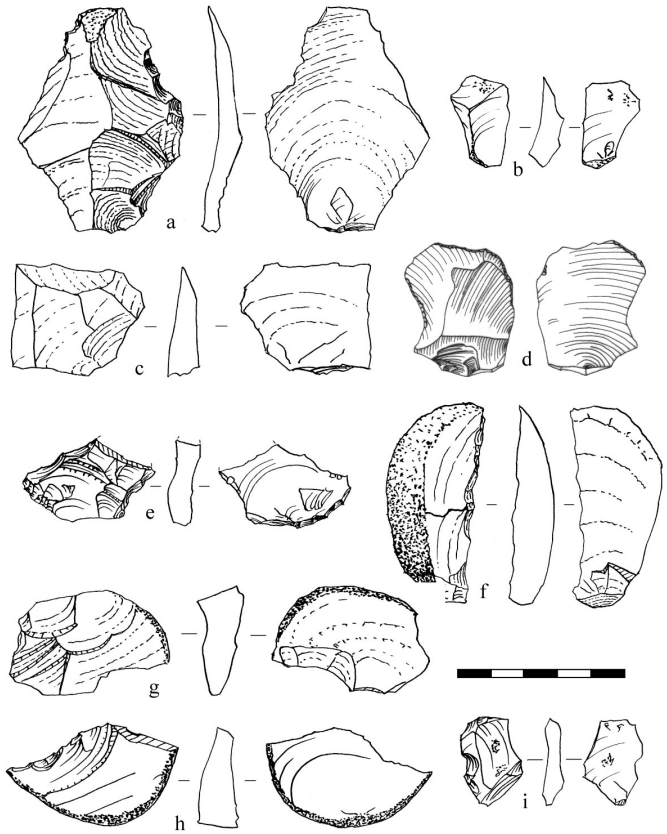

Figure 24. Flakes and retouched tools from the Mousterian (non-tanged) assemblages. a-d: Levallois flakes; e, g-i: notches; f: denticulate.

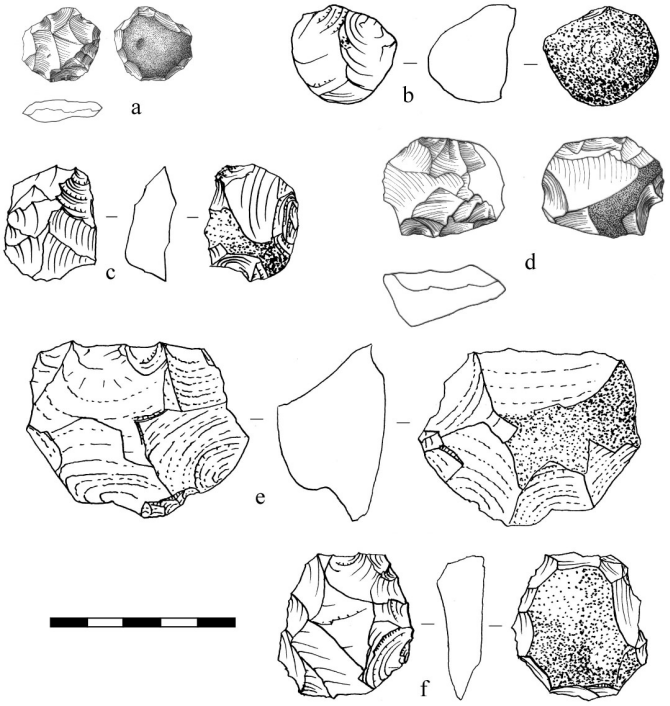

Figure 25. Cores from the Mousterian (non-tanged) assemblages.

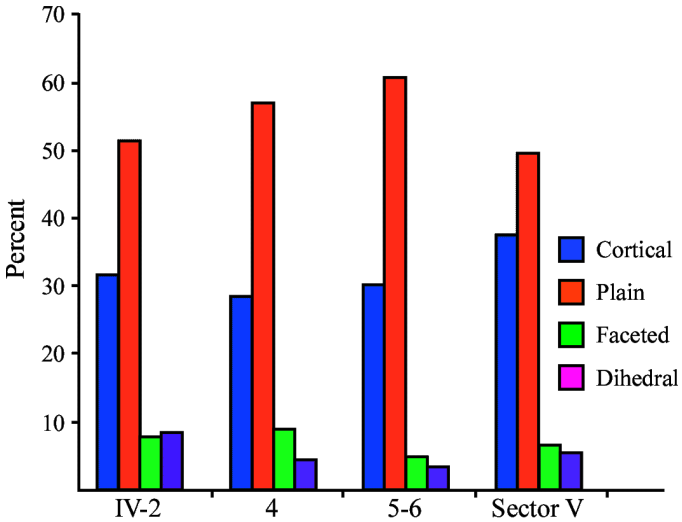

Figure 26. Platform preparation by major stratigraphic unit.

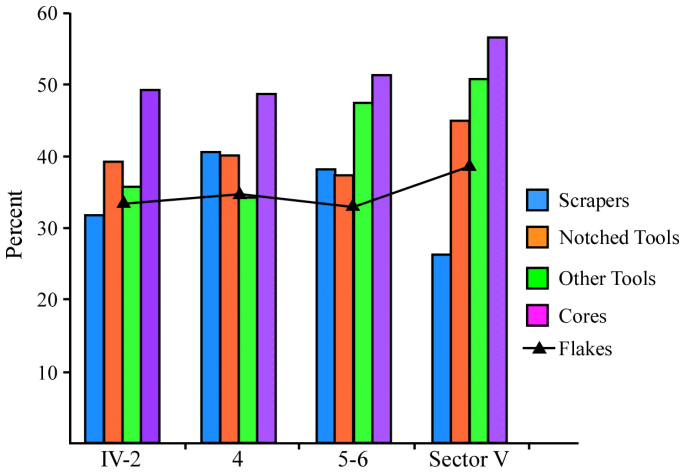

Figure 27. Average lengths of various artifact classes and by major stratigraphic unit.

(Layers 4, 5, IV-2, V-1, and V-2) the amount of cortex is quite low (Figure 33). As defined by Dibble et al. (2005), the Cortex Ratio should equal 1 if all of the lithic objects were knapped and remained on site; a Cortex Ratio greater than 1 indicates that too much cortex is present, while ratios as low as those shown here for Contrebandiers Cave indicates a deficit of cortex relative to assemblage volume at the site. This same pattern occurs with both fine and coarse grain materials.

The Cortex Ratio is based on an estimate of the number of whole nodules, and there are two ways of arriving at this estimate. One is to use the number of cores present as an estimate of original nodule frequency. When we do this, fine grained artifacts produced Cortex Ratios range from 0.57 to 0.37 between the five layers (see Figure 33), which indicate that cortex is underrepresented in these assemblages. Because fine grain materials (i.e., flint and chalcedony) do not

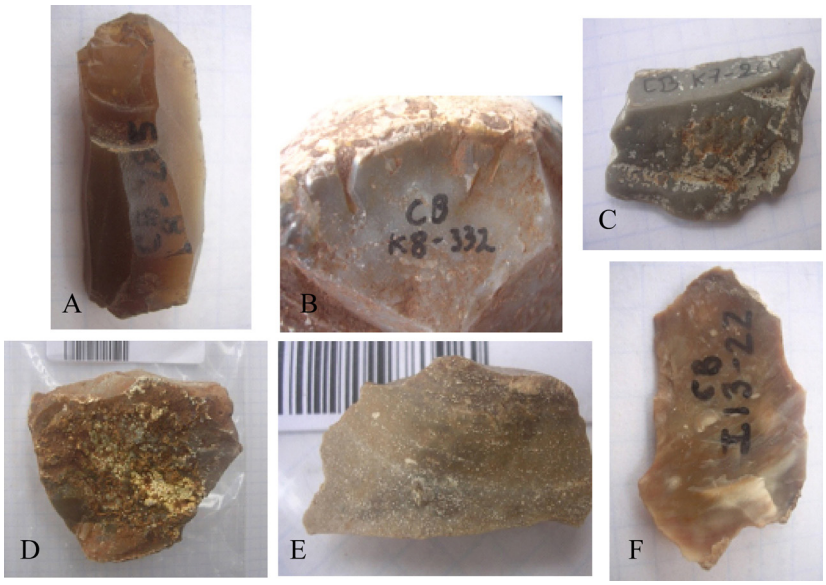

Figure 28. Assorted raw materials identified in the Contrebandiers lithic assemblages.

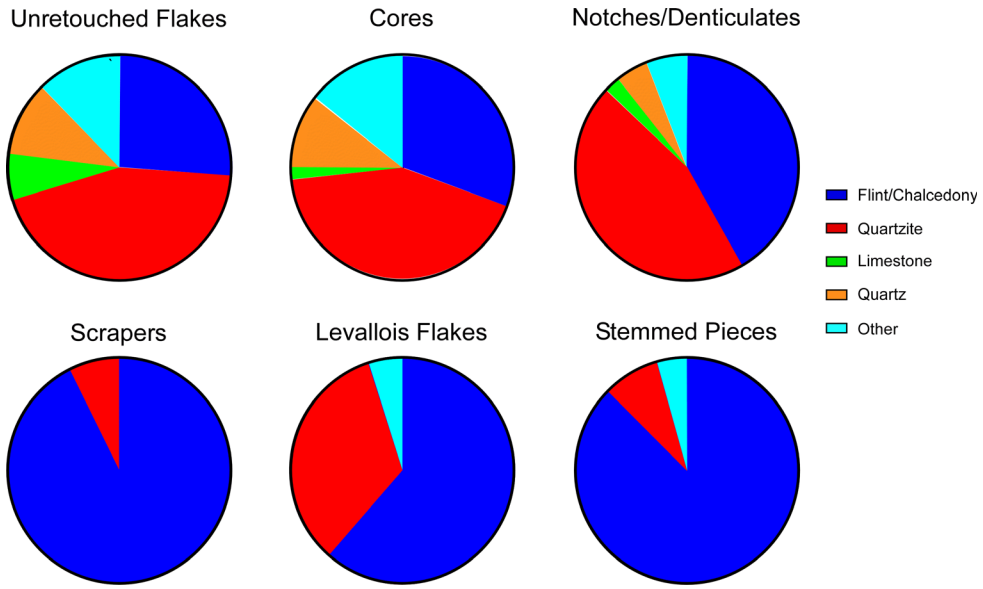

Figure 29. Breakdown of major raw material classes by artifact class.

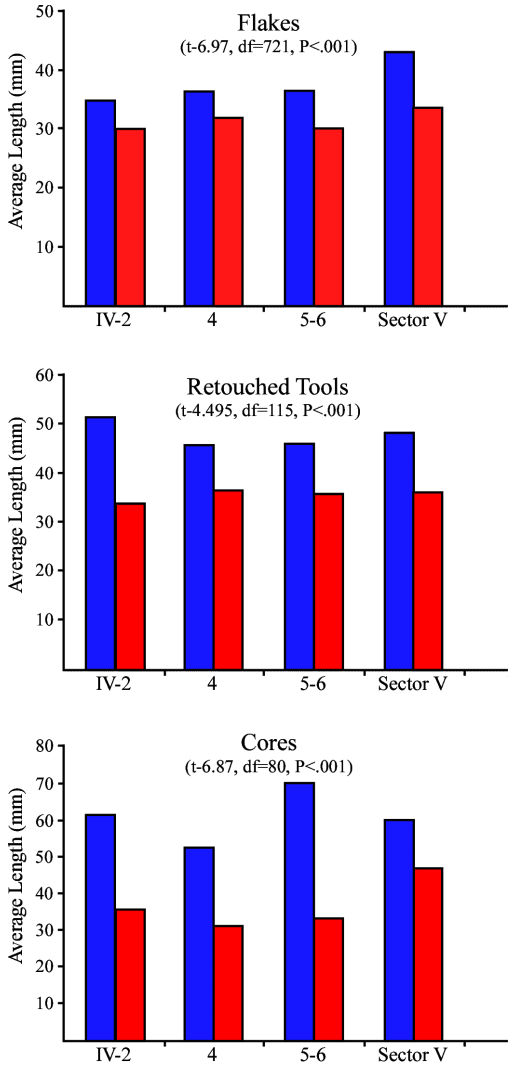

Figure 30. Difference in average lengths of objects made in either flint/chalcedony (red) or quartzite (blue).

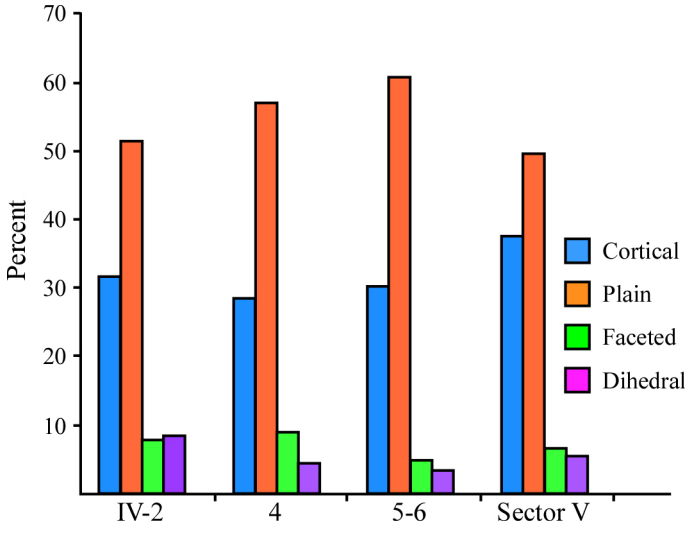

Figure 32. Edge damage by major stratigraphic unit.

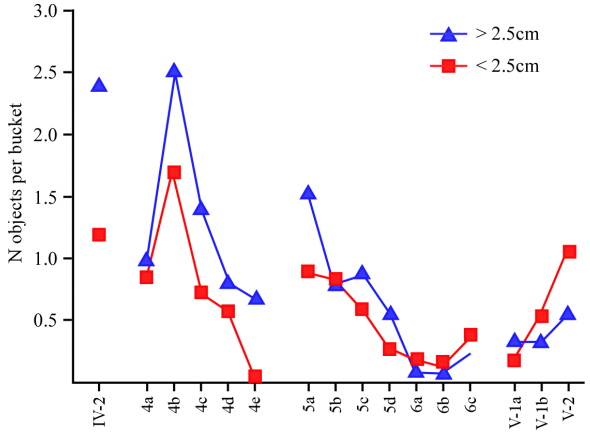

Figure 31. Average number of blanks (proximal or complete flakes, retouched or not) per 7-liter bucket of excavated sediment. Flakes >2.5cm in maximum dimension were piece-plotted, while flakes below that size cutoff were recovered in the 1cm coarse fraction after wet screeening.

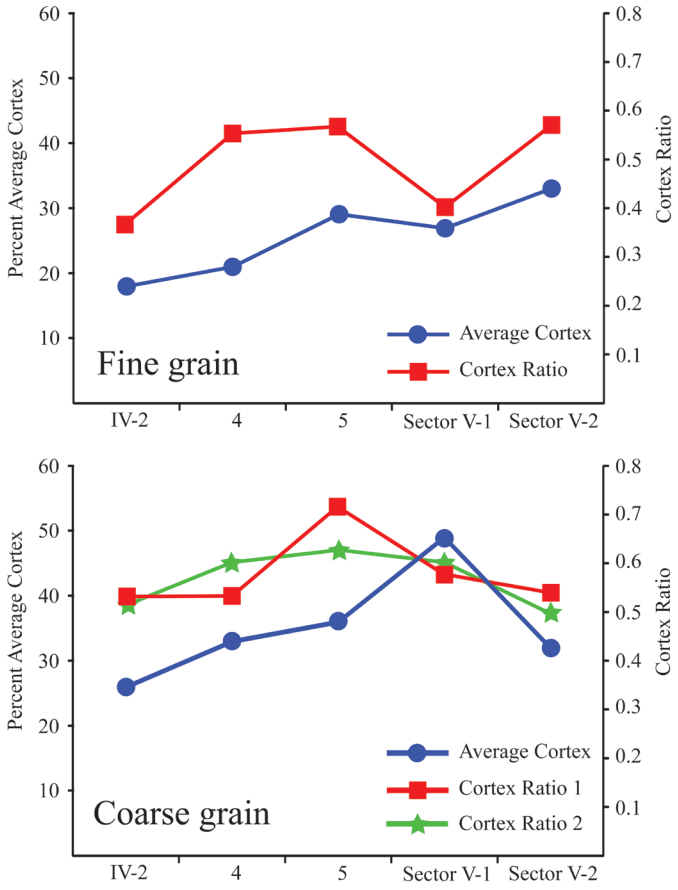

Figure 33. Average cortex per lithic object and Cortex Ratio (Dibble et al. 2005) for the major stratigraphic units. Top: Fine grain material with Cortex Ratio based on core frequency within each assemblage. Bottom: Coarse grain material with Cortex Ratio 1 based on core frequency within each assemblage, and Cortex Ratio 2 based on a constant nodule morphology (cylindrical) and size (334g).

occur naturally in the immediate proximity and thus had to be transported to the site (Bouzouggar 1997), these low ratios are the results of the movement of fine grain artifacts in and out of the site. Layers 4, 5 and V-2 have ratios higher than Layers IV-2 and V-1. This variation likely reflects differences in the type of fine grain artifacts that were being transported as well as the degree of mobility.

For coarse grain materials, again using the number of cores as a proxy for nodule frequency, the Cortex Ratios are still below 1. Layer 5 from the CEA yields the highest ratio of 0.72, which contrasts with a set of relatively consistent values ranging from 0.58–0.53 for the other four layers. Because coarse grain nodules are readily available along the coast, the underrepresentation of cortex across the assemblages indicates a general absence of coarse grain artifacts at the site.

Applying a different method for estimating the original number of coarse grain nodules, by assuming a constant nodule size of 334g estimated from the more cortical cores that have more than 60% of cortex surface (N=25) (see Douglass 2010: 153 for experimental justification), results in a set of more similar Cortex Ratios across the five layers being studied (ranging from 0.65–0.50). Because this method does not rely on the number of cores present in the assemblage, it is independent from the uncertainties of core breakage or material recycling. Instead, the similarity between the values in the second set of Cortex Ratios suggests that if the occupants represented by the different layers at Contrebandiers exploited the same quartzite source, and thus that the nodules were similar in shape and size, the strategies of artifact transport were relatively similar among the various assemblages. This method was not employed for fine grain materials because cores with more than 60% of cortex are too rare (n=3).

Because the first set of Cortex Ratios is derived by using the number of cores present in the assemblage and the second set of ratios is based on a constant nodule size, the difference between the two sets of Cortex Ratios reflects the different type of artifacts responsible for the apparent cortex deficit (see in Figure 33 the difference between the red and green lines). For Layers IV-2, V-1, and V-2, the similarity between the two sets of Cortex Ratios (0.58–0.53 vs. 0.60–0.50) suggests that the number of cores present in the assemblage do resemble the original nodule frequency. This is to say, the nodules utilized for producing these assemblages were not subsequently transported away after they were reduced. Since these coarse grain nodules occur naturally in close proximity and their cortex composition would have been close to, if not completely, cortical as they were brought to the site (i.e., Cortex Ratio of 1), the deficit in cortex across these assemblages had to be created by the export of cortical flakes. In the case of Layer 4, the difference between the two sets of ratios (0.53 vs. 0.60) shows that the number of cores present (n=13) is slightly more than the number of nodules estimated by the reconstructed nodule size (n=9). This slight overabundance of cores relative to assemblage volume can be explained by either a greater variability in original nodule size or the breakage of nodules into multiple cores during core reduction.

In contrast to Layer 4, the discrepancy between the two sets of Cortex Ratio in Layer 5 (0.72 vs. 0.63) indicates an overabundance of assemblage volume relative to the number of cores. This is also seen in the lower number of cores present (n=7) compared to the number of nodules estimated (n=10). One possibility for this disparity can be that the Layer 5 occupants were utilizing different types of coarse grain material that originally occurred in larger sizes. This is unlikely, however, because the cores in this assemblage are similar in size and shape to those of other layers. The more likely explanation for the apparent Cortex Ratio discrepancy is that, along with flake export, artifact transport in Layer 5 also was marked by the transport of cores away from the site, potentially as cores or core tools.

The overall small sample sizes prevent more conclusive discussion regarding Cortex Ratio patterns in relation to wider mobility models. However, there seems to be a difference between the artifact transport strategy of both fine and coarse grain material across the different layers at Contrebandiers Cave.

In summary, the earlier assemblages from Contrebandiers Cave reflect relatively ephemeral occupations of the site, with little to no core reduction taking place in the cave. In traditional terminology, both Aterian (with stemmed pieces) and Mousterian (without) assemblages are present, with the Aterian overlying the Mousterian stratigraphically, but as discussed above, the absolute dates overlap statistically. Both assemblage types are quite similar, with low tool counts (with notched pieces dominant) and low frequencies of Levallois flake production, though, of course, the Aterian assemblages do contain both stemmed pieces and one bifacial foliate. There are interesting patterns in terms of the use of the different raw materials, with both scrapers and stemmed pieces most often being made on finer grain materials.

In comparing the lithic assemblages from Contrebandiers Cave to other assemblages in the region, it should be noted that many collections remain unpublished, or data are presented in ways that considerably limits any direct comparison. Furthermore, in many key regions—especially in the Sahara—most data come from surface contexts (e.g., Caton-Thompson 1946; Cremaschi et al. 1998: 279–208; Pasty 1999; Hawkins 2004, 2008; Barich et al. 2006; Barich and Garcea 2008) and many collections were either acquired before the advent of modern excavation standards or have an insufficient amount of material for comparison. It is for these reasons that we do not include lithic data from the collections like Dar es-Soltane I (Ruhlman 1951; Roche 1956), Mugharet al-Aliya (Howe 1967; Bouzouggar et al. 2002), Aïn Fritissa (Tixier 1958–1959) and Station Météo (Wengler 1997) in the area from the Atlantic coast of Morocco to the Oujda Mountains; Koudiat Bou Gherara (Cadenat 1953) and Bérard (Vaufrey 1955) near the Atlas Tellien Mountains of northern Algeria; Oued Djouf el-Djemel (Morel 1978), Bir el-Ater (Oued Djebbana) (Reygasse 1921–1922; Morel 1974), Aïn Métherchem (Vaufrey 1955) and Aïn El-Guettar (Gruet 1958–1959; Aouadi-Abdeljaouad

and Belhouchet 2008) between the Great Eastern Sand Sea and Mediterranean coast of Algeria and Tunisia; Zaouïa el-Kebira (Chavaillon 1960) and Hassi Ouchtat (Chavaillon 1985) in Wadi Saoura, western Algeria; Uan Afuda in the Tadrart Acacus Mountains of western Libya (Cremaschi et al. 1998); Jebel Uweinat in the Libyan Desert (de Heinzelin et al. 1969), etc. A number of Late Pleistocene contexts have been reported from the Jebel Gharbi Mountains in Tripolitania, northwestern Libya, but to date they have been investigated by test excavations only (Garcea and Giraudi 2006; Barich et al. 2006; Barich and Garcea 2008). The relevant material from the Haua Fteah in Cyrenaica, Libya, is also equivocal both in regards to its classification as either Mousterian or Aterian, and the nature of the excavation units employed (McBurney 1967: 105–134).

Using what data are available, Figures 34 and 35 present some comparisons among the assemblages from Contrebandiers Cave and other sites in the region. In terms of typology, the Contrebandiers assemblages are relatively low in scrapers and relatively high in notched and denticulated tools. The assemblages from Taforalt, as reported by Roche (1967, 1969) have the highest Levallois, Blade, and Faceting Indices, while the Contrebandiers assemblages are relatively low in these measures. Clearly, however, there is considerable variability among these various sites and assemblages.

THE IBEROMAURUSIAN LITHIC ASSEMBLAGES

Roche's (1963) excavations identified Iberomaurusian deposits in the area of the mouth of the cave, which were thought to have been completely removed. However, during the 2008 field season this assumption was tested by excavating several squares in the Sector IV area that largely abutted the region excavated by Roche. Additional excavations occurred here in 2009 and 2010. All together, the new excavations yielded a total of 3,454 Iberomaurusian artifacts from Layers IV-1a and IV-1b, which have together a total thickness of about 80 cm (see Figure 9); this total count includes artifacts from the screens, which contain high numbers of very small flakes. The distribution of the Iberomaurusian artifacts by general class is shown in Table 14. In Table 15, the weight of these artifacts is shown by raw material type, which follows earlier work in Olszewski et al. (2011). Coarse-grained quartzite is the most common material (by weight), followed by finer grained flint/chert. If the two ground stone pestles (weighing 618.2g total) are removed from these tabulations, then the chipped stone coarse-grain material weighs 0.7kg and fine-grained raw material becomes the most common.

Not unexpectedly, the diversity of tool classes and types mainly is similar to those recorded for the 1950s Iberomaurusian collections (Figure 36; Roche 1963; Olsze-

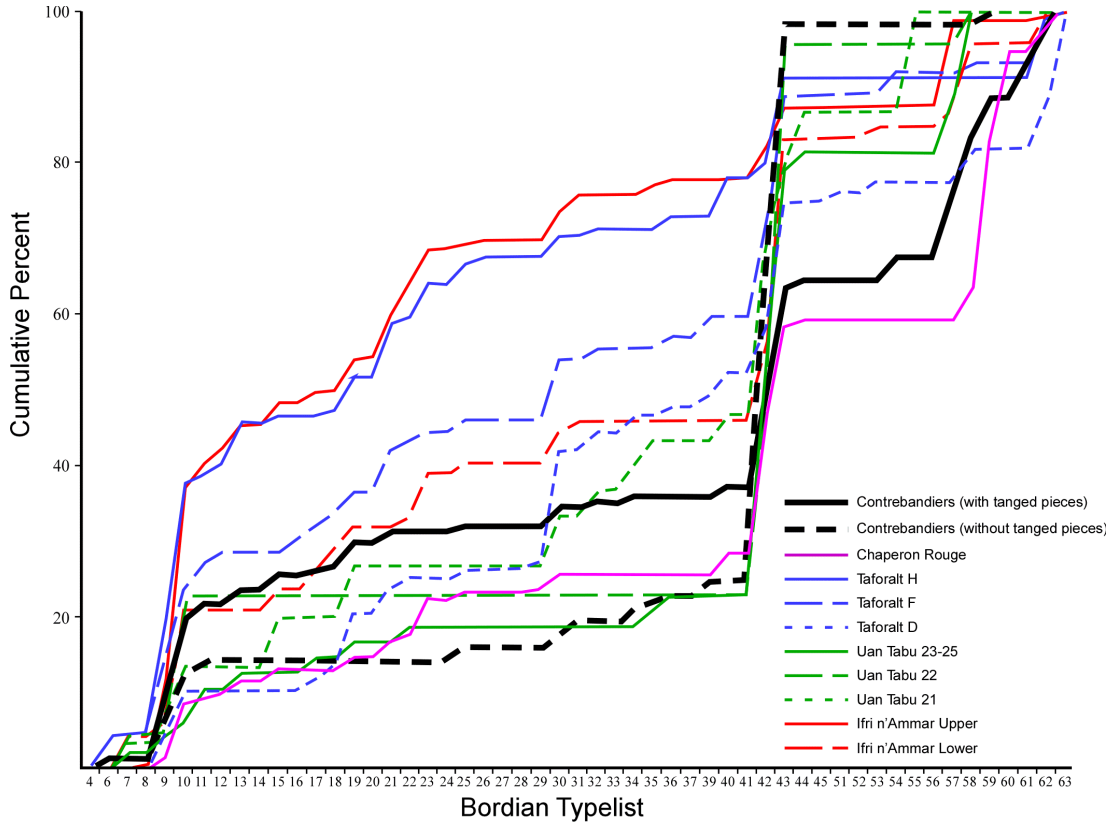

Figure 34. Bordian "essential" cumulative graph (see Debénath and Dibble 1995 for details). The horizontal axis refers to the list of Bodian types (excluding unretouched pieces, and in this case, tanged pieces). The vertical axis represents the cumulative sum of the percentages of each type. Data taken from Rhafas Cave (Wengler 1997), Taforalt (Roche 1967, 1969), Chaperon Rouge (Texier 1985–1986), Uan Tabu (Garcea 1998, 2001), and Ifri N'Ammar (Nami and Moser 2010).

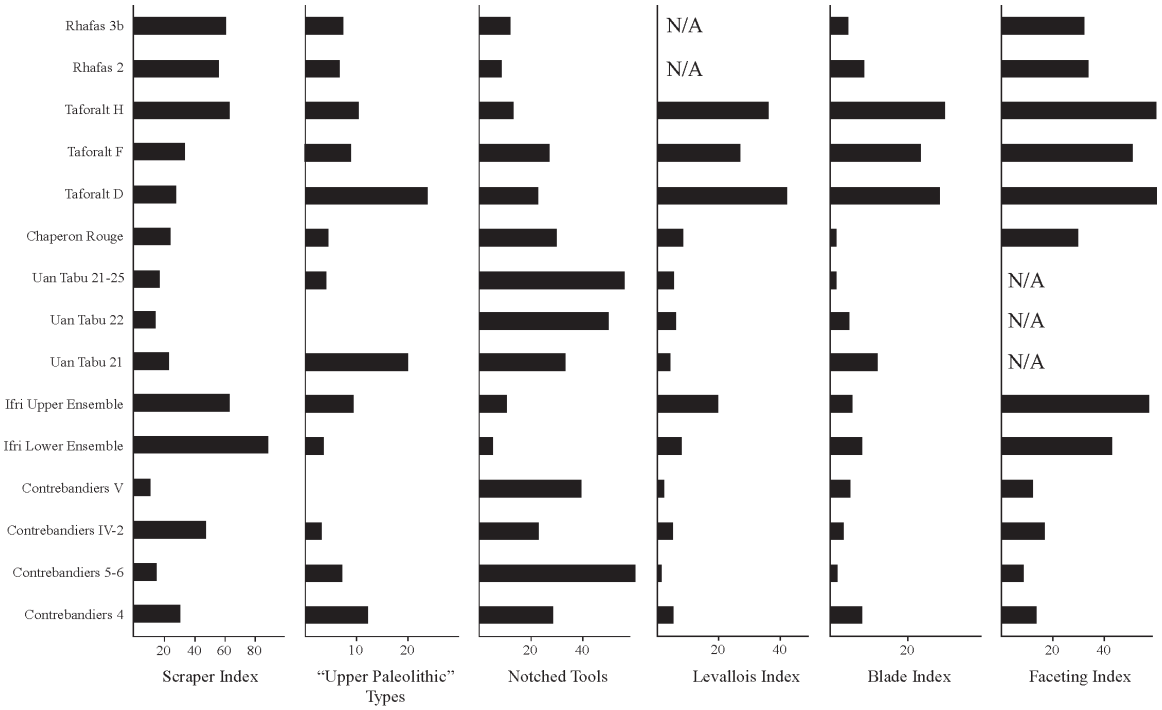

Figure 35. Major typological and technological indices (see Debénath and Dibble 1995 for details) for Contrebandiers and other nearby sites. See Figure 34 for sources.

TABLE 14. IBEROMAURUSIAN LITHIC CLASS DISTRIBUTION.

Class	N	Percentage
Tools	262	7.6
Hammerstones	1	<0.1
Cores	32	<0.1
Debitage	3,157	91.4
Pestles	2	<0.1
Total	**3,454**	

TABLE 15. IBEROMAURUSIAN STONE RAW MATERIALS.

Stone Raw Material	Weight
Fine-grained	1.2 kg
Chalcedony	0.3 kg
Coarse-grained	1.3 kg
Quartz	0.1 kg
Other	0.1 kg
N/A	< 0.1 kg
Total	**3.0 kg**

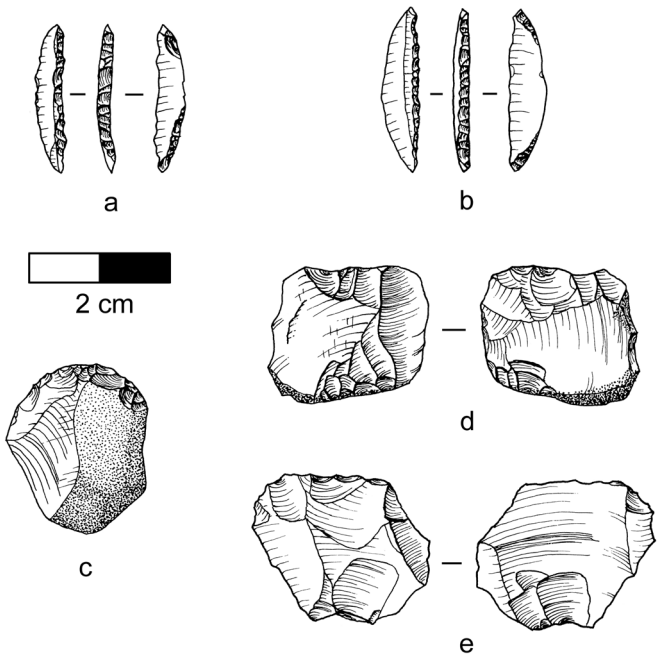

Figure 36. Examples of Iberomaurusian tools. a, b: Ain Keda points; c: flake endscraper; d, e: pieces esquillées.

wski et al. 2011). However, the recent excavations yielded more nongeometric microliths (which are also the most frequent tool class [Table 16]) than did Roche's excavation (Olszewski et al. 2011). By comparison, in the 1950s' excavations, nongeometric microliths, special tools, and retouched pieces are about equally represented. The recovery of more nongeometric microliths is the result of water screening of all excavated sediments in the new excavations, and is reflected in the comparison of the recovery of the nongeometrics from the coarse versus the fine screens (microliths are usually less than 2.5cm and thus are not often point provenienced). For example, there are 139 total nongeometrics from the new excavations, of which 9 were point provenienced, 65 acquired from the coarse screen fraction and 65 discovered in the fine screen. The context of recovery (coarse versus fine screen) shows that nearly half of the nongeometric component derives from fine screen, a technique not used during the 1950s.

The nongeometrics include pointed bladelets (n=35), Ain Keda points (n=18), blunt-ended bladelets (n=12), Ouchtata bladelets (n=16), curved bladelets (n=5), truncated bladelets (n=3), other nondiagnostic types, and 36 fragments. Special tools consist of sidescrapers and pièces esquillées (Table 17). Study of the 1950s' Iberomaurusian assemblage (Olszewski et al. 2011) showed a high frequency of *pièces esquillées* (so-called splintered pieces), an observation that continued to be true of the artifacts from the new excavations. The 34 *pièces esquillées* recovered represent 12.9% of all chipped stone tools (compared to 18.6% in the 1950s' collections). Given the ubiquity of this tool type in the Iberomaurusian and its similarities (11.4mm length, 7.4mm width, 2.6mm thickness, 3.8g weight) to small opposed platform cores (12.2mm length, 7.8mm width, 2.9mm thickness, 4.6g weight), it is quite likely that *pièces esquillées* functioned not as tools, but as cores for small flakes (Dibble and McPherron 2006; see also Olszewski et al. 2011). Here, we follow the historical precedent of including these elements in tool counts, partly because not all researchers agree that they are cores. Moreover, as *pieces esquillées* (sometimes referred to as *outils écaillés*) are widely known from many Later Stone Age assemblages across the African

TABLE 16. IBEROMAURUSIAN TOOLS.

Tool Class	N	Percentage
Endscrapers	13	4.9
Burins	6	2.3
Backed Pieces	7	2.7
Perforators	1	0.4
Truncations	1	0.4
Nongeometric Microliths	139	53.0
Geometric Microliths	3	1.1
Special Tools	44	16.8
Notch/Denticulates	10	3.8
Retouched Pieces	38	14.5
Composite Tools	-	-
Core Tools	-	-
Varia	-	-
Total	262	
Hammerstones	1	
Pestles	2	
Grand Total	265	

TABLE 17. IBEROMAURUSIAN SPECIAL TOOLS.

Special Tools	N
single sidescraper	5
double sidescraper	5
pièces esquillées	34
Total	**44**

continent (e.g., Close 1989; Parsons 2003; Willoughby 2001, among others), it is possible that their function(s) was situational; that is, in some cases, they represent cores while in others they were used as tools, or both. This is an issue of typological systematics and beyond the scope of this paper.

Rarer tools include notches/denticulates, and overall retouch present on the retouched pieces tends to be of high quality. Together, these features suggest that not much damage or movement has occurred in the Iberomaurusian deposits.

Few cores were recovered from the recent excavations. Among them, opposed platforms are slightly more frequent, followed by cores-on-flakes, and then multiple platforms and ninety-degree and single platforms (Table 18). Somewhat unexpectedly, single platform cores are not common, whereas the 1950s' collections yielded about equal numbers of single platform and opposed platform types (19.1% and 20.4%, respectively) (Olszewski et al. 2011). This discrepancy between the recent and the 1950s' core types distribution may be due to small sample size in the new excavations.

Quite surprisingly, there is a close comparability of the frequency of small debitage in our new excavations and the 1950s collection, especially given that Roche did not employ wet screening and examination of the fine fraction. Small bladelets from the 1950s collections represent 9.5% of the debitage, while small flakes constitute 52.6% (compare to Table 19 below). One major discrepancy between the new and old excavations is the lower frequency of flakes in the new excavations.

In addition to nongeometric microliths, the fine screen sorting was useful in the recovery of microburins, small

TABLE 18. CORE TYPES (broken down by removals) IN THE IBEROMAURUSIAN AT CONTREBANDIERS.

Core Type	Blade	Bladelet	Flake	Mixed	NA	Total	%
single platform	2	-	1	-	-	3	9.4
opposed platforms	-	6	-	-	-	6	18.7
ninety-degree platforms	-	-	1	2	-	3	9.4
discoidal	-	-	1	-	-	1	3.1
multiple platforms	-	1	2	1	-	4	12.5
core-on-flake	-	1	4	-	-	5	15.6
core fragment	-	-	-	-	10	10	31.2
Total	**2**	**8**	**9**	**3**	**10**	**32**	**100**

TABLE 19. BREAKDOWN OF IBEROMAURUSIAN DEBITAGE.

Debitage Class	N	Percentage
Blade	51	1.6
Bladelet	76	2.4
Flake	171	5.4
Burin spall	33	1.0
Microburin	24	0.8
Small bladelet	310	9.9
Small flake	2,082	65.9
Shatter	406	12.8
n/a	4	0.1
Total	**3,157**	

bladelets, and small flakes. For example, 11 microburins were recovered from the coarse screens and 13 from the fine. For small bladelets and small flakes, the ratio is more than 3:1 for recovery from fine compared to coarse mesh (244:66 [small bladelets fine:coarse] and 1592:490 [small flakes fine:coarse]).

Our new excavations in the Sector IV Iberomaurusian deposits at Contrebandiers Cave confirm many of the observations made about the 1950s' Roche collections (Olszewski et al. 2011). One of the main differences is due to the use of wet screening and the analysis of fine screened material during the new excavations. Important small diagnostics, including microburins, nongeometric microliths, and small bladelets, were considerably augmented by sorting of the fine screen fraction, as was the small flake component. Although Roche used traditional screening in the 1950s excavations, interestingly, the small elements in his recovered assemblage are quite comparable in most cases (except perhaps for microliths). This suggests that exceedingly careful attention to dry screening was characteristic of the Roche excavations, and confirms the value of these older collections for interpretations of the Iberomaurusian.

The numerous *pièces esquillées* are an important element in Iberomaurusian collections (see Olszewski et al. 2011), and along with cores-on-flakes, and small opposed and single platform cores, these types suggest a small flake production focus (most often less than 20mm in length). Although these small flakes are not microliths, their tiny size makes them microlithic; possibly they were used as composite tool elements (e.g., as barbs along arrow shafts).

In summary, only small pockets of sediments containing Iberomaurusian assemblages remain at the site, just outside the current dripline. While there are clear similarities between what can be seen in Roche's earlier collections and what was recovered in the new excavations, the major difference is the higher proportion of nongeometric microliths (including Ain Keda points) in the latter collection. This is probably due to the more meticulous excavation techniques currently being used. In addition to these pieces, the Iberomaurusian assemblage contains endscrapers, burins, and backed tools, *pièces esquillées*, cores, blades and bladelets, and many small flakes. The Contrebandiers Iberomaurusian is thus similar to assemblages found throughout much of northwestern Africa, including the relatively well-published assemblages from the older excavations at Taforalt (Roche 1963: 43–156; lithics from the recent excavations are not yet published) and Ifri n'Ammar (Moser 2003).

THE FAUNAL RECORD AT CONTREBANDIERS CAVE

The primary goal in analyzing the Contrebandiers Cave fauna is to describe the diet and environments of early *Homo sapiens* in coastal Morocco. However, because studies of the faunal assemblages are still on-going, the results presented here should be considered preliminary. In this report, the presentation and discussion of the evidence to date will be broken down into four major sections—the macrofaunal assemblages, the microvertebrates, the molluscan fauna, and the *Nassarius* remains.

THE MACROFAUNAL ASSEMBLAGES

The current macrofaunal sample includes bones that were piece-plotted (all teeth and all bones with a maximum size >25mm) and those that were discovered after screening with the 1cm screens. Identifications were made to the lowest taxonomic level possible, and the Number of Identified Specimens (NISP) was recorded for each taxon. So far, 549 macrofaunal specimens (out of a total of 5,663 piece-plotted bones) are taxonomically identifiable from all layers at Contrebandiers Cave (Table 20).

Carnivore remains were present in nearly all layers, and include large-bodied taxa (e.g., *Ursus arctos bibersoni*) as well as small-bodied animals (e.g., *Vulpes rueppelli*). Species of *Gazella*, including *Gazella cuvieri* and *Gazella dorcas*, dominate the majority of the identifiable faunal remains. Throughout most of the sequence larger mammals such as aurochs (*Bos primigenius*) tend to be juvenile individuals, perhaps indicating that the hunters or accumulators focused on particular sized animals. In contrast, *Bos* and equids tend to be adult individuals in the Iberomaurusian layers. Ostrich eggshells and tortoise carapaces also are present in all layers.

The lower layers of the CEA, Layers 5c, 5b, and 5a, have a total of 119 taxonomically identifiable faunal remains. *Gazella* species represent the highest frequency of bovids present. *Oryx* cf. *gazella*, typically found in short-grass steppe/semi-desert habitats, was only found in Layer 5a. Likewise, *Bos primigenius* (wet woodland/swamp species) and *Alcelaphus buselaphus* (grassland/woodland edge species) were only found in Layer 5c. Nearly all *Sus scrofa* remains were recovered from Layers 5c, 5b, and 5a, while only one was recovered from Layer V-2. *Phacochoerus africanus*, a savannah grassland/open woodland species, was found in Layers 5c and 5b. Carnivores from Layers 5c, 5b, and 5a include *Canis aureus* (arid/open grassland species), *Vulpes rueppelli* (true desert species), and *Ursus arctos bibersoni*.

The layers containing Aterian assemblages, specifically Layer 4 from the CEA, and Layers IV-2, V-1a, V-1b, V-2, yielded a total of 338 taxonomically identifiable faunal remains. As in the underlying layers, *Gazella* species represent the majority of bovids, and there is also a high frequency of *Bos primigenius*. Since *Gazella dorcas* is typically found in arid to semi-arid habitats, the presence of this species in Layers V-2, V-1b, and V-1a indicates the presence of arid environments near Contrebandiers Cave. *Alcelaphus buselaphus* (grassland/woodland edge species) and *Connochaetes taurinus* (short-grass plains species) were also found, though in very low frequencies. *Sus scrofa* and *Phacochoerus africanus* were only present in Layer V-2. A nearly complete maxilla of *Dicerorhinus sp.* was found in Layer V-2. Carnivore remains include *Canis aureus, Vulpes rueppelli, Felis sylvestris libyca, Genetta genetta, Mellivora capensis, Hyaena hyaena,* and *Ursus arctos bibersoni*.

Layers IV-1b and IV-1a have a total of 91 taxonomically identifiable faunal remains; the low sample size being pri-

TABLE 20. MACROFAUNA: NUMBER OF IDENTIFIED SPECIMENS (NISP) BY LAYER.

Class/Order	Taxon	Common Name	Iberomaurusian		Aterian		Mousterian			Aterian			
			IV-1A	IV-1B	IV-2	4	5A	5B	5C	V-1A	V-1B	V-2	Grand Total
Mammalia (Class)													
Artiodactyla	*Oryx* cf. *gazella*	Oryx	-	-	-	-	1	-	-	-	-	-	**1**
	Bos primigenius	Aurochs	5	3	5	2	-	-	5	7	10	3	**40**
	Bovini gen. et sp. indet.		-	-	-	-	-	-	-	-	-	2	**2**
	Alcelaphus buselaphus	Hartebeest	5	2	3	-	-	-	3	-	-	2	**15**
	Connochaetes taurinus	Blue wildebeest	-	-	-	-	-	-	-	1	-	-	**1**
	Alcelaphini gen. et sp. indet.		-	-	-	1	-	-	-	-	-	1	**2**
	Gazella dorcas	Dorcas gazelle	-	3	-	-	-	-	-	13	6	6	**28**
	Gazella cuvieri	Cuvier's gazelle	-	15	-	-	-	-	-	-	-	-	**15**
	Gazella sp. indet.		8	-	22	8	2	3	3	17	28	20	**111**
	Antelopini gen. et sp. indet.		-	-	-	-	-	-	-	-	-	3	**3**
	Bovidae gen. et sp. indet.		5	9	13	7	6	3	20	10	12	5	**90**
	Phacochoerus africanus	Warthog	-	-	-	-	1	-	1	-	-	1	**3**
	Sus scrofa	Wild boar	-	-	-	-	2	2	2	-	-	1	**7**
	Suidae gen. et sp. indet.		3	2	-	-	1	-	1	-	-	-	**7**
	Artiodactyla gen. et sp. indet.		-	5	-	13	8	3	10	2	2	-	**43**
Perissodactyla	*Equus mauritanicus*	Zebra	2	-	-	1	-	-	2	-	-	-	**5**
	Equus sp. indet.		-	-	1	-	-	-	-	3	1	3	**8**
	Dicerorhinus sp. indet.	Rhinoceros	-	-	-	-	-	-	-	-	-	2	**2**
Carnivora	*Canis aureus*	Golden jackal	-	-	-	-	1	-	1	1	1	-	**4**
	Vulpes rueppelli	Rüppel's fox	2	-	2	-	-	-	-	5	3	4	**16**
	Genetta genetta	Small-spotted genet	-	-	3	-	-	-	-	-	1	-	**4**
	Felis sylvestris libyca	African wildcat	-	-	-	-	-	1	-	2	2	-	**5**
	Hyaena hyaena	Striped hyena	-	2	-	-	-	-	-	-	1	1	**4**
	Hyaenidae gen. et sp. indet.		-	-	-	-	-	-	3	1	-	-	**4**
	Ursus arctos bibersoni	Brown bear	-	1	-	-	-	-	1	-	-	1	**3**
	Mellivora capensis	Honey badger	-	-	-	-	-	-	-	2	1	-	**3**
	Carnivora gen. et sp. indet.		4	2	1	1	1	3	6	3	1	1	**23**
Lagomorpha	*Lepus capensis*	Cape hare	-	1	-	-	-	-	-	1	1	2	**5**
	Oryctolagus cuniculus	European rabbit	1	-	-	-	-	1	-	1	-	-	**3**
	Leporidae gen. et sp. indet.		2	3	-	1	-	-	-	3	5	1	**15**
Rodentia	*Hystrix cristata*	Crested porcupine	-	-	-	2	-	2	-	7	7	1	**18**
	Rodentia gen. et sp. indet.		-	-	1	-	-	-	-	-	-	-	**1**

TABLE 20. continued

Class/Order	Taxon	Common Name	Iberomaurusian		Aterian		Mousterian			Aterian			
			IV-1A	IV-1B	IV-2	4	5A	5B	5C	V-1A	V-1B	V-2	Grand Total
Sauropsida (Class)													
Testudines	*Testudo graeca*	Greek tortoise	1	3	7	10	3	7	5	2	2	2	**42**
Reptilia (Class)													
Squamata	Squamata gen. et sp. indet.	Lizards/snakes	1	-	-	-	-	-	-	-	2	-	**3**
Aves (Class)			-	1	-	-	-	1	-	-	-	-	**2**
Struthioniformes	*Struthio camelus*	Ostrich	-	-	2	-	-	-	2	-	-	1	**5**
	Aves gen. et sp. indet.		-	-	1	-	-	-	2	-	1	-	**4**
		Grand Total	**39**	**52**	**61**	**46**	**26**	**26**	**67**	**81**	**87**	**63**	**549**

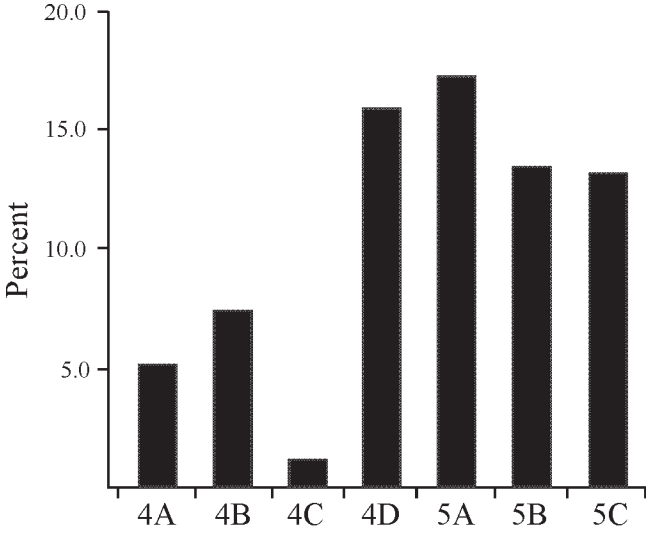

Figure 37. Frequency of cut-marked bones by layer.

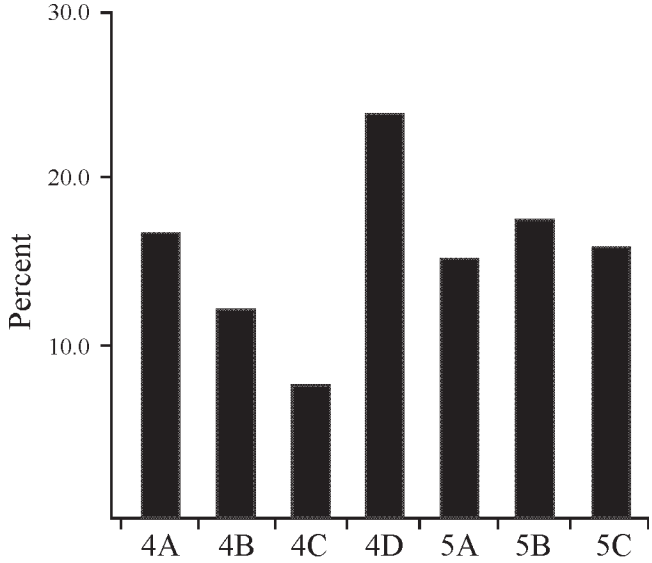

Figure 38. Frequency of percussion-marked bones by layer.

marily due to the lack of Iberomaurusian deposits remaining at the site. Results to date show that *Gazella* species are the most represented bovid, as in the other layers. *Alcelaphus buselaphus* (grassland/woodland edge species) and *Bos primigenius* (wet woodland/swamp species) were the only other species of bovid found in the Iberomaurusian layers. Carnivores include *Vulpes rueppelli*, *Hyaena hyaena* and *Ursus arctos bibersoni*.

Surface Modification on Bones

The current sample of bones that were analyzed for surface modification includes all of the bones that were piece-plotted from one square (I17) during the recent excavation (see Figure 2). This sample is composed of 723 bones from Layers 4a–4d and 5a–5c, which represents about 13% of the total number of piece-plotted bones. The number of tooth marks, tooth notches, hammerstone percussion marks, cut marks, and gastric etching marks were recorded for each bone following the standards outlined in Blumenschine et al. (1996). A 40X zoom binocular microscope and bright incident light were used to analyze each specimen. Only those fragments with a mark that could be identified with high confidence were used in this study.

Figure 37 shows that the highest frequency of observed cut-marks occurs in Layers 4d and 5a, and these two layers also yielded the lowest frequency of bones identified as carnivores. However, the frequencies of cut-marks in Layers 5b and 5c indicate that occupants of the site were accumulating bones despite the frequency of carnivore bones found in these layers. Such evidence most likely indicates that Contrebandiers Cave was occupied by carnivores when hominins were not present and vice versa, perhaps reflecting seasonal or migratory patterns.

Figure 38 shows the high frequency of percussion-marked bones in Layer 4d, indicating heavy butchery of carcasses for nutrient-rich marrow. Layer 4c displays the lowest frequency of percussion-marked bones as well as cut-marked bones, perhaps indicating an occupation hiatus of Contrebandiers Cave by *H. sapiens*.

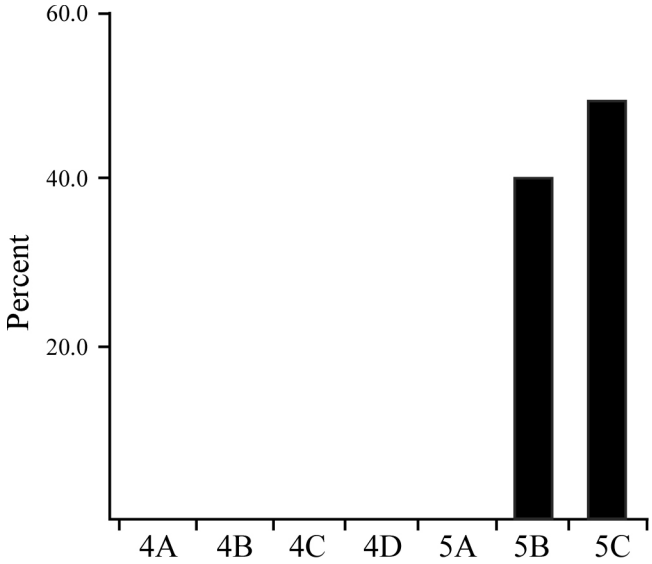

Figure 39. Frequency of tooth-marked bones by layer.

Figure 39 shows the absence of any observable tooth-marks on bones in all layers aside from Layers 5b and 5c. This is likely due to the small sample size of bone analyzed. In addition, the excavated area of these layers within the cave is not to the rear of the cave, where carnivores typically den, and where the majority of their remains were found. Future surface modification analyses will include bones from Sector V at the rear of the cave, and will most likely increase the observed frequencies of tooth-marked bones.

Summary of the Macrofaunal Record

Agents of accumulation in archaeological assemblages can include both hominins and carnivores, as both occupy natural shelters (Marean and Kim 1998). The results of this preliminary study, based on analyses of only 13% of the faunal remains at Contrebandiers Cave, so far indicate that the faunal assemblage was primarily accumulated by

hominins, although the presence of tooth-marked bones in Mousterian layers (Layers 6 to 5) indicates a carnivore accumulator in the lower layers of the cave and in the back of the cave (Sector V). Layer 4d, associated with the Aterian, has the highest rates of cut-marks and percussion-marks, and is also the only layer with no carnivore remains; however, it is also possible that the apparent lack of carnivore activity on bone in the Aterian layers is likely a result of low sample sizes available at this time. On-going analysis of the remainder of the faunal assemblages, along with estimates of the minimum number of skeletal elements (MNE) following the guidelines described in Marean et al. (2001) will undoubtedly clarify the extent to which hominins and carnivores competed for use of the cave.

MICROVERTEBRATES

The microvertebrates (i.e., a vertebrate species with an estimated body mass of <500g) recovered during the recent excavations at Contrebandiers Cave include mammalian, reptilian, and avian remains. A preliminary analysis of the rodent component of the mammalian assemblage has been completed and is presented below. It should be noted, however, that smaller material, such as microvertebrate fossils, was not point-provenienced during excavation and was instead recovered after wet screening of the sediments collected in the buckets. During excavation seasons up to and including 2009, the sediments were wet screened through stacked 1cm and 2mm meshes. Finer 1mm wet screens were introduced in 2010 to test for possible size bias in the microvertebrate assemblage.

The microvertebrate material from Contrebandiers that has been studied so far comprises 931 specimens, of which 526 are rodents, and the remainder are crociduran shrews, bats, and reptiles. The rodent portion of the fauna was analyzed first because they are often the best indicators of past environment. Analysis of the non-rodent portion of the present sample is on-going, as is the recovery of additional specimens from the screened sediments.

Of the rodents, at least three species are preserved at Contrebandiers Cave. Morphological and metric descriptions of the more abundant taxa have been published (Reed and Barr 2010), but a brief summary of the each taxon in given below.

Family Muridae Illiger, 1811, Subfamily Gerbillinae Gray, 1825, *Meriones* sp. Today four species of Meriones inhabit North Africa: *M. crassus*, *M. grandis*, *M. libycus*, and *M. shawii* (Aulagnier and Thevenot 1986; Musser and Carleton 2005). Additionally, *M. shawii*, *M. maghrebianus*, and *M. maximus* are known from Pleistocene age fossil deposits in Morocco (Tong 1986; 1989; Geraads 1994). The sample of more than 350 specimens from Contrebandiers Cave is below the size range of *M. grandis* and *M. maximus*, and is instead similar in size and morphology to both *M. libycus* and *M. shawii*. The current sample of *Meriones* is also very close in size and morphology to *M. maghrebianus*. Distinguishing among these closely related species represents an ongoing subject of investigation. Of particular interest are anatomical differences between *M. libycus* and *M. shawii*. In their modern distributions, *M. shawii* generally inhabits its coastal zones of northern Africa while *M. libycus* ranges further into the interior and occupies more xeric conditions (Aulagnier and Thevenot 1986). Finding morphological features that distinguish between these taxa and that refine the diagnosis of the specimens from Contrebandiers Cave will help improve the paleoenvironmental reconstruction of the region around the site.

Gerbillus campestris (Loche 1867). Numerous extant species of *Gerbillus* are known from Morocco (Aulagnier and Thevenot 1986; Musser and Carleton 2005). The modest sample of 16 specimens from Contrebandiers Cave is indistinguishable in size and morphology from extant and fossil forms of *G. campestris* (Reed and Barr 2010). Generally species in the genus *Gerbillus* are xeric adapted and have a distribution that reflects their adaptations for arid environments. North African gerbils (*G. campestris*) have a broad coastal distribution from Morocco east to Egypt and the Sudan (Musser and Carelton 2005), and like *Meriones shawii*, *G. campestris* has a more littoral distribution compared to other members of the genus *Gerbillus*.

Subfamily Murinae, *Mus spretus* (Lataste 1883). Two extant species of mouse are known in Morocco, *Mus musculus* and *Mus spretus*. The sample of more than 100 specimens from Contrebandiers Cave exhibits the small body size, elongate first molars with an offset t1 cusp on the upper M1 and the reduced third molars characteristic of the genus *Mus*. Size and additional morphological details ally the Contrebandiers Cave sample to *M. spretus* (Reed and Barr 2010). Two extinct species, *M. haouzi* (Jaeger 1975) and *M. hamidae* (Geraads 1994), are known from Morocco. The Contrebandiers sample is larger than either of these extinct forms, and also larger than extant forms of *M. spretus* (Reed and Barr 2010) and is most similar to *M. spretus* from the nearby site of El Harhoura II (Stoetzel 2005).

The Algerian mouse (*M. spretus*) is distributed broadly around the Mediterranean basin from southern portions of Western Europe, through the Levant and into North Africa. Though similar to the common house mouse, *M. musculus*, the two species have unique niches in most areas. *M. musculus* is commensal with humans while *M. spretus* is generally not, though it is common in agricultural fields and grasslands (Aulagnier and Thevenot 1986; Musser and Careleton 2005). *M. spretus* is very common in the prey of barn owls and other predators in Morocco (Aulagnier and Thevenot 1986). In Morocco, *M. spretus* has a littoral distribution (Aulagnier and Thevenot 1986) and is not associated with true desert conditions.

Taphonomically, Contrebandiers Cave is distinct from other nearby cave sites with regard to microvertebrate accumulations. The *in situ* fossil microvertebrates recovered at this site are sparsely distributed in the excavation, and no dense lenses of micromammals, as are often found in cave sites occupied for long periods by owls (Andrews 1990; Reed 2003, 2005), were found in the sediments. However, some areas, such as in Sector V at the rear of the cave, have higher densities of micromammals suggesting that lenses of dense microvertebrate remains may exist in other unex-

cavated areas. The taphonomic situation at Contrebandiers Cave is in stark contrast to the preservation patterns at the nearby site of El Harhoura 2, where dense microvertebrate concentrations are reported (Stoetzel 2005; Stoetzel et al. 2007).

There is also evidence for a size bias in the assemblage. The largest taxon, *Meriones*, is the most abundant and is known from numerous isolated teeth, which are large enough to be recovered in the 2mm sieves. The smaller taxa, *Gerbillus campestris* and *Mus spretus*, on the other hand, are less abundant and few isolated elements were recovered from the sediments screened with 2mm mesh. Thus, the relative abundance of species at the site remains for now insufficiently documented because the smaller species are likely under-represented in the assemblage.

Biodiversity estimates are an important component for understanding local paleoenvironments around the site. Contrebandiers Cave shows low rodent biodiversity. Taxonomic richness in an archaeological assemblage is a direct function of sampling effort (Grayson 1984) yet, even with relatively large samples of over 900 specimens, the rodent diversity in the rodent fraction of the assemblage remains low, with only three rodents represented. By comparison the modern rodent species richness in the area surrounding the cave is between 8–10 species (Aulagnier and Thevenot 1986).

One challenge to interpreting the relative biodiversity at Contrebandiers Cave is that few other reports on microvertebrate assemblages in Morocco document the sample sizes of the microvertebrate assemblages. Two exceptions are from El Harhoura I and II (Stoetzel 2005; Stoetzel et al. 2007). The site of El Harhoura I, based on a sample size approximately half that of Contrebandiers, has yielded three species—*Hystrix* aff. *cristata, Meriones shawii*, and *Mastomys* sp. (Abbasi and Aouraghe 2002). Given the preponderance of the very large rodent, *Hystrix*, the El Harhoura I assemblage is probably size-biased against small taxa, making it difficult to make meaningful comparisons between the two sites. El Harhoura II, with a sample size comparable to that of Contrebandiers, has six species of rodent—*Apodemus sylvaticus, Mus musculus, Mus spretus, Gerbillus campestris, Meriones shawii, and Hystrix campestrix* (Stoetzel 2005). If the unresolved species at Contrebandiers Cave match those at El Harhoura II, and there is as yet no reason to think they cannot, then the two samples have a high degree of correspondence, with the Contrebandiers Cave sample being a subset, in terms of richness, to the El Harhoura II sample. The two additional taxa in the El Harhoura II assemblage are the small-bodied murines *Apodemus sylvaticus* and *Mus musculus*. Given that the El Harhoura II fauna was screened at 1mm and the majority of the Contrebandiers sample was from 2mm screens, it is possible that recovery of smaller taxa has been negatively biased in the Contrebandiers Cave assemblage.

PALEOENVIRONMENTAL RECONSTRUCTION

Macrofaunal and microfaunal remains were used to reconstruct local paleoenvironment at Contrebandiers Cave. Fortunately, the macrofaunal taxa found at Contrebandiers Cave are indistinguishable from extant species living in the region, and all three rodent taxa found in the excavation are today found in both coastal and inland regions of Morocco. For the former, 73 species lists were created for modern African game parks following the methods outlined in Reed (2008). These extant sites encompass overall habitat types from forests through deserts, and each species at each site was assigned to a trophic and substrate category (for example, *Equus burchelli*, the common zebra, is a terrestrial grazer). We then added the numbers of each of the adaptations at each extant site. These data were then analyzed with correspondence analysis (CA) to group similar habitat types together, which has been effective in previous analyses (Reed 2008; Rector and Reed 2010). For the current study, several North African localities were added to the modern dataset to include Mediterranean vegetation types, and the combined faunal assemblages representing the Aterian and Mousterian layers were plotted. The result is displayed in Figure 40 where forests are to the left and open grasslands are to the right. Intermediate habitats such as woodland, bushland, shrubland, etc., are plotted such that those with higher mean annual rainfall are to the left of the graph and lower mean annual rainfall is to the right. In addition, localities which have rivers, wetlands, or lakes within their borders are positioned towards the bottom of the graph, and those lacking these categories of ground water are positioned near the top of the graph. The Mousterian layers at Contrebandiers Cave (Layers 6 and 5 in the CEA) are reconstructed as an open grassland habitat similar to the Serengeti Plains along the x-axis. The Aterian layers (Layers 4, IV-2, V-1, and V-2) are positioned between Chambi National Park in Algeria and the Serengeti Plains, indicating a drier and mosaic habitat of Mediterranean shrubland and open grasslands. Further identification of fauna in each of the separate layers will help us refine the habitat reconstructions in the future.

Figure 41 is a map of Morocco indicating those areas in which the three rodent taxa from Contrebandiers Cave co-occur. The absence of arid adapted gerbils, jerboas, and elephant shrews suggests the site was not situated in a true desert as occurs today in southern and eastern Morocco. Similarly the absence of wood mice (Genus *Apodemus*) suggests that the more mesic woodlands as found today in northern Morocco were not present. The rodents present at Contrebandiers Cave are consistent with a low-elevation scrub-grassland to treed-grassland semi-arid Mediterranean habitat similar to the current day habitat in the area around the cave.

Since the macrofauna suggest that during the time of deposition of Layers 5–6, habitats surrounding the cave included those ranging from woodlands/grasslands to dry shrublands, the small discrepancy in the datasets may indicate that while habitats near the cave were dry (as indicated by the microvertebrates), habitats further from the cave were wetter. Later in time, in the Aterian layers, the microfauna suggest a dry shrubland habitat that was simi-

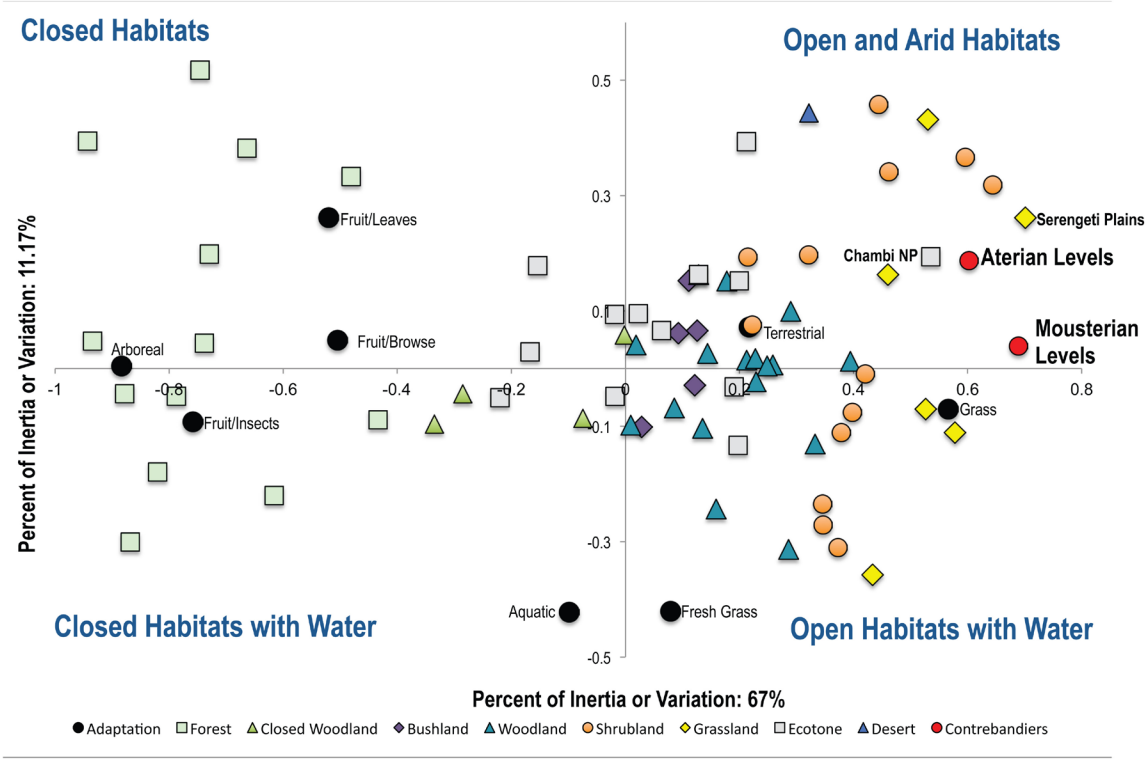

Figure 40. Habitat reconstruction of Mousterian and Aterian layers at Contrebandiers based on recovered fauna. Mousterian and Aterian layers are interpolated into the 73 modern localities as represented by the adaptations of the large mammals that exist at each locality. These adaptations included: arboreal, terrestrial, aquatic, fruit and leaf eating, fruit and browse eating, fruit and insect eating, fresh grass grazing, and grazing. This enables groupings of like habitats together. See key on the x-axis for types of habitats by symbol and color.

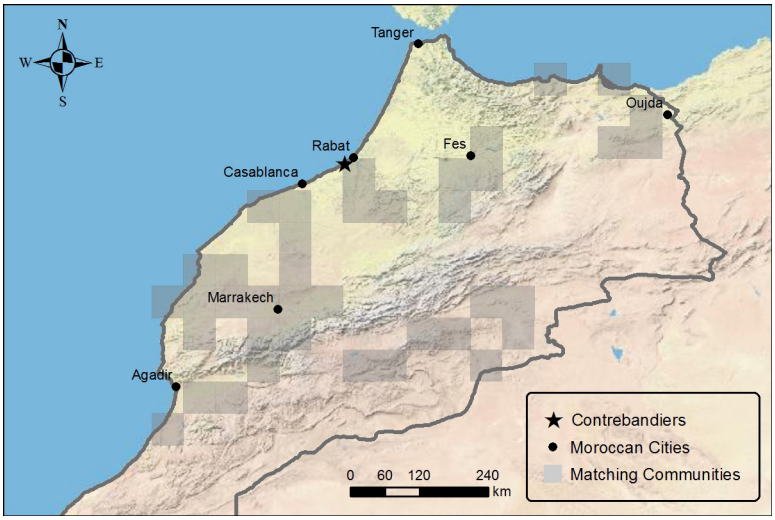

Figure 41. Relief map of Morocco showing regions where the rodent species excavated at Contrebandiers, Meriones shawii/lybicus, Gerbillus campestris, and Mus Musculus, occur together today. These species are found in coastal regions and inland in areas that are neither mountainous nor desert. This assemblage of species is also absent from the northern area around Tangier, which is more wooded.

lar to the habitat in the Mousterian layers, which is also supported by the macrofauna. Therefore, the microfauna indicate consistent dry grassland to dry shrubland environment throughout the sequence; while the macrofauna indicate a minor change to drier shrubland habitats in the Aterian (the woodland/grassland component is lost). The past habitat near Contrebandiers Cave was likely a coastal Mediterranean mosaic, with more shrubland type habitats

*Figure 42. Example of state of preservation of Molluskan fauna (*Osilinus*) from Layer 4c.*

consistently near the cave, and habitats ranging from grasslands/woodlands to arid shrublands further from the cave.

THE MOLLUSCAN FAUNA

Previous excavations at Contrebandiers Cave yielded abundant limpets in the Aterian (Roche and Texier 1976), and Bouzouggar's (1997b) subsequent work at the site provided a species list of mussels, limpets and topshells (Bouzouggar et al. 2002: 241). Nearby, only the early work at Dar es-Soltan I provided a species list for comparisons (Ruhlman and Neuville 1951). Our current excavations at Contrebandiers Cave have yielded mollusks throughout the sequence, thus providing new opportunities to study mollusk exploitation in detail (see also Steele and Álvarez Fernández 2011, which includes a review of North African evidence). To date, over 10,000 shell fragments have been recorded, representing almost 3,000 individuals (Tables 21a, 21b). Work on the mollusks is continuing.

The current mollusk sample consists of shells that were piece-plotted during the first season and subsequent bulk samples sorted out of the material recovered from the 1cm screens of each bucket; *Nassarius* sp. and other shells potentially used as ornaments continued to be piece-plotted whenever possible. Identifications are made to the lowest taxonomic level possible, and for each taxon, the MNI (Minimum Number of Individuals; right or left hinges for bivalves; apices for limpets and snails) and NISP (Number of Identified Specimens minus those used for MNI) is recorded. It is common in archaeomalacological analyses to quantify an assemblage using mass. However, much of the Contrebandiers Cave material is covered in carbonate precipitates (Figure 42), which significantly biases this measure. Likewise, quantifying the assemblage by NISP is can be problematic because it is dependent on the degree of fragmentation, which occurs pre- and post-depositionally, during excavation, curation, and analysis. However, MNI counts should remain consistent and will form the basis for most analyses.

Limpets are the most common taxa throughout the sequence and multiple species typical of Atlantic and Mediterranean shores have been identified along the Moroccan coast in the past. The dominant taxon appears to be *P. vulgata*, but this species was not recognized in the previous analyses at Contrebandiers Cave, although it was recognized at Dar es-Soltan I (Neuville in Ruhlmann 1951) only a few kilometers to the north. Limpet species can be difficult to separate because *P. vulgata* exhibits high variability in its morphology, as do many of the other possible species;

TABLE 21a. MOLLUSCAN FAUNA (Number of Identified Specimens [NISP]).

		Iberomaurusian		Aterian						Mousterian						Aterian			
Species	**Common Name**	**IV-1A**	**IV-1B**	**IV-2**	**4A**	**4B**	**4C**	**4D**	**4E**	**5A**	**5B**	**5C**	**5D**	**6A**	**6B**	**V-1A**	**V-1B**	**V-2**	**Grand Total**
Mytilus sp.	Mediterranean or blue mussel	14	8	4	67	9	25	9	-	2	-	-	-	-	-	-	1	-	**139**
Perna perna	Brown mussel	10	8	-	5	-	12	55	-	11	1	21	-	1	-	43	1	-	**168**
	Mussel	109	69	18	186	48	254	459	2	93	62	52	-	3	-	113	6	-	**1,474**
Patella caerulea	Rayed Mediterranean limpet	7	5	3	-	-	1	-	-	-	2	-	-	-	-	-	-	-	**18**
Patella ferruginea	Ribbed Mediterranean limpet	2	-	-	-	-	-	-	-	-	1	-	-	-	-	-	-	-	**3**
Patella nigra	Safian limpet	1	-	1	1	-	1	-	-	-	-	-	-	-	-	-	-	-	**4**
Patella ulyssiponensis	China limpet	4	2	-	-	-	2	-	-	-	1	-	-	-	-	-	-	-	**9**
Patella vulgata	Common/European limpet	26	19	185	189	66	201	27	1	21	22	41	-	2	-	5	11	-	**816**
Patella sp.	Limpet	76	106	514	962	300	841	218	1	152	122	206	1	12	-	64	25	-	**3,600**
Osilinus lineatus	Atlantic marine snail/topshell	9	3	78	149	33	229	181	-	5	6	6	-	-	-	23	1	-	**723**
Stramonita haemastoma	Oyster drill/rock shell	7	5	-	3	1	26	61	-	-	1	-	-	-	-	40	2	-	**146**
Charonia lampas	Predatory sea snail	-	-	-	-	1	-	-	-	-	-	1	-	-	-	-	-	-	**2**
	Terrestrial snails	20	44	60	394	64	300	184	-	11	23	85	-	13	-	37	14	-	**1,249**
	Other	35	45	37	45	21	24	84	-	9	9	16	-	1	-	2	2	-	**330**
	Unknown	-	1	-	-	-	1	3	-	1	-	-	-	-	-	3	-	-	**9**
	Water-worn shell	-	-	-	-	1	-	-	-	-	-	-	-	-	-	-	-	-	**1**
	Unidentifiable fragment	28	28	57	176	36	320	551	2	82	34	82	-	15	2	150	6	-	**1,569**
OTHER MARINE																			
	Fish	-	-	-	-	-	-	1	-	-	-	-	-	-	-	2	1	-	**4**
Crustacea-*Balanus perforatus*	Common barnacle	-	-	-	-	-	-	2	-	1	31	152	1	1	1	8	12	12	**221**
Crustacea-*Pollicipes pollicipes*	Goose neck barnacle	1	-	-	-	-	-	-	-	-	-	2	-	-	-	-	-	3	**6**
Crustacea-Brachyura	Crabs	4	3	-	-	-	-	-	-	-	-	-	-	-	-	1	-	1	**9**
Echinodermata-*Paracentrotus*?	Sea urchin	-	-	-	-	-	-	1	-	-	10	2	-	-	-	-	-	-	**13**
	Grand Total	**339**	**338**	**953**	**2,110**	**571**	**2,212**	**1,827**	**6**	**386**	**325**	**666**	**2**	**48**	**3**	**491**	**81**	**16**	**10,374**

TABLE 21b. MOLLUSCAN FAUNA (Minimum Number of Individuals [MNI]).

		Iberomaurusian		Aterian						Mousterian						Aterian			
Species	**Common Name**	**IV-1A**	**IV-1B**	**IV-2**	**4A**	**4B**	**4C**	**4D**	**4E**	**5A**	**5B**	**5C**	**5D**	**6A**	**6B**	**V-1A**	**V-1B**	**V-2**	**Grand Total**
Mytilus sp.	Mediterranean or blue mussel	6	5	2	18	3	9	6	-	1	-	-	-	-	-	-	1	-	**51**
Perna perna	Brown mussel	8	4	-	4	-	7	30	-	9	1	7	-	1	-	23	1	-	**95**
	Mussel	20	15	4	22	8	25	45	1	5	8	7	-	1	-	19	1	-	**181**
Patella caerulea	Rayed Mediterranean limpet	7	5	3	-	-	1	-	-	-	2	-	-	-	-	-	-	-	**18**
Patella ferruginea	Ribbed Mediterranean limpet	2	-	-	-	-	-	-	-	-	1	-	-	-	-	-	-	-	**3**
Patella intermedia	Black-footed limpet	-	-	-	-	-	-	-	-	-	-	-	-	-	-	-	-	-	**-**
Patella nigra	Safian limpet	1	-	1	1	-	1	-	-	-	-	-	-	-	-	-	-	-	**4**
Patella ulyssiponensis	China limpet	4	2	-	-	-	1	-	-	-	1	-	-	-	-	-	-	-	**8**
Patella vulgata	Common/European limpet	25	19	177	189	65	165	27	1	21	22	41	-	2	-	5	11	-	**770**
Patella sp.	Limpet	35	35	183	271	103	259	47	1	45	23	52	1	1	-	7	5	-	**1,068**
Osilinus lineatus	Atlantic marine snail/topshell	1	1	7	13	3	18	2	-	1	1	2	-	-	-	4	1	-	**54**
Charonia lampas	Predatory sea snail	-	-	-	-	1	-	-	-	-	-	1	-	-	-	-	-	-	**2**
Stramonita haemastoma	Oyster drill/rock shell	1	1	-	1	1	1	3	-	-	1	-	-	-	-	1	1	-	**11**
	Terrestrial snails	2	8	16	45	9	28	11	-	1	2	13	-	1	-	1	2	-	**139**
	Other	25	24	30	45	20	23	83	-	9	4	12	-	1	-	1	1	-	**278**
	Unknown	-	1	-	-	-	1	1	-	1	-	-	-	-	-	1	-	-	**5**
OTHER MARINE																			
	Fish	-	-	-	-	-	-	1	-	-	-	-	-	-	-	1	1	-	**3**
Crustacea-*Balanus perforatus*	Common barnacle	-	-	-	-	-	-	2	-	1	31	152	1	1	1	8	12	12	**221**
Crustacea-*Pollicipes pollicipes*	Goose neck barnacle	1	-	-	-	-	-	-	-	-	-	1	-	-	-	-	-	1	**3**
Crustacea-Brachyura	Crabs	2	1	-	-	-	-	-	-	-	-	-	-	-	-	1	-	1	**5**
Echinodermata-*Paracentrotus*?	Sea urchin	-	-	-	-	-	-	1	-	-	1	1	-	-	-	-	-	-	**3**
	Grand Total	**140**	**121**	**423**	**609**	**213**	**539**	**259**	**3**	**94**	**98**	**289**	**2**	**8**	**1**	**72**	**37**	**14**	**2,922**

Figure 43. Large specimen of Charonia lampas *recovered from Layer 5c.*

local environmental factors may also influence their shell morphology and coloration (Mauro et al. 2003). At Contrebandiers Cave, the problem is again complicated by the carbonates adhering to the shells, and uncertain specimens were recorded simply as *Patella* sp. *P. vulgata* lives in the intertidal of rocky shores and dominates the areas of open rock and patchy seaweed where wave-action is moderate, making them easily accessible to ancient foragers.

At least two types of mussels are apparent in the Contrebandiers Cave assemblages, *Mytilus* and *Perna*. Within *Mytilus*, there may be *M. edulis*, the blue mussel typical of the Atlantic Ocean, or *M. galloprovincialis*, the Mediterranean mussel. However, the genetic distinction, let alone morphological distinction, between these two taxa is subtle or unclear (Gosling 1992; Poppe and Goto 1991; Tebble 1966), and therefore we have not attempted to differentiate between the two. Although mostly complete shells are distinct, fragments of *Mytilus* and *Perna* can also be difficult to separate, and these fragments were assigned to a general mussel category. *Mytilus* can be found on hard substrates in both the intertidal and subtidal and can reach densities of up to 1,000 individuals/m^2; typically intertidal specimens are smaller and subtidal are larger (Poppe and Goto 1991). *Perna* lives on rocks below the low tide mark (Poppe and Goto 1991), and therefore would have been less accessible.

Completing the complement of common marine taxa in the Contrebandiers Cave assemblages is *Osilinus*, a marine snail or topshell, which is also an intertidal rocky shore dweller. Two predatory sea snails also are found in the assemblage, primarily *Stramonita* but also a few examples of *Charonia* (Figure 43); some of these shells have pits from bioeroders inside, suggesting that they were already dead when collected (see also Jerardino and Marean 2010). A few fragments of *Haliotis*, or abalone, were present in the Iberomaurusian assemblage. *Haliotis* also was identified from the Iberomaurusian assemblage at Dar es-Soltan I (Neuville in Ruhlmann 1951) but has not been recognized in any Aterian or Mousterian assemblages. Remains of some small fish, crabs, goose neck barnacles, and sea urchins also were found throughout the samples; the common barnacles are those that live on the backs of limpets and mussels, and therefore were unlikely to have been a source of human subsistence in the past.

Limpet species diversity is higher in the Iberomaurusian sample than in the other assemblages at Contrebandiers Cave, although it is true that the better preservation may have allowed for easier identification of these more recent specimens. At Dar es-Soltan I, the Iberomaurusian occupants also exploited a higher diversity of mollusks than the Aterian occupants (Neuville in Ruhlmann 1951). The limpets, especially the *P. vulgata*, in the Contrebandiers Iberomaurusian sample, are significantly smaller than the same species in the older assemblages, which may be the result of increased human predation on the Iberomaurusian limpets (Steele and Klein 2008). Unfortunately, the hiatus between the youngest Aterian and oldest Iberomaurusian samples limits our ability to discern when this change may have begun.

As seen elsewhere in North Africa (e.g., Lubell 2004), terrestrial snails also are found throughout the Contrebandiers Cave sequence; these specimens may reflect natural deaths or human food refuse. We are currently investigating this assemblage, and further detailed analyses, such as those currently being conducted at Taforalt (Taylor et al. 2011), are needed to understand the landsnails' place within the Contrebandiers Cave assemblages.

To investigate why species composition may change in the Moroccan assemblages, future research will use exist-

Figure 44. Nassarius *sp. shells from the Aterian assemblages at Contrebandiers. Top row:* Nassarius gibbosulus*. Bottom row:* Nassarius circumcinctus*.*

ing off-shore bathymetry data to investigate how changing sea-levels affected the proximity of the ocean to the caves and the proportions of rocky to sandy shores. Fluctuating species abundances also may reflect fluctuating biogeographic boundaries. The Atlantic coast of Morocco belongs to the Saharan Upwelling ecoregion of the Lusitanian province ,while the Mediterranean coast belongs to the Alboran Sea ecoregion of the Mediterranean Sea province (Spalding et al. 2007). Currently, the Lusitanian biogeographic region contains a mix of characteristically Atlantic and Mediterranean taxa. However, due to changing environmental conditions such as changing sea levels, water temperatures, or salinity, more or less Mediterranean species may have been present along the Atlantic shores of Morocco. Future research will investigate these potential fluctuations in species abundances.

NASSARIUS REMAINS POTENTIALLY USED FOR HUMAN ORNAMENTATION

The assemblage of shells from Contrebandiers Cave also contains mollusks with no dietary interest. Humans selected from the local beaches very small gastropods shells; the most abundant are *Nassarius* (*N. gibbosulus* and *N. cincumcinctus*) tick shells, but several other species of small gastropods have been identified (mainly *N. corniculus*, but also *N. incrassatus*, *N. reticulatus*, *Columbella rustica*, *Trivia* sp. and *Littorina obtusata*).

To date research has been focused on the *Nassarius* from the Aterian layers (n=132), but they are also present in the Mousterian (n=19); approximately one-quarter of this sample has been studied in detail. A large number of these specimens have a perforation (as do some of the other small gastropods) usually located on the edge of the labrum in the part next to the columella (Figure 44). Although the Contrebandiers Cave sample of *Nassarius* is the largest yet described, elsewhere in North Africa and the Near East, similar examples of these species have been considered to be shell beads. They have been found at Skhul Cave (two without clear context), Oued Djebbana (one), Ifri n´Ammar (one), Rhafas (one in context and four without context) and Taforalt (38; 11 without context), and finally, there is one example from Bouzouggar´s work at Contrebandiers Cave (Bouzouggar et al. 2007; d´Errico et al. 2009; Nami and Moser 2010; Vanhaeren et al. 2006). *Nassarius* also have been documented in fossil beaches in Morocco (Brébion 1983; see also Barton et al. 2009), and natural Late Pleistocene *Nassarius* sp. were found at the base of the Dar es-Soltan I sequence (Layer M, identified by Ruhlman in 1951) dated by OSL between 150 and 130 ka (D´Errico et al. 2009; Barton et al. 2009).

One aspect of the methodology for studying these remains was to photograph the different sides of each shell, followed by an examination under a microscope equipped with a digital camera. This allowed for the identification of surface modifications on the shells and perforation edges, including damage inflicted by bioeroders, perforations made by predators, marine erosion, carbonate precipitation, use wear, color changes made by heating and absence of oxygen, post-depositional damage like decalcification, and manganese traces, and examination of sediment resi-

Figure 45. Nassarius *sp. with marine erosion in the apex and smooth faceting in the perforation and natural black color on the surface (Layer 4c).*

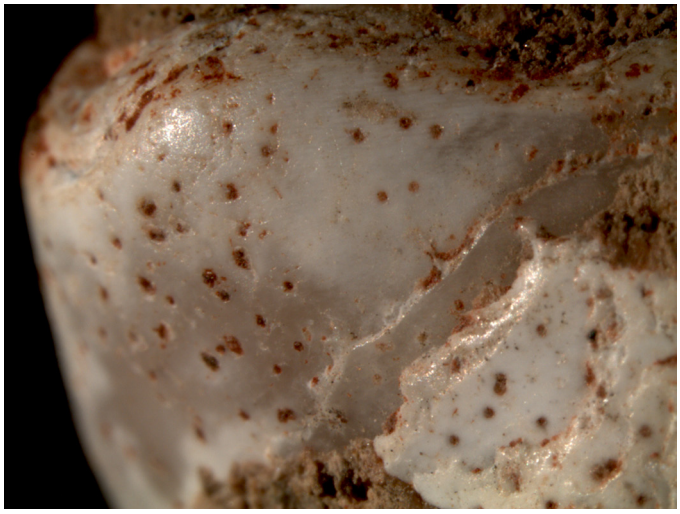

Figure 46. Nassarius gibbosulus *with holes (from bioerosion) filled with ochre and exhibiting marine erosion in the apex (Layer 4d).*

dues. Maximum shell height, width, and thickness (in mm) on all archaeological shells were measured with digital calipers, along with maximum and minimum diameter (in mm) of unbroken perforations. When necessary for the analysis, specimens were cleaned under the microscope with a dry soft brush and a wooden toothpick. An experimental program is underway to reproduce the perforations and use wear on recent and geological *Nassarius* for comparisons with the archaeological specimens. The study of the geological specimens is important because they are closer in size and preservation to the specimens from Contrebandiers Cave.

All of the specimens present a muted shell sculpture with a smoothing of the apex that is typical of mechanical abrasion on the shore (Figure 45 and Figure 46). Additional evidence supporting this conclusion is that some of them present gastropods predator holes or bioeroders pits (see Figure 45) and alterations by other marine organism (e.g., *Polydora*) on their surfaces. One of them is partially blackened because the shell was buried in beach sand in anaerobic conditions (without oxygen) (see Figure 46). This evidence indicates that the shells were collected after they were already dead on the shore and therefore they cannot be interpreted as the remains of subsistence-related activities. *Nassarius* are scavengers that inhabit the calm waters and sandy-muddy bottoms of brackish and marine environments.

Furthermore, microscopic features diagnostic of human intervention in the production of the perforation are absent; there are no traces of preparation of the perforations (by abrasion, incision, etc.). Some perforations show intense shine on the edge (Figure 47). It is hoped that in the course of the experimental studies it will be possible to determine if these patterns could be due to human use or other causes. Microscopic residues of red sediment are detected on some perforated *N. gibbosulus* and *N. circumcinctus* shells. The residues are located in different parts of the shells—on the body whorl and the parietal shield, on the perforation edges, or on the entire surface. In one case, red sediment fills pits left by bioeroders located on its entire outer surface (see Figure 46). In our experimental studies, we will investigate the source of the pigments, including potential human application.

There are also a significant number of shell surfaces that were affected by the post-depositional percolation of water in the cave. The resulting decalcification and precipitation of carbonate and manganese makes it difficult to study these shells under the microscope and so these will await further treatment and study.

SUMMARY AND CONCLUSIONS

The recent excavations at Contrebandiers Cave have recovered many important elements that have not only clarified the situation at this site, but which also contribute to un-

Figure 47. Nassarius gibbosulus *with smooth faceting in the perforation (Layer 4d).*

derstanding the larger role of Morocco in the emergence of modern humans.

This work allowed for a re-assessment of the stratigraphy in the central portion of the cave and the characterization of the deposits in one new loci of the site, namely in Sector V, located towards the back of the cave. The new stratigraphic layout can be roughly correlated overall with the previously developed stratigraphy by Roche and Texier (1976), but it adds a more comprehensive view of lateral variations of the deposits and their overall geometry. For instance, in the area of sector IV the Aterian layer (Layer IV-2) is truncated and Iberomaurusian associated sediments are only locally preserved in a cut/fill type of structure. Roche had identified the Iberomaurusian occupations as representing pit infills. However, since our excavations in this area are located more than 2m away from the original profile of Roche, it seems doubtful that these features represent anthropic pits, given their elliptical shape and total width of several meters. While the processes responsible for this unconformity are still being investigated, the local erosion of an undetermined thickness of the underlying deposits has clear implications for understanding these late Aterian occupations at Contrebandiers. It seems reasonable to assume, for instance, that in this area, the ages obtained for Layer IV-2 do not necessarily express the final Aterian occupations at Contrebandiers, since part of the deposits were, at least locally, eroded.

In the CEA, lateral variation of the deposits is expressed in several ways, but especially in the localized presence of carbonated crusts and calcium carbonate cementation of the sediments. In addition, at least from lithostratigraphic Unit C1 onwards (i.e., the top of archaeological Layer 6a/b) there is a clear dip of the deposits towards the interior of the cave, roughly in the areas of squares G-H 15/13, presumably due to the presence of a swallow hole in this area. Such slumping of the sediments also affects the cemented crust C1 that shows a clear fracture (which occurred sometime after the sediments were cemented) visible in Square G 18/17. Further excavations in this location of the site can help determine the causes for the observed dip directions. Episodes of roof/wall collapse are expressed throughout the CEA in the contact between Layers 5a and 4, and localized blocks are also present in the Aterian layers in Squares H-J 14/13 and in Layer IV-1, which is associated with the Iberomaurusian.

The basal layer at the site, that is, Layer 7, exposed in the CEA presents lithostratigraphic characteristics that can be associated with a marine incursion during the last high sea level stand around 125 ka (MIS 5e). MIS 5e beach deposits have also been identified in other cave sites in the area of Témara, namely at the base of the stratigraphic sequence at Dar-es-Soltan I (Barton et al. 2009). All of the above deposits can be associated with terrestrial depositional conditions with varying inputs of anthropogenic components.

The first human occupations at Contrebandiers Cave occur in the deposits that rest just above the marine beach sands (Layer 7) and are seen in the presence of localized combustion features and artifacts. Human occupations also are well expressed in the somewhat more organic archaeological Layer 5 where there is a relative abundance of combustion associated sediments (ashes, charcoal, burned bone and lithics, etc.). Combustion residues in association with the Aterian are present in Sector V in the form of ash and charcoal lenses. The depositional environment in Sector V is characterized by an increase of clay components when compared with the CEA and Sector IV deposits. Phosphatization is also an important process in this area at the back of the cave and the degree of alteration of the deposits is currently being analyzed. Rodent and insect bioturbation (namely by wasps) is ubiquitous throughout the excavated areas.

In order to obtain an absolute chronology to compliment the stratigraphic and archaeological observations, three different dating techniques were used, namely OSL dating of sediments, TL dating of burned lithics, and ESR dating of ungulate teeth. These three methods produced broadly comparable results, suggesting that the layers in which the Mousterian (Layers 5 and 6) and Aterian (Layers 4, IV-2, V-1, and V-2) assemblages were found are between ~90 and 120 ka old, and started to accumulate shortly after deposition of the basal beach sand during MIS 5e at ~125 ka. At the present time it is not possible to resolve with sufficient precision any difference in the timing of the Mousterian and Aterian, but it is clear that the majority of the pre-Iberomaurusian deposits accumulated relatively rapidly during MIS 5. Further chronological work is ongoing to resolve the timing of the Iberomaurusian and Neolithic deposits in the cave, and to further our understanding of the time of formation and subsequent modification of some of the geological features observed in the stratigraphy.

Regarding the lithic assemblages, only small pockets of sediments containing Iberomaurusian assemblages remain at the site, just outside the current dripline in excavation Sector IV. While there are clear similarities between what can be seen in Roche's earlier collections and what was recovered in the new excavations, the major difference is the higher proportion of nongeometric microliths (including Ain Keda points) in the latter collection. This is probably due to the more meticulous excavation techniques currently being used. In addition to these pieces, the Iberomaurusian assemblage contains endscrapers, burins, and backed tools, *pièces esquillées*, cores, blades and bladelets, microburins, and many small flakes.

The bulk of the lithic assemblages from Contrebandiers Cave represent both Aterian and Mousterian assemblages, with or without tanged pieces, respectively. It is quite clear, however, that aside from the presence/absence of this one distinctive element, the two kinds of assemblages are quite similar, with low percentages of Levallois, few retouched tools, and some production of small flakes (see Dibble et al. submitted). Overall, the generally low density of lithic artifacts suggests that the cave was occupied only ephemerally. Based on the analysis of cortex, there is a high probability that most of the flakes, tools, and cores were brought into the site after having been, at least preliminarily, flaked elsewhere, and this is especially true for the fine-grained

materials. In some of the assemblages, the coarser-grain quartzite appears to have been exported from the site. Ongoing analyses of the raw materials that were used, and their sources, should help to shed some light on patterns of mobility of these groups.

The faunal assemblages from the Mousterian and Aterian layers at Contrebandiers Cave, as represented by large and small mammals and reptiles, as well as shellfish, indicate shrubland or grassland habitats in a coastal setting. The microfauna suggests a consistent dry grassland to dry shrubland environment throughout the deposition, while the macrofauna indicate a minor change to drier shrubland habitats in the Aterian. This may suggest that during the initial occupations of the cave the habitat closer to the cave was drier, as represented by the microfauna, than habitats further afield, because the larger fauna from these layers indicate habitats that were slightly wetter. The macro and microfauna from the Aterian layers both indicate overall dry shrubland environments. The ancient habitat was likely a coastal Mediterranean mosaic, with more shrubland type habitats consistently near the cave, and similar to the stone artifacts, there are not strong distinctions between the Aterian and Mousterian. The mollusks indicate that the sea level did not fluctuate much during the depositional period, or at least that sea levels did not drop enough to alter the human occupants' shellfish acquisition patterns. Complete zooarcheological analyses of the fauna from Contrebandiers Cave have not been finished, but there are preliminary indications that both carnivores and humans accumulated the fauna in varying degrees per layer.

Contrebandiers Cave has also yielded a large sample of non-subsistence related shells, principally *Nassarius*. Ongoing studies of these gastropods will hopefully help to reveal why they were being brought into the site.

Altogether, the new excavations at Contrebandiers Cave have clarified many of the details surrounding this important site. Along with the results from several other excavations currently underway in the surrounding area, the data that are emerging from this site will help to shed light into many of the conditions under which early modern *H. sapiens* lived.

ACKNOWLEDGEMENTS

The project at Contrebandiers Cave is a joint Moroccan-American project under the auspices of the Moroccan Institut National des Sciences de l'Archéologie et du Patrimoine (INSAP). While all of the authors contributed in the writing of the overall article, various sections primarily reflect the results of particular individuals—geology and site formation (Aldeias and Goldberg); OSL dating (Jacobs, Meyer, and Roberts); TL dating (Richter); ESR dating (Blackwell and Skinner); Aterian and Mousterian lithic assemblages (el-Hajraoui, Dibble, Lin, Sandgathe, and Rezek); Iberomaurusian lithics (Olszewski); lithic raw materials (Morala); macrofauna (K. Reed and Hallet-Desguez); microvertebrates (D. Reed); and malacology (Steele and Alvarez-Fernández).

The majority of this research was funded by the National Science Foundation (BCS-0935491), the Australian Research Council through Discovery Project grants DP0666084 to Jacobs and DP1092843 to Jacobs and Dibble, and with other contributions from the National Science Foundation, Leakey Foundation, the National Geographic Society, the Max Planck Society for Evolutionary Anthropology, the Institute for Human Origins (Arizona State University), McMaster University, Williams College, the RFK Science Research Institute, and the University Research Foundation of the University of Pennsylvania. The funders had no role in study design, data collection and analysis, decision to publish, or preparation of the manuscript.

Thanks are due to Rita Gaspar and Ekaterina Doronicheva for the artifact illustrations; Alice Pidruczny who performed the NAA analyses at McMaster University, and to Elizabeth Pasipodany (Williams College), E.K.Cho, J.J.Huang, Tiffany Yau, and C. X. Y.Zhou (RFK Science Research Institute) for ESR sample preparation. The authors would especially like to thank the administration and personnel of INSAP for their help and hospitality.

REFERENCES

Abbasi, M. and Aouraghe, H. 2002. The rodents form the Aterian site of El Harhoura 1 (Témara, Morocco). *Quaternaire* 13, 125–136.

Aitken, M.J. 1985. *Thermoluminescence Dating*. Academic Press, London.

Alperson-Afil, N., Richter, D., and Goren-Inbar, N. 2007. Phantom hearths and the use of fire at Gesher Benot Ya'aqov, Israel. *PaleoAnthropology* 2007, 1–15.

Andrews, P. 1990. *Owls, Caves, and Fossils*. University of Chicago Press, Chicago.

Aouadi-Abdeljaouad, N. and Belhouchet, L. 2008. Recent prehistoric field research in Central Tunisia: Prehistoric occupations in the Meknassy Basin. *African Archaeological Review* 25, 75–85.

Arnold, L.J. and Roberts, R.G. 2009. Stochastic modelling of multi-grain equivalent dose (D_e) distributions: Implications for OSL dating of sediment mixtures. *Quaternary Geochronology* 4(3), 204–230.

Aulagnier, S. and Thevenot, M. 1986. Catalogue des mammifères sauvages du Maroc. *Travaux de l'Institut Scientifique, Rabat, Série Zoologie*, 41, pp. 1–164.

Balter, M. 2011. Was North Africa the launch pad for modern human migration? *Science* 331, 20-23.

Barich, B.E., Garcea, E.A.A., and Giraudi, C. 2006. Between the Mediterranean and the Sahara: Geoarchaeological reconnaissance in the Jebel Gharbi, Libya. *Antiquity* 80, 567–582.

Barich, B.E. and Garcea, E.A.A. 2008. Ecological patterns in the upper Pleistocene and Holocene in the Jebel Gharbi, Northern Libya: Chronology, climate and human occupation. *African Archaeological Review* 25, 87–97.

Barton, R.N.E., Bouzouggar, A., Collcutt, S.N., Gale, R., Higham, T.F.G., Humphrey, L.T., Parfitt, S., Rhodes, E., Stringer, C.B., and Malek, F. 2005. The late upper Palaeolithic occupation of the Moroccan Northwest

Maghreb during the last glacial maximum. *African Archaeological Review* 22, 77–100.

Barton, R.N.E., Bouzouggar, A., Collcutt, S.N., Schwenninger, J.-L., and Clark-Balzan, L. 2009. OSL dating of the Aterian levels at Dar es-Soltan I (Rabat, Morocco) and implications for the dispersal of modern *Homo sapiens*. *Quaternary Science Reviews* 28, 1914–1931.

Belcastro, M.G., Condemi, S. and Mariotti, V. 2010. Funerary practices of the Iberomaurusian population of Taforalt (Tafoughalt, Morocco, 11-12,000 BP): the case of Grave XII. *Journal of Human Evolution* 58, 522–532.

Bellomo, R.V. 1993. A methodological approach for identifying archaeological evidence of fire resulting from human activities. *Journal of Archaeological Science* 20, 525–553.

Blackwell, B.A. 1989. *Laboratory Procedures for ESR Dating of Tooth Enamel*. McMaster University Department of Geology Technical Memo 89.2.

Blackwell, B.A. 2006. Electron spin resonance (ESR) dating in karst environments. *Acta Carsologica* 35, 123–153.

Blackwell, B.A., Porat, N.P., Schwarcz, H.P., and Debénath, A. 1992. ESR dating of tooth enamel: Comparison with $^{230}Th/^{234}U$ speleothem dates at La Chaise-de-Vouthon (Charente), France. *Quaternary Science Reviews* 11, 231–244.

Blackwell, B.A., Rutter, N.W., and Last, W.M. 2000. Biogeochemical diagenesis in recent mammalian bones from saline lakes in western Victoria, Australia. In: *Perspectives in Amino Acid and Protein Geochemistry*, Goodfriend, G.A., Collins, M.J., Fogel, M.L., Macko, S.A., and Wehmiller, J.F. (eds.). Oxford University Press, New York, pp. 88–107.

Blackwell, B.A., Skinner, A.R., Blickstein, J.I.B., Lebel, S., and Leung, H.Y.M. 2001. ESR isochron analyses at Bau de l'Aubesier, Provence: Clues to U uptake in fossil teeth. *Geoarchaeology* 16, 719–761.Blumenschine, R.J., Marean, C.W., and Capaldo, S.D. 1996. Blind tests of interanalyst correspondence and accuracy in the identification of cut marks, percussion marks, and carnivore tooth marks on bone surfaces. *Journal of Archaeological Science* 23, 493–508.

Bordes, F. 1961 Mousterian cultures in France. *Science* 134, 803–810.

Bouzouggar, A. 1997a. Économie des matières premières et du débitage dans la séquence atérienne de la grotte d'El Mnasra I (ancienne grotte des Contrebandiers-Maroc). *Préhistoire Anthropologie Méditerranéenne* 6, 35–52.

Bouzouggar, A. 1997b. *Matières premières, processus de fabrication et de gestion des supports d'outils dans la séquence atérienne de la grotte des Contrebandiers à Temara*. Ph.D. Dissertation, Université de Bordeaux.

Bouzouggar, A., Kozlowski, J.K., and Otte, M. 2002. Étude des ensembles lithiques atériens de la grotte d'El Aliya à Tanger (Maroc). *L'Anthropologie* 106, 207–248.

Bouzouggar, A., Barton, N., Vanhaeren, M., d´Errico, F., Collcutt, S., Higham, T., Hodge, E., Parfitt, S., Rhodes, E., Schwenninger, J.L., Stringer, C., Turner, E., Ward, S., Moutmir, A., and Stambouli, A. 2007. 82,000-year-old shells beads from North Africa and implications for the origins of modern human behavior. *Proccedings of the National Academy of Sciences USA* 104, 9964–9969.

Brébion, P. 1983. Paleoclimatologie du Quaternaire Marin du Maroc Atlantique. Methodes d'etude—Variations dans le temps and dans l'espace. *CNRS Cahiers du Quaternaire*, 179–186.

Brennan, B.J., Rink, J.W., McGuire, E.L., and Schwarcz, H.P. 1997. β doses in tooth enamel by "one-group" theory and the Rosy ESR dating software. *Radiation Measurements* 27, 307–314.

Briggs, L.C. 1967. Appendix B. The mollusks. In: *The Palaeolithic of Tangier, Morocco: Excavations at Cape Ashakar, 1939-1947*, Howe, B. (ed.). Cambridge, MA: The Peabody Museum, pp. 187.

Cadenat, P. 1953. Une nouvelle station atérienne au Koudiat bou Gherara (Commune Mixte de Tiaret). *Libyca* A/P/E I, Janvier 1953.

Caton-Thompson, G. 1946. The Aterian industry: its place and significance in the Palaeolithic world. *Royal Anthropological Institute of Great Britain and Ireland* 76, 87–130.

Chavaillon, N. 1960. L'Atérien de Zaouia el Kebira (Saoura). *Bulletin de la Société préhistorique française* 57, 214–222

Chavaillon, N. 1985. L'Atérien du Foum el Hartani au Sahara nord-occidental (République Algérienne). *Bulletin de la Société préhistorique française*, 82, 307–337.

Close, A.E. 1989. Report on Site E-81-1: an early Kubbaniyan site on the edge of the Kubbaniyan dune field. In: *The Prehistory of Wadi Kubbaniya*, Volume 3. *Late Paleolithic Archaeology*, Wendorf, F., Schild, R., and Close A.E. (eds.). Southern Methodist University Press, Dallas, pp. 490–523.

Cremaschi, M., Lernia, S.D., and Garcea, E.A.A. 1998. Some insights on the Aterian in the Libyan Sahara: chronology, environment, and archaeology. *African Archaeological Review* 15, 261–285.

David, B., Roberts, R.G., Magee, J., Mialanes, J., Turney, C., Bird, M., White, C., Fifield, K., and Tibby, J. 2007. Sediment mixing at Nonda Rock: investigations of stratigraphic integrity at an early archaeological site in northern Australia and implications for the human colonisation of the continent. *Journal of Quaternary Science* 22, 449–479.

Debénath, A. 1976. Le site de Dar Es Soltane 2 a Rabat (Maroc). *Bulletin et Mémoires de la Societé d'Anthropologie de Paris* 3, 181–182.

Debénath, A. 2000. Le peuplement préhistorique du Maroc : Données récentes et problèmes. *L'Anthropologie* 104, 131–145.

Debénath, A. and Dibble. H. 1994. *Handbook of Paleolithic Typology Vol 1: The Lower and Middle Paleolithic of Europe*. The University Museum, University of Pennsylvania, Philadelphia, PA.

De Heinzelin, J., Clark, J.D., White, T., Hart, W., Renne, P., WoldeGabriel, G., Beyene, Y., and Vrba, E. 1999. Environment and behavior of 2.5-million-year-old Bouri hominids. *Science* 284, 625–629.

d´Errico, F., Vanhaeren, M., Barton, N., Bouzouggar, A.,

Mienis, H., Richter, D., Hublin, J.-J., McPherron, S, and Lozouet, P. 2009. Additional evidence on the use of personal ornaments in the Middle Paleolithic of North Africa. *Proccedings of the National Academy of Sciences USA* 106, 16051–16056.

Dibble, H.L. and McPherron, S.P. 2006. The Missing Mousterian. *Current Anthropology* 47, 777–803.

Dibble, H.L., Lenoir, M., Holdaway, S., Roth, B., and Sanders-Gray, H. 1995. Techniques of excavation and analysis. In: *The Middle Paleolithic Site of Combe-Capelle Bas (France)*, Dibble, H. and Lenoir, M. (eds.). University Museum Press, University of Pennsylvania, Philadelphia, PA, pp. 27–40.

Dibble, H.L., Schurmans, U.A., Iovita, R.P., and McLaughlin, M.V. 2005. The measurement and interpretation of cortex in lithic assemblages. *American Antiquity* 70, 545–560.

Dibble, H.L., Aldeias, V., Jacobs, Z., Olszewski, D.I., Rezek, Z., Lin, S., Alvarez-Fernández, E., Barshay-Szmidt, C., Hallett-Desguez, E., Reed, D., Reed, K.E., Richter, D., Steele, T., Skinner, A., Blackwell, B.A., Doronicheva, E., and El-Hajraoui, M.A. Submitted. On the Industrial Attribution of the Moroccan Aterian and Mousterian. *Journal of Human Evolution*

Douglass, M. 2010. *The Archaeological Potential of Informal Lithic Technologies: A Case Study of Assemblage Variability in Western New South Wales, Australia*. Ph.D. thesis, Anthropology Departent, The University of Auckland.

Duller, G.A.T. 2008. Single-grain optical dating of Quaternary sediments: why aliquot size matters in luminescence dating. *Boreas* 37, 589–612.

El Hajraoui, M.A. 2004. *Le Paléolithique du domaine mésetien septentrional. Données récentes sur le littoral: Rabat, Témara et la Mamora*. Ph.D. Dissertation, Université Mohamed.

Falguères, C., Bahain, J.J., Dolo, J.M., Mercier, N., and Valladas, H. 2007. On the interest and the limits of using combined ESR/U-series model in the case of very late uranium uptake. *Quaternary Geochronology* 2, 403–308.

Ferembach, D. 1976. Les restes humains Atériens de Témara (Campagne 1975). *Bulletin et Mémoires de la Societé d'Anthropologie de Paris* 3–13, 175–180.

Ferembach, D. 1985. On the origin of the Iberomaurusians (Upper Palaeolithic: North Africa). A new hypothesis. *Journal of Human Evolution* 14, 393–397.

Ferembach, D. 1998. Le crâne Atérien de Témara (Maroc Atlantique). *Bulletin D'Archéologie Marocaine* 18, 19–66.

Galbraith, R.F. 2003. A simple homogeneity test for estimates of dose obtained using OSL. *Ancient TL* 21, 75–78.

Galbraith, R.F., Roberts, R.G., Laslett, G.M., Yoshida, H., and Olley , J.M. 1999. Optical dating of single and multiple grains of quartz from Jinmium Rock Shelter, Northern Australia: Part I, experimental design and statistical models. *Archaeometry* 41, 339–364.

Garcea, E.A.A. 2010. The spread of Aterian peoples in North Africa. In: *South-Eastern Mediterranean Peoples Between 130,000 and 10,000 Years Ago*, Garcea, E.A.A. (ed.). Oxbow Books, Oxford, pp. 37–53.

Garcea, E.A.A. and Giraudi, C. 2006. Late Quaternary human settlement patterning in the Jebel Gharbi. *Journal of Human Evolution* 51, 411–421.

Geraads, D. 1994. Rongeurs et lagomorphes du Pléistocène moyen de la "Grotte des Rhinocéros", carrière Oulad Hamida 1, à Casablanca, Maroc. *Neues Jahrbuch für Geologie und Paläontologie Abhandlungen* 191, 147–172.

Gosling, E.M. 1992. Systematics and geographic distribution of *Mytilus*. In: *The Mussel Mytilus: Ecology, Physiology, Genetics and Culture*, Gosling, E.M. (ed.). Elsevier, Amsterdam, pp. 1–20.

Grayson, D.K. 1984. *Quantitative zooarchaeology: topics in the analysis of archaeological faunas*. Academic Press, Orlando.

Gruet, M. 1958-1959. Le gisement d'El Guettar es sa flore. *Libyca* 6-7, 79–126.

Grün, R., Chadam, J., and Schwarcz, H.P. 1988. Electron spin resonance (ESR) dating of tooth enamel: Coupled correction for U uptake and U-series disequilibrium. *Nuclear Tracks & Radiation Measurements* 14, 237–241.

Grün, R. 2006. Direct dating of human remains. *Yearbook of Human Anthropology* 49, 2–48.

Hawkins, A.L. 2004. A model for Aterian usage of Dakhleh Oasis and the surrounding area. In: Settlement Dynamics of the Middle Paleolithic and Middle Stone Age II, Conard, N. (ed.). Kerns Verlag, Tübingen, pp. 37–64.

Hawkins, A.L. 2008. Preliminary report on the Aterian at Dakhleh Oasis, Western Desert of Egypt. In: *The Oasis Papers 2: Proceedings of the Second International Conference of the Dakhleh Oasis Project*, Wiseman, M.F. (ed.). Oxbow Books, Oxford, pp. 73–82.

Henshilwood, C.S., d'Errico, F., Yates, R., Jacobs, Z., Tribolo, C., Duller, G.A.T., Mercier, N., Sealy, J.C., Valladas, H., Watts, I., and Wintle, A.G. 2002. Emergence of modern human behavior: Middle Stone Age engravings from South Africa. *Science* 295, 1278–1280.

Henshilwood, C.S., d'Errico, F., and Watts, I. 2009. Engraved ochres from the Middle Stone Age levels at Blombos Cave, South Africa. *Journal of Human Evolution* 57, 27–47.

Horai, S., Hayasaka, K., Kondo, R., Tsugane, K., and Takahata, N. 1995. Recent African origin of modern humans revealed by complete sequences of hominoid mitochondrial DNAs. *Proccedings of the National Academy of Sciences USA* 92, 532–536.

Howe, B. 1967. *The Palaeolithic of Tangier, Morocco. Excavation at Cape Ashakar, 1939-1947*. American School of Prehistoric Research, Bulletin 22. Cambridge, MA, Peabody Museum, Harvard University.

Hublin, J.-J. 1992. Recent human evolution in northwestern Africa. *Philosophical Transactions of the Royal Society* 337, 185–191.

Hublin, J.-J. 1993. Recent human evolution in Northwestern Africa. In: *The Origin of Modern Humans and the Impact of Chronometric Dating*, Aitken, C.S.M. and Mellars, P. (eds.). Princeton University Press, Princeton, pp. 118–131.

Hublin, J.-J. 2001. Northwestern African Middle Pleistocene hominids and their bearing on the emergence of *Homo*

sapiens. In: *Human Roots: Africa and Asia in the Middle Pleistocene*, Barham, L. and Robson, K. (eds.). Western Academic and Specialist Press Ltd, Bristol, pp. 99–122.

Ikeya, M. 1982. A model of linear uranium accumulation for ESR age of Heidelberg. Mauer, and Tautavel bones, *Japanese Journal of Applied Physics* 21, L690–692.

Jacobs, Z., Roberts, R.G., Nespoulet, R., El Hajraoui, M.A., and Debénath, A. 2012. Single-grain OSL chronologies for Middle Palaeolithic deposits at El Mnasra and El Harhoura 2, Morocco: implications for Late Pleistocene human–environment interactions along the Atlantic coast of northwest Africa. *Journal of Human Evolution* 62, 377–394.

Jacobs, Z., Meyer, M.C., Roberts, R.G., Aldeias, V., Dibble, H., and El Hajraoui, M.A. 2011. Single-grain OSL dating at La Grotte des Contrebandiers ('Smugglers' Cave'), Morocco: improved age constraints for the Middle Paleolithic levels. *Journal of Archaeological Science* 38, 3631–3643.

Jacobs, Z. 2010. An OSL chronology for the sedimentary deposits from Pinnacle Point Cave 13B—A punctuated presence. *Journal of Human Evolution* 59, 289–305.

Jacobs, Z., Duller, G.A.T., Wintle, A.G., and Henshilwood, C.S. 2006. Extending the chronology of deposits at Blombos Cave, South Africa, back to 140ka using optical dating of single and multiple grains of quartz. *Journal of Human Evolution* 51, 255–273.

Jacobs, Z. and Roberts, R.G. 2007. Advances in optically stimulated luminescence dating of individual grains of quartz from archaeological deposits. *Evolutionary Anthropology* 16, 210–223.

Jacobs, Z., Roberts, R.G., Galbraith, R.F., Deacon, H.J., Grün, R., Mackay, A., Mitchell, P., Vogelsang, R., and Wadley, L. 2008. Ages for Middle Stone Age of Southern Africa: implications for human behaviour and dispersal. *Science* 322, 733–735.

Jaeger, J.-J. 1975. *Les Muridae (mammalia, Rodentia) du Pliocène et du Pléistocene du Maghreb. Origine; Evolution; Données biogéographiques et paléoclimatiques*. Ph.D. Dissertation, Université de Montpellier.

Jerardino, A. and Marean, C.W. 2010. Shellfish gathering, marine paleoecology and modern human behavior: perspectives from cave PP13B, Pinnacle Point, South Africa. *Journal of Human Evolution* 59, 412–424.

Klein, R.G. 2001. Southern Africa and modern human origins. *Journal of Anthropological Research* 57, 1–16.

Klein, R.G. and Scott., K. 1986. Re-analysis of faunal assemblages from the Haua Fteah and other Late Quaternary archaeological sites in Cyrenaican Libya. *Journal of Archaeological Science* 13, 515–542.

Lombard, M., Wadley, L., Jacobs, Z., Mohapi, M., and Roberts, R.G. 2010. Still Bay and serrated points from Umhlatuzana Rock Shelter, Kwazulu-Natal, South Africa. *Journal of Archaeological Science* 37, 1773–1784.

Lubell, D. 2004. Prehistoric edible land snails in the circum-Mediterranean : the archaeological evidence. In: *Petits animaux sociétés humaines: du complément alimentaire aux ressources utilitaires*, Brugal, J.-P. and Desse, J. (eds.). Éditions APDCA, Antibes, pp. 77–98.

Marean, C.W. and Kim, S.Y. 1998. Mousterian large-mammal remains from Kobeh Cave: behavioral implications for Neanderthals and early modern humans. *Current Anthropology* 39, S79–S114.

Marean, C.W. and Thompson, J.C. 2003. Research on the origins of modern humans continues to dominate paleoanthropology. *Evolutionary Anthropology* 12, 165–167.

Marean, CW., Abe., Y., Nilssen, P.J., and Stone, E.C. 2001. Estimating the minimum number of skeletal elements (MNE) in zooarchaeology: a review and a new image-analysis GIS approach. *American Antiquity* 66, 333–348.

Marean, C.W., Bar-Matthews, M., Bernatchez, J., Fisher, E., Goldberg, P., Herries, A.I.R., Jacobs, Z., Jerardino, A., Karkanas, P., Minichillo, T., Nilssen, P.J., Thompson, E., Watts, I., and Williams, H.M. 2007. Early human use of marine resources and pigment in South Africa during the Middle Pleistocene. *Nature* 449, 905–908.

Mauro, A., Arculeo, M., and Parrinello, N. 2003. Morphological and molecular tools in identifying the Mediterranean limpets *Patella caerulea*, *Patella aspera* and *Patella rustica*. *Journal of Experimental Marine Biology and Ecology* 295, 131–143.

McBrearty, S. and Brooks, A.S. 2000. The revolution that wasn't: a new interpretation of the origin of modem human behavior. *Journal of Human Evolution* 39, 453–563.

McBurney, C. 1967. *The Haua Fteah (Cyrenaica) and the Stone Age of the Eastern Mediterranean*. Cambridge University Press, Cambridge, UK.

McDougall, I., Brown, F.H., and Fleagle, J.G. 2005. Stratigraphic placement and age of modern humans from Kibish, Ethiopia. *Nature* 433, 733–736.

McPherron, S. and Dibble. H. 2002. *Using Computers in Archaeology: A Practical Guide*. McGraw-Hill Mayfield, Boston.

Ménard, J. 1998. Odontologie des dents de la grotte de Temara (Maroc). *Bulletin d'Archéologie Marocaine* 18, 67–97.

Mercier, N., Wengler, L., Valladas, H., Joron, J.L., Froget, L., and Reyss, J.L. 2007. The Rhafas Cave (Morocco): Chronology of the Mousterian and Aterian archaeological occupations and their implications for Quaternary geochronology based on luminescence (TL/OSL) age determinations. *Quaternary Geochronology* 2, 309-313.

Michel, P., Campmas, E., Stoetzel, E., Nespoulet, R., El Hajraoui, M.A., and Amani, F. 2010. La grande faune du Paléolithique supérieus (niveau 2) et du Paléolithique moyen (niveau 3) de la grotte d'El Haroura 2 (Témara, Maroc): etude peléontologique, reconstitutions paléoécologiques et paléoclimatiques. Historical Biology 22, 327–340.

Minugh-Purvis, N. 1993. Reexamination of the immature hominid maxilla from Tangier, Morocco. *American Journal of Physical Anthropology* 92, 449–461.

Morel, J. 1974. La station éponyme de l'Oued Djebbana à Bir-el-ater (est algérien). Contribution à la connaissance de son industrie et de sa faune. *L'Anthropologie* 78, 53-80.

Morel, J. 1978. L'industrie atérienne de l'Oued Djouf El Djemel. Comparaison avec l'industrie de l'Oued Djebbana. Le complexe atérien du Maghreb Oriental. *Bulletin de la Société Préhistorique Française* 75, 487–500.

Moser, J. 2003. *La Grotte d'Ifri n'Ammar*. Tome 1. *L'Ibéromaurusien*. Linden Soft, Deutsches Archaologisches Institut, Köln.

Murray, A.S. and Wintle, A.G. 2000. Luminescence dating of quartz using improved single-aliquot regenerative-dose protocol. *Radiation Measurements* 32, 57–73.

Musser, G. and Carleton, M.D. 2005. Superfamily Muroidea; In: *Mammal Species of the World: A Taxonomic and Geographic Reference* (3rd edition), Volume 2, Wilson, D. and Reeder, D. (eds.). Johns Hopkins University Press, Baltimore, pp. 894–1531.

Nami, M. and Moser, J. 2010. *La Grotte D'Ifri n'Ammar*. Tome 2. *Le Paléolithique Moyen*. Reichert Verlag, Deutsches Archaologisches Institut, Wiesbaden.

Nespoulet, R. and El Hajraoui, M.A. 2004. Mission archaeologique El Haroura-Temara. Rapport d'áctivites 2004, p. 117.

Nespoulet, R., El Hajraoui, M.A., Amani, F., Ben Ncer, A., Debénath, A., El Idrissi, A., Lacombe, J.-P., Michel, P., Oujaa A., and Stoetzel. E. 2008. Palaeolithic and Neolithic occupations in the Témara region (Rabat, Morocco): recent data on hominin contexts and behavior. *African Archaeological Review* 25, 21–39.

Niftah, S. 2003. *Étude géologique des grottes du littoral atlantique marocain: El Harhoura 2, El Mnasra et grotte des Contrebandiers à Témara*. Ph.D. Dissertation, Université de Perpignan.

Niftah, S., Debenath, A., and Miskovsky, J.C. 2005. Origine du remplissage sédimentaire des grottes de Temara (Maroc) d'après l'étude des minéraux lourds et l'étude exoscopique des grains de quartz. *Quaternaire* 16, 73–83.

Olszewski, D.I., Schurmans, U.A., and Schmidt, B.A. 2011. The Epipaleolithic (Iberomaurusian) from Grotte des Contrebandiers, Morocco. *African Archaeological Review* 28, 97–123.

Parsons, I. 2003. Lithic expressions of Later Stone Age lifeways in the Northern Cape. *South African Archaeological Bulletin* 57, 33–37.

Pasty, J.-F. 1999. *Contribution à l'étude de l'Atérien du nord mauritanien*. British Archaeological Reports International Series 758. Archaeopress, Oxford.

Poppe, G.T. and Goto, Y. 1991. *European Seashells*, Volume I. Verlag Christa Hemmen, Wiesbaden.

Prescott, J.R. and Hutton, J.T. 1994. Cosmic ray contributions to dose rates for luminescence and ESR dating: large depths and long–term time variations. *Radiation Measurements* 23, 497–500.

Rector, A.L. and Reed, K.E. 2010. Middle and late Pleistocene faunas of Pinnacle Point and their paleoecological implications. *Journal of Human Evolution* 59, 340–357.

Reed, D.N. 2003. *Micromammal Paleoecology: Past and Present Relationships Between East African Small Mammals and their Habitats*. Ph.D. Dissertation, Stony Brook University.

Reed, D.N. 2005. Taphonomic implications of roosting behavior and trophic habits in two species of African owl. *Journal of Archaeological Science* 32, 1669–1676.

Reed, D.N. and Barr, W.A. 2010. A preliminary account of the rodents from Pleistocene levels at Grotte des Contrebandiers (Smuggler's Cave), Morocco. Historical Biololgy 22, 286–294.

Reed, K.E. 2008. Paleoecological patterns at the Hadar hominin site, Afar Regional State, Ethiopia. *Journal of Human Evolution* 54, 743–768.

Reygasse, M. 1921–1922. Etudes de Palethnologie Maghrébine (deuxième série). *Recueil des Notices et Mémoires de la Société Archéologique Historique et Géographique de Constantine* 53, 159–204.

Reyss, J.-L., Valladas, H., Mercier, N., Froget, L., and Joron J.-L. 2007. Application des méthodes de la thermoluminescence et des déséquilibres dans la famille de l'uranium au gisement archéologique d'El Akarit. In: *El Akarit. Un site archéologique du Paléolithique moyen dans le sud de la Tunisie*, Roset, J.P. and Harbi-Riahi, M. (eds). Éditions Recherche Sur Les Civilisations, Culturefrance, pp. 357–363.

Richter, D. 2007. Advantages and limitations of thermoluminescence dating of heated flint from Paleolithic sites. *Geoarchaeology* 22, 671–683.

Richter, D., Moser, J., Nami, M., Eiwanger, J., and Mikdad., A. 2010. New chronometric data from Ifri n'Ammar (Morocco) and the chronostratigraphy of the Middle Palaeolithic in the Western Maghreb. *Journal of Human Evolution* 59, 672–679.

Rink, W.J. 1997. Electron spin resonance (ESR) dating and ESR applications in Quaternary science and archaeometry. *Radiation Measurements* 27, 975–1025.

Roberts, R.G., Bird, M., Olley, J., Galbraith, R., Lawson, E., Laslett, G., Yoshida, H., Jones, R., Fullagar, R., Jacobsen, G., and Hua, Q. 1998. Optical and radiocarbon dating at Jinmium rock shelter in northern Australia. *Nature* 393, 358–362.

Roche, J. 1956. Étude sur l'industrie de la grotte de Dar es Soltan. *Bulletin d'Archéologie Marocaine* 1, 93–118.

Roche, J. 1963. *L'Épipaléolithique Marocain*. Fondation Calouste Gulbenkian, Lisbon.

Roche, J. 1967. L'Atérien de la grotte de Taforalt (Maroc oriental). *Bulletin d'Archéologie Marocaine* 7, 11–56.

Roche, J. 1969. Fouilles de la Grotte des Contrebandiers (Maroc). *Palaeoecology of Africa and of the surrounding islands and Antarctica* 4, 120–121.

Roche, J. 1976a. Cadre chronologique de l'Épipaléolithique marocain. *Actes du IXè Congrès de l'UISPP: Chronologie et synchronisme dans la préhistoire circum-méditerranéenne*, pp. 153–167.

Roche, J. 1976b. Chronostratigraphie des restes atériens de la Grotte des Contrebandiers à Témara (Province de Rabat). *Bulletin et Mémoires de la Societé d'Anthropologie de Paris* 3, 165–173.

Roche, J. and Texier, J.-P. 1976. Découverte de restes humains dans un niveau atérien supérieur de la grotte des Contrebandiers, à Temara (Maroc). *Comptes Rendus de*

l'Académie des Sciences de Paris, Série D 282, 45–47.

Ruhlmann, A. 1951. *La Grotte Préhistorique de Dar es-Soltan*. Larose, Paris.

Saban, R. 1998. Les vaisseaux méningés de l'homme de Témara (Maroc Atlantique). *Bulletin d'Archéologie Marocaine* 18, 99–107.

Schwenninger, J.-L., Colcutt, S.N., Barton, R.N.E., Bouzouggar, A., El Hajraoui, M.A., Nespoulet, R., and Debénath, A. 2010. Luminescence chronology for Aterian cave sites on the Atlantic coast of Morocco. In: *South-Eastern Mediterranean Peoples between 130,000 and 10,000 years ago*, Garcea, E.A.A. (ed.). Oxbow Books, Oxford, pp. 19–37.

Skinner, A.R., Blackwell, B.A., Chasteen, D.E., Shao, J.M., and Min, S.S. 2000. Improvements in dating tooth enamel by ESR. *Applied Radiation and Isotopes* 52, 1337–1344.

Smith, T.M., Tafforeau, P., Reid, D.J., Grün, R., Eggins, S., Boutakiout, M., and Hublin, J.J. 2007. Earliest evidence of modern human life history in North African early *Homo sapiens*. *Proccedings of the National Academy of Sciences USA* 104, 6128–6133.

Spalding, M.D., Fox, H.E., Allen, G.R., Davidson, N., Ferdaña, Z.A., Finlayson, M., Halpern, B.S., Jorge, M.A., Lombana, A., Lourie, S.A., Martin, K.D., McManus, E., Molnar, J., Recchia, C.A., and Robertson, J. 2007. Marine ecoregions of the world: a bioregionalization of coastal and shelf areas. *BioScience* 57, 573–583.

Steele, T.E. and Álvarez-Fernández, E. 2011. Initial investigations into the exploitation of coastal resources in North Africa during the Late Pleistocene at Grotte des Contrebandiers, Morocco. In: *Trekking the Shore: Changing Coastlines and the Antiquity of Coastal Settlement*, Bicho, N., Haws, J., and Davis, L.G. (eds.). Springer, New York, pp. 383–403.

Steele, T.E. and Klein, R.G. 2008. Intertidal shellfish use during the Middle and Later Stone Age of South Africa. *Archaeofauna* 17, 63–76.

Stoetzel, E. 2005. *Les microvertebres de la couche 1 d'El Harhoura II. Donnees systematiques, taphonomiques et paleoecologiques*. Masters Thesis, Museum National d'Histoire Naturelle.

Stoetzel, E., Michel, P., Nespoulet, R., and El Hajraoui, M.A. 2007. Les environnements holocènes du littoral atlantique du Maroc. Exemple des petits et grands vertébrés en contexte archéologique provenant de la grotte d'El Harhoura 2, région de Temara. *Quaternaire* 18, 359–367.

Stoetzel, E., Marion, L., Nespoulet, R., El Hajraoui, M.A., and Denys, C. 2011. Taphonomy and palaeoecology of the late Pleistocene to middle Holocene small mammal succession of El Harhoura 2 cave (Rabat-Témara, Morocco). *Journal of Human Evolution* 60, 1–33.

Taylor, V.K., Barton, R.N.E., Bell, M., Bouzouggar, A., Collcutt, S.N., Black, S., and Hogue, J.T. 2011. The Epipaleolithic (Iberomaurusian) at Grotte des Pigeons (Taforalt), Morocco: A preliminary study of the land Mollusca. *Quaternary International* 244, 5–14.

Tebble, N. 1966. *British Bivalve Seashells: A Handbook for Identification.* The British Museum of Natural History, London.

Tixier, J. 1958-1959. Les pièces pédonculées de l'Atérien. *Libyca* A/P/E VI-VII: 127–158.

Tong, H. 1986. The Gerbillinae (Rodentia) from Tighennif (Pleistocene of Algeria) and their significance. *Modern Geology* 10, 197–214.

Vanhaeren, M., d´Errico, F., Stringer, C., James, S.L., Todd, J.A., and Mienis, H.K. 2006. Middle Palaeolithic Shell Beads in Israel and Algeria. *Science* 312, 1785–1788.

Vallois, M.H.V. and Roche, J. 1958. La mandibule acheuléene de Témara, Maroc. *Comptes Rendus de l'Acádemie des Sciences* 246, 3113–3116.

Van Peer, P. 2001. Observations on the Palaeolithic of the south-western Fezzan and thoughts on the origin of the Aterian. In: *Uan Tabu in the Settlement History of the Lybian Sahara*, Garcea, E.A.A. (ed.). Arid Zone Archaeology. Roma, Edizioni all'insegna del giglio, pp. 51–62.

Vaufrey, R. 1955. *Préhistoire de l'Afrique*, Vol. 1: Maghreb. Masson, Paris.

Wengler, L. 1997. La transition du Moustérien à l'Atérien. *L'Anthropologie* 101, 448–481.

White, T.D., Asfaw, B., Degusta, D., Gilbert, H., Richards, G.D., Suwa, G., and Howell, F.C. 2003. Pleistocene *Homo sapiens* from Middle Awash, Ethiopia. *Nature* 423, 742–747.

Willoughby, P.R. 2001. Middle and Later Stone Age technology from the Lake Rukwa Rift, southwestern Tanzania. *South African Archaeological Bulletin* 56, 34–45.